8-18-2014 12:00 AM

Tissue Engineering Scaffolds with Enhanced Oxygen Delivery Using a Cyclodextrin Inclusion Complex

Tierney GB Deluzio, *The University of Western Ontario*

Supervisor: Dr. Kibret Mequanint, *The University of Western Ontario*
A thesis submitted in partial fulfillment of the requirements for the Master of Engineering
Science degree in Chemical and Biochemical Engineering
© Tierney GB Deluzio 2014

TISSUE ENGINEERING SCAFFOLDS WITH ENHANCED OXYGEN DELIVERY USING A CYCLODEXTRIN INCLUSION COMPLEX

(Thesis format: Integrated-Article)

by

Tierney Grace Blakeborough <u>Deluzio</u>

Graduate Program in Chemical & Biochemical Engineering

A thesis submitted in partial fulfillment of the requirement for the degree of

Master of Engineering Science

The School of Graduate and Postdoctoral Studies
The University of Western Ontario
London, Ontario, Canada

ABSTRACT

The development of a strategy to improve oxygen delivery to cells seeded on scaffolds is essential for the success of tissue engineering applications. The focus of this work was to explore the application of cyclodextrin inclusion complexes (CD:ICs) with perfluorocarbons as oxygen carriers. CD:ICs were prepared from alpha-cyclodextrin and perfluoroperhydrophenanthrene via co-precipitation, paste mixing, and dry mixing complexation techniques. Characterization indicated that paste mixing at a 2:1 host:guest ratio was the most effective method for complexation between the parent molecules. The CD:ICs were then successfully incorporated in 3D fibrous mats via electrospinning with poly(carbonate urethane) and polycaprolactone as biostable and biodegradable polymer matrices, respectively. Electrospinning conditions were optimized to achieve appropriate fiber morphology for tissue engineering applications and material characterization indicated some of the CD:ICs were present on the fiber surface. The dissolved oxygen concentration increased significantly in the presence of either CD:ICs or CD:IC-functionalized fibrous mats at various conditions in model solutions. Overall, this study demonstrates that CD:ICs prepared with perfluorocarbons are potential oxygen carriers, and when embedded in scaffolds they may present a viable approach to enhancing oxygen delivery to cells seeded on tissue engineering scaffolds.

Keywords: tissue engineering, oxygen delivery, scaffold, electrospinning, perfluorocarbons, cyclodextrin, inclusion complex

ACKNOWLEDGEMENTS

TABLE OF CONTENTS

LIST OF TABLES

LIST OF FIGURES

LIST OF APPENDICES

LIST OF ABBREVIATIONS

2D	Two-dimensional
3D	Three-dimensional
ANOVA	Analysis of variance
ATR	Attenuated total reflectance
BE	Binding energy
CD	Cyclodextrin
CD:IC	Cyclodextrin inclusion complex
CPO	Calcium peroxide
DCM	Dichloromethane
d.i.	De-ionized water
DMF	*N,N*-Dimethylformamide
DO	Dissolved oxygen
ECM	Extracellular matrix
FTIR	Fourier transform infrared spectroscopy
FZ	Fluorinated-zeolite
HBSS	Hank's balanced salt solution
HCASMC	Human coronary artery smooth muscle cells
IC	Inclusion complex
MTT	3-(4,5-dimethylthiazol-2-yl)-2,5-diphenyltetrazolium bromide
NC	Nanocapsule
PBS	Phosphate-buffered saline
PCL	Polycaprolactone

PCU	Poly(carbonate urethane)
PDMS	Polydimethylsiloxane
PFC	Perfluorocarbon
PFD	Perfluorodecalin
PFP	Perfluoroperhydrophenanthrene
PLGA	Poly(lactic-co-glycolic acid)
$p\mathrm{O}_2$	Oxygen partial pressure
POG	Polymeric oxygen generating
RT	Room temperature
SD	Standard deviation
SEM	Scanning electron microscopy
SPO	Sodium percarbonate
TGA	Thermogravimetric analysis
XPS	X-ray photoelectron spectroscopy
XRD	X-ray diffraction

1 INTRODUCTION

1.1 Scope

Tissue engineering continues to emerge as a strategy for the repair and regeneration of diseased or damaged tissues and organs as an alternative to current therapies.[1] Scaffold-guided tissue engineering involves seeding cells onto a porous three-dimensional (3D) scaffold that supports *in vitro* tissue formation and maturation. The resulting engineered tissue is envisioned to be implanted in a patient where it further grows, going through self-repair remodeling. The ultimate objective of tissue engineering is thus to develop responsive living tissues with properties similar to those of the native tissues they are intended to replace, and can be applied to many, if not all, tissues in the body. However, one of the major factors hindering the success of scaffold-guided tissue engineering is the inability to deliver sufficient oxygen to the growing constructs *in vitro*. Previous attempts to overcome this limitation have been riddled with drawbacks; so the task remains a fundamental consideration for fabricating engineered tissues.[2-4]

Oxygen delivery, in particular, is a limiting step for developing tissues of a clinically-relevant size because of the low solubility of oxygen in culture media, which is further exacerbated by the high oxygen requirements for cells, which consume five to six moles of oxygen per mole of monosaccharide.[5] Clearly, the delivery of oxygen to cells requires the development of an oxygen delivery system that is more efficient than molecular diffusion alone. When designing an alternative oxygen delivery strategy, arguably the most important factor is the length of and extent of delivery with the goal of continuous and sustained delivery such that sufficient quantities are available until the cells seeded on the scaffold are adequately matured into clinically-relevant thick tissues. If the developed strategy involves altering the scaffold in some way, it must be done such that the scaffold properties, particularly porosity and morphology, are not adversely affected. Finally, it is imperative that the materials used are cytocompatible and do not introduce any toxic or otherwise harmful by-products.

In this work, cyclodextrin inclusion complexes were prepared with a perfluorocarbon, and explored for their ability to enhance oxygen delivery when embedded in tissue engineering scaffolds.

1.2 Thesis Outline

In view of the scope described above, the work presented in this thesis underscores the importance of addressing oxygen delivery limitations in fabricating engineered tissues of clinical relevance. Firstly, Chapter 2 provides an in-depth literature review covering pertinent information related to the topics being discussed, specifically tissue engineering, oxygen mass transfer in tissues, the chemistry of perfluorocarbon compounds, and cyclodextrin inclusion complexes. This thesis is separated into three main objectives, with all materials and methods, including experimental parameters, presented at the beginning of each chapter. Chapter 3 describes the initial objective of preparation and characterization of cyclodextrin inclusion complexes with perfluorocarbons. Chapter 4 describes the fabrication and characterization of tissue engineering scaffolds incorporating the prepared cyclodextrin inclusion complexes. Chapter 5 describes the *in vitro* analysis of oxygen delivery for both the cyclodextrin/perfluorocarbon inclusion complexes and the functionalized three dimensional scaffolds. Finally, Chapter 6 provides a general conclusion of the major findings in this study, its strengths and limitations, and future directions.

1.3 References

1.   Langer, R.; Vacanti, J. P., Tissue engineering. *Science* **1993,** 260, (5110), 920-6.

2.   Malda, J.; Rouwkema, J.; Martens, D. E.; Le Comte, E. P.; Kooy, F. K.; Tramper, J.; van Blitterswijk, C. A.; Riesle, J., Oxygen gradients in tissue-engineered PEGT/PBT cartilaginous constructs: measurement and modeling. *Biotechnol Bioeng* **2004,** 86, (1), 9-18.

3.   Radisic, M.; Deen, W.; Langer, R.; Vunjak-Novakovic, G., Mathematical model of oxygen distribution in engineered cardiac tissue with parallel channel array perfused with culture medium containing oxygen carriers. *Am J Physiol Heart Circ Physiol* **2005,** 288, (3), H1278-89.

4.   Radisic, M.; Malda, J.; Epping, E.; Geng, W.; Langer, R.; Vunjak-Novakovic, G., Oxygen gradients correlate with cell density and cell viability in engineered cardiac tissue. *Biotechnol Bioeng* **2006,** 93, (2), 332-43.

5.   Rappaport, C., Review-progress in concept and practice of growing anchorage-dependent mammalian cells in three dimension. *In Vitro Cell Dev Biol Anim* **2003,** 39, (5-6), 187-92.

2 LITERATURE REVIEW[*]

2.1 Tissue Engineering

Tissue engineering is the assembly of cells and their support structures for the repair and regeneration of diseased or damaged tissues and organs as an alternative to current therapies.[1] One strategy of tissue engineering (**Figure 2-1**), involves seeding cells onto a porous three-dimensional (3D) scaffold that supports *in vitro* tissue formation and maturation. The resulting engineered tissue is implanted in a patient where it further grows, through self-repair remodeling. The ultimate objective of tissue engineering is thus to develop responsive living tissues with properties similar to those of the native tissues they are intended to replace, and can be applied to many, if not all, tissues in the body. Not surprisingly, tissue engineering continues to be a promising alternative to current treatments for diseased and damaged organs, and it has already found applications in a variety of other areas such as drug research and discovery.[2-4] The strategies of tissue engineering are conceptually simple and appealing yet they have proven to be challenging engineering tasks. Despite rapid advances made in this field,[5, 6] success is still limited due to significant knowledge gaps in the ability to control, coordinate, and direct tissue formation, which are the ultimate goals for tissue engineering.

2.1.1 Scaffolds

With the few exceptions,[7-9] exogenous porous 3D scaffolds which mimic the extracellular matrix (ECM) are required for the growth of cells to form an engineered construct.[10, 11] Depending on the intended application, scaffolds may be designed to be biodegradable so that only the neo-tissue will remain after a given period of culture time or following implantation, or they may be biostable such that a composite tissue that provides long-term support could be fabricated.[12-15] In the case of biodegradable scaffolds, cells will remodel the scaffold with their own ECM proteins creating the intended tissue without

---

[*] Parts of this chapter have been published: Tierney GB Deluzio, Dawit G Seifu, Kibret Mequanint, 3D scaffolds in tissue engineering and regenerative medicine: beyond the structural templates? *Pharmaceutical Bioprocessing* **2013**, 1(3), 267-281.
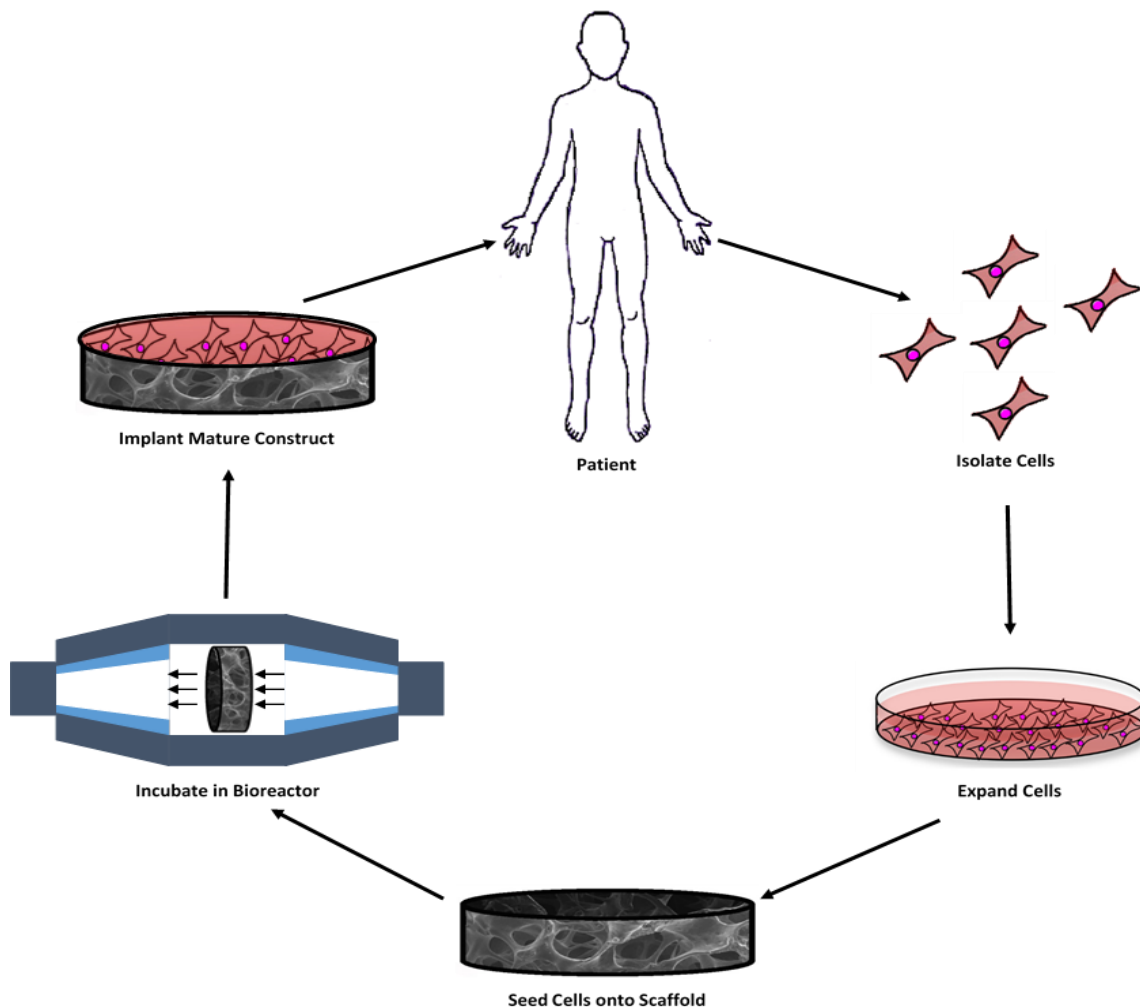
Figure 2-1: Schematic diagram showing the essential stages of scaffold-guided tissue engineering

compromising the tissue structural integrity. This, however, requires strict coordination of the scaffold biodegradation rate with the biosynthetic rate and is one of the major obstacles in the field today. In addition, a scaffold must have several required characteristics: biocompatibility, appropriate mechanical strength and compliance, optimal porosity for cell seeding, *in vitro* nutrient and oxygen transport, and the ability to bind to cells and release growth factors when needed. Although some of these criteria could be met with existing scaffolds, they do not always provide biological cues for embedded cells and do not interact with the cells. In the body, cells reside within the ECM, which provides tissues with the appropriate architecture as well as signaling cues that influence key cell function such as adhesion, migration, proliferation, differentiation, and secretion of ECM components.[16] Fabrication of tissues *in vitro* thus requires that cells be given a more

specific level of instruction so that tissue regeneration in the host is successful. With the discovery of cell adhesion peptide domains in fibronectin, collagen, and laminin, the design of synthetic extracellular matrices with biological activity has become a valuable strategy to impart biomimetic properties.[17-19]

The selection of scaffold type and material depends on the specific tissue engineering application, as well as the applicable design criteria. Natural materials such as collagen,[20] chitosan,[21] and hyaluronic acid[22] have the advantage of being generally nontoxic in addition to providing biological cues to promote cell attachment and proliferation. However, these natural materials are difficult to fabricate due to their limited processing parameters and often result in constructs with poor mechanical properties. Synthetic materials, on the other hand, are readily available and generally easy to modify, with minimal batch to batch variations. However, they do not innately possess appropriate sites to enhance cellular interactions and therefore lack bioactivity. The method of scaffold fabrication also significantly impacts the physical and chemical properties of the resulting tissue engineered construct. Other aspects, including reproducibility and cost-effectiveness, should also be considered when selecting materials and fabrication techniques. Common methods for scaffold fabrication include solvent casting/particulate leaching and electrospinning, with more advanced techniques, such as rapid 3D plotting, solid free form, and 3D projection stereolithography, being developed.[23-26] Since the work in this thesis utilized electrospinning to fabricate scaffolds, a succinct review of the electrospinning process is described in the following section (2.1.1.1).

2.1.1.1 Electrospinning

One of the most commonly utilized methods for scaffold fabrication is electrospinning. Electrospinning was initially developed in 1902,[27, 28] and it has been applied to fabricate tissue engineering scaffolds since the mid-1990s. Electrospinning is a versatile technique that enables the production of multi-functional fibers in the nano- to micrometer range from a wide variety of materials including but not limited to polymers, polymer blends, sol-gels, composites, and ceramics.[29-31] In general, electrospinning is a relatively simple, versatile, and cost-effective method. The typical electrospinning setup consists of a syringe pump, a

high voltage source, and a collector (**Figure 2-2**). The selected polymer is dissolved in a solvent and the resulting polymer solution is loaded into a syringe. A strong electrostatic force is applied to the needle tip via a high voltage supply, inducing a charge in the solution. As the polymer solution is forced through the syringe via the syringe pump, the charge induced within the polymer begins to overcome the surface tension holding the polymer solution suspended at the needle tip. The solution at the tip begins to elongate and form a conical shape known as a Taylor cone.[28, 32, 33] When the critical value at which the surface tension is overcome is reached, the solution is ejected from the tip of the Taylor cone as a charged jet.[32, 34, 35] The solvent evaporates during the flight of the jet in air across the distance between the needle tip and collector, resulting in the continuous accumulation of solid polymer fibers in a non-woven arrangement on the grounded collector. The collector can be one of several configurations, including a stationary plate or a rotating mandrel.[27, 28] The electrospinning jet is composed of four regions: the base, jet, splay, and collection.[36] In the first region, the base, the jet emerges to form the Taylor cone. The polymer jet is then accelerated and stretched by the electric forces, decreasing its diameter and increasing the charge density. The jet then appears to splay into many small fibers of approximately equal diameter, yet the jet is actually a single, rapidly whipping jet that undergoes bending and stretching.[32, 35] The fibrous mats that result from electrospinning possess important characteristics for tissue engineering scaffolds. These characteristics include a large surface-to-volume ratio, pore sizes and fibers in the nano-range, and an interconnected structure,[36] and make the fibrous configurations that result from electrospinning useful in mimicking of the ECM. Electrospinning is generally a simple and cost-effective technique. Furthermore, it is relatively simple to incorporate various additives during the electrospinning process in order to improve on the functionality of the fibers.[29, 31] The main disadvantage of electrospinning is that the small pore spacing leads to difficulties with cell infiltration during cell delivery and fostering; however, electrospun nanofibers best mimic several ECM proteins.[37, 38]
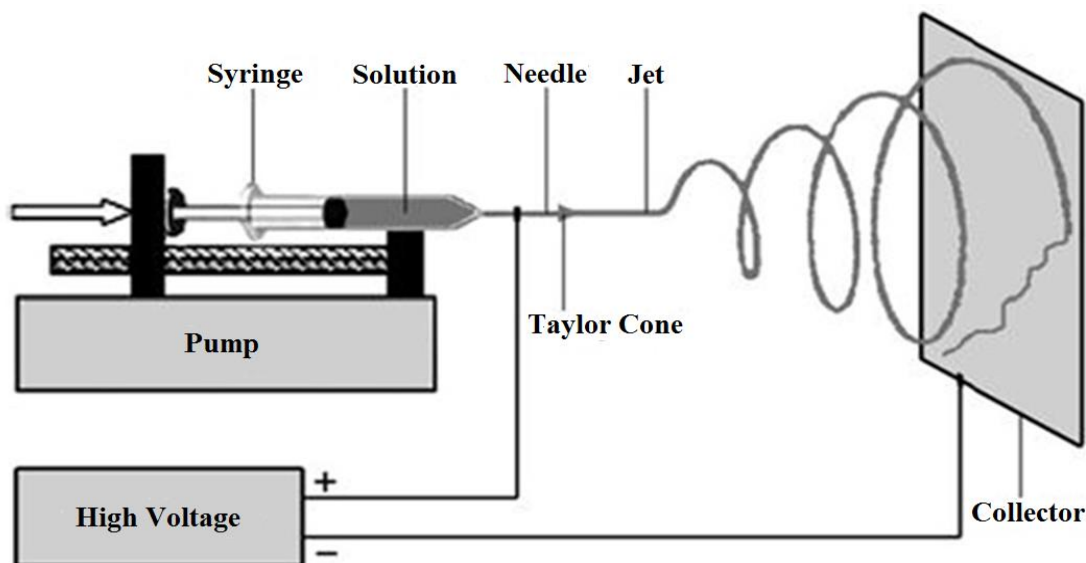
Figure 2-2: Schematic of electrospinning set-up

The characteristics of the resultant fibrous mats can be controlled by a number of parameters: solution properties, controlled variables, and ambient parameters.[32, 36] The solution properties include viscosity, conductivity, surface tension, polymer molecular weight, dipole moment, and dielectric constant of the polymer solution. It is difficult to determine the effect of individual solution properties as they are usually connected and are therefore difficult to isolate. Nevertheless, the viscosity of the solution, as controlled by altering the polymer concentration, has a significant effect on the fiber size and morphology; they are directly proportional, with fiber diameter generally increasing as solution viscosity is increased. At very low viscosities, there are not enough chain entanglements and overlapping to create a stable jet, so the process is characteristic of electrospraying, yielding beads or fibers possessing defects such as beading.[39] Increasing the molecular weight of the polymer also decreases the number of beads and droplets formed on the fibers.[36] Increasing the conductivity of the solution generally decreases beading, resulting in more uniform and smaller fibers. The controlled variables include flow rate, electric field strength, distance between tip and collector, needle tip design, and collector composition and geometry. Decreasing the flow rate generally results in fibers with smaller diameters, as flow rate and fiber diameter are directly proportional. If the flow rate is too high, the wet fibers will not have enough time to dry before reaching the collector, resulting in beading and fiber fusion. Similarly, there is a minimum distance

between the needle tip and collector required in order to give the fibers enough time to dry, with beading observed at distances that are too close or far. In general, increasing the voltage also causes an increase in beading. Overall, fiber diameter is inversely proportional to both distance and electric potential.[36] Furthermore, a solvent with suitable volatility should be selected to facilitate sufficient evaporation over the allocated needle tip to collector distance.[35]

Incorporating cyclodextrins (CDs) or their inclusion complexes (ICs) into an electrospun mat can impart unique characteristics to the fibers, creating interesting functionality, and potentially improving the application of cyclodextrin and/or electrospun fibers.[31] A number of studies have explored the functionalization of electrospun nanofibers with CDs incorporated for a variety of applications, for example poly(methyl methacrylate) containing CD-menthol-ICs,[29] polystyrene fibers containing CD-menthol-ICs,[40] polyvinyl alcohol nanofibers incorporating CD-vanillin-ICs,[41] polystyrene incorporating CDs as molecular filters,[42] and polyacrylonitrile with silver/β-CD nanoparticles.[30] Moreover, polymer-free nanofibers have been prepared by electrospinning cyclodextrin, its derivatives, and their inclusion complexes alone.[39] For instance, polymer-free nanofibers have been obtained from hydroxypropyl-β-cyclodextrin and its inclusion complexes with triclosan, and the resulting fibrous mats possess some mechanical integrity and can be handled and folded as a free-standing web.[43] The success of this procedure is dependent upon considerable aggregates and adequate interactions between the CD molecules, effectively acting as chain entanglements in the solution in order to create a stable jet.[39] Cyclodextrin has been shown to positively affect the electrospinning of polymer solutions. The addition of CD increases the conductivity of the polymer solution, allowing for successful electrospinning of bead-free fibers from low polymer concentrations.[29, 40] This is because the polymer solution is subjected to higher stretching under the high electric field.[31] The addition of CD can also influence the viscosity of the polymer solution, potentially furthering the effect of CD on fiber morphology. However, in the case of electrospinning polyvinyl alcohol with a CD-vanillin-ICs, the conductivity of the resulting polymer solution was lower, resulting in less stretching of the electrified jet, and in turn thicker fibers, contradictory to the general observed trend.[41]

2.2 Oxygen Mass Transfer in Tissues

2.2.1 The Challenges of Oxygen Transfer in Engineered Tissues

The success of engineered tissues has been limited by the inability to deliver sufficient oxygen to the growing constructs. Oxygen delivery, in particular, is a limiting step for clinically-relevant size tissues because of its low solubility in culture media.[44] This is further exacerbated by the fact that cells consume five to six moles of oxygen per mole of monosaccharide according to the following mole balance.

$$C_6H_{12}O_6 + 6O_2 \rightarrow 6CO_2 + 6H_2O \tag{2-1}$$
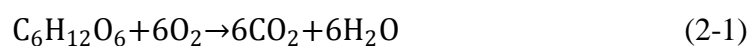
Clearly, the delivery of this much oxygen to cells requires the development of an oxygen delivery system that is more efficient than molecular diffusion alone.[45]

The lack of sufficient oxygen supply to cells is exemplified by results showing cellular spheroids containing a hypoxic and necrotic center surrounded by a rim of viable cells.[46,47] This is because the cells located in the center of the tissue engineered constructs experience different environmental conditions than those located at the peripheral boundaries.[48] It has been shown that oxygen concentrations decline rapidly from the exterior to the interior within the structure and that the oxygen gradients are more pronounced during the early stages of tissue development.[48] In addition to cellular necrosis, insufficient oxygen levels result in a shift to anaerobic metabolism and energy conservation.[49] For the tissue engineering approach to become a clinical success, it is vital that the challenge of delivering sufficient oxygen to cells seeded on scaffolds is overcome.

2.2.2 *In vivo* Oxygen Transfer

In the body, oxygen is supplied in sufficient amounts via two specialized systems: convection and hemoglobin. Firstly, the circulatory system enhances the delivery of oxygen to vascularized tissues via convection of blood through the capillary network which has the effect of decreasing the distance required for diffusion. Furthermore, hemoglobin,

a natural oxygen carrier protein, overcomes the very low solubility of oxygen in plasma by carrying 65 times more oxygen than blood plasma alone.[50]

2.2.3 Alternative Oxygen Delivery Strategies

The delivery of nutrients and the removal of metabolic waste materials remains to be a fundamental consideration for fabricating engineered tissues.[51, 52, 53] A number of approaches have been developed to improve the delivery of oxygen to cells seeded on tissue engineering constructs, as summarized in **Figure 2-3**, adapted from Malda *et al*.[48] This section evaluates a few such studies with the intent of bringing attention to the limitations of current strategies and rationale for this research.

One approach to reducing hypoxia *in vitro* is the use of perfusion bioreactors where oxygen dissolved in the culture medium diffuses to the scaffold interior. For this purpose, bioreactors have been developed with the intent to mechanically stimulate the growing tissue constructs with physiologically relevant forces and to improve mass transfer within the tissue. Although the former is largely successful, the latter has shown to be a formidable engineering task. Therefore, the delivery of nutrients and the removal of metabolic waste materials remained to be a fundamental consideration for fabricating engineered tissues.[52,54,55]

In the case of flow-induced mass transfer, the high flow rate required to maintain an adequate oxygen concentration for cell viability often surpasses the shear stress tolerance of the cells.[56] Alternatively, one feasible approach involves the use of perfluorocarbon (PFC) emulsions as an oxygen carrier emulating the role of hemoglobin in the physiologic system.[52] PFCs have a high dissolving power for oxygen and are hydrophobic, lipophobic, and stable which makes them generally biologically compatible. However, unlike oxygen chemically bound to hemoglobin, solubilized oxygen can be rapidly and extensively extracted from PFC molecules.[57] As oxygen is depleted from the culture medium, it is replenished via diffusion of dissolved oxygen from the PFC particles.[52] The oxygen unloading of the PFC emulsion is facilitated by its increased surface area. One disadvantage of these emulsions is their lack of stability, resulting in stringent storage

requirements and an overall lack of user-friendliness.[57] Moreover, their high density causes them to settle in the culture well or medium reservoir.[50] From this, it can be inferred that binding the oxygen carrier molecules to the scaffold would be advantageous.
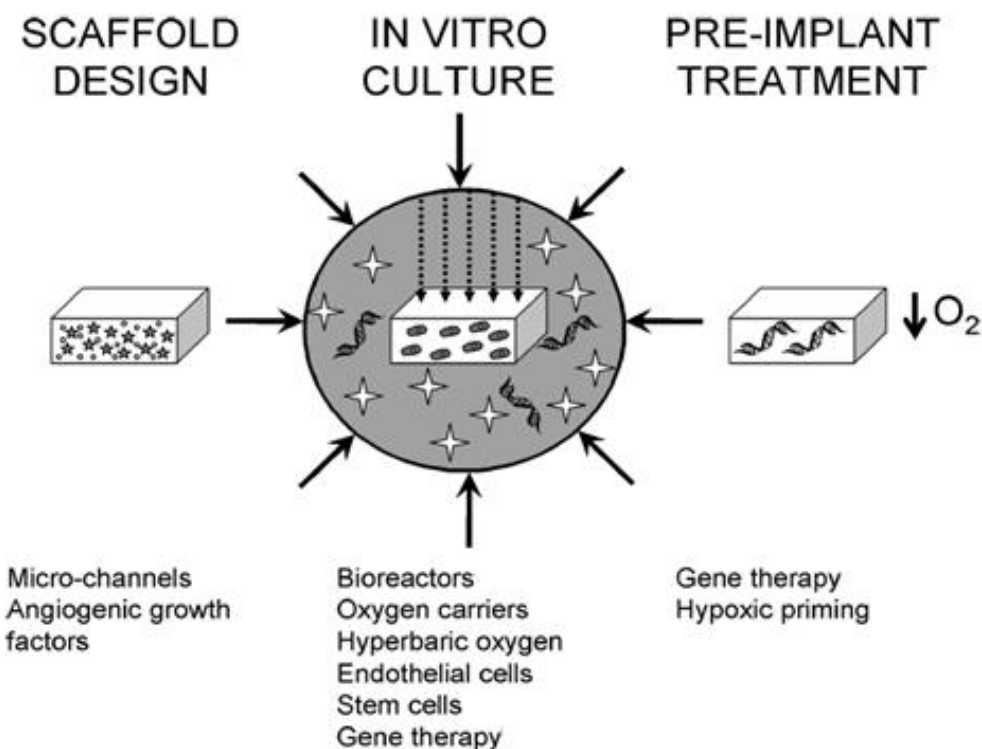
Figure 2-3: Approaches to reduce hypoxia in vitro, promote angiogenesis, or both after implantation of engineered tissues. Adapted from Malda, J.; Klein, T.J.; Upton, Z., The roles of hypoxia in the in vitro engineering of tissues. *Tissue Engineering* **2007, 13, (9), 2153-2162 with permission from Mary Ann Liebert, Inc.**

One study aimed to closely mimic the biological environment by incorporating a parallel array of channels within the porous 3D scaffold, representing the capillary network, and supplementing the medium with a PFC emulsion, representing the hemoglobin.[50] Porous biorubber scaffolds, made of poly(glycerol-sebacate), were fabricated using a salt leaching technique with sodium chloride as a porogen and an array of cubically packed parallel channels was created using a computerized carbon dioxide laser system. Although it was demonstrated that the channel walls were highly porous, as required for efficient nutrient and oxygen transport, technical restrictions limited the size and spacing of the channels,

resulting in channels that were much larger than the native capillaries. Increased availability of oxygen resulted in significantly lower levels of lactate dehydrogenase, an enzyme indicative of tissue breakdown signifying decreased cell death; increased DNA content and cell density, indicating higher construct cellularity; and lower lactate to glucose ratio, suggestive of more aerobic metabolism than the control. Electron microscopy of the constructs following cell culturing showed that the channels remained open with cells present between them; however, a compact and continuous tissue was not formed. Moreover, settling of the PFC droplets was still evident within the experimental setup, owing to the high density of the PFC emulsion, and the cells exhibited a rounded morphology owing to the direct exposure to shear stress above their tolerance, due to the perfusion culture conditions. As such, a number of the limitations associated with the perfusion bioreactor and PFC emulsion strategies remained apparent with this technique.[50]

Another method for improving the delivery of oxygen to cells is incorporating oxygen generating chemicals into the 3D scaffolds. Calcium peroxide (CPO), which decomposes in water to produce oxygen according to the following set of equations, was embedded into poly(lactic-co-glycolic acid) (PLGA) scaffolds.

$$2CaO_2 + 4H_2O \rightarrow 2Ca(OH)_2 + 2H_2O_2 \qquad\qquad (2\text{-}2)$$

$$2H_2O_2 \rightarrow O_2 + 2H_2O \qquad\qquad (2\text{-}3)$$
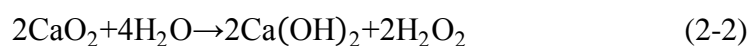
The porous 3D PLGA constructs were prepared via particulate leaching with paraffin as a porogen and contained CPO at concentrations of 0, 1, 5, and 10 wt. %. Scanning electron microscopy data suggested that the pore size and porosity of the scaffold were unaffected by the incorporation of CPO and the scaffold maintained a highly porous and open pore structure. To test the effect on oxygen delivery, NIH3T3 fibroblasts were seeded onto PLGA and PLGA-CPO scaffolds with the addition of catalase to capture the hydrogen peroxide by-products that may be toxic to cells. Under normoxic conditions (21 % oxygen, 5 % carbon dioxide), significant cell viability with the incorporation of 5 % CPO was shown. When scaffolds containing 5 % CPO were seeded with cells and cultured in a

hypoxic environment (1 % oxygen, 5 % carbon dioxide), the metabolic activity on the PLGA-CPO scaffold increased significantly compared with control scaffolds. The hypoxic condition was chosen to test the oxygen generation from the CPO.[58]

A similar study of incorporating CPO into 3D polycaprolactone (PCL) nanofibers was carried out to test the antibacterial properties of the calcium hydroxide produced during oxygen generation.[59] The reported results were not consistent with the previous study[58] since the scaffolds were reported to be cytotoxic to human osteoblast cells. The cytotoxicity, however, appeared to be temporary as cells regained a healthy status and spread over the nanofiber mesh. This negative effect may be attributed to the initial burst release of calcium hydroxide, suggesting that the effect may be transient, causing no long-term harm to tissue development.

As an alternative to calcium peroxide, sodium percarbonate (SPO) can be used as an oxygen generating biomaterial. SPO decomposes in water according to the following equations.[60]

$$[Na_2CO_3]_2 \cdot 3H_2O_2 \rightarrow 4Na^+ + 2CO_3^{2-} + 3H_2O_2 \qquad (2\text{-}4)$$

$$2H_2O_2 \rightarrow O_2 + 2H_2O \qquad (2\text{-}5)$$
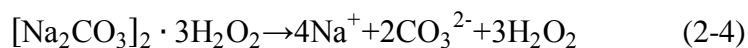
In a feasibility study, SPO was incorporated in a PLGA film using a solvent casting fabrication technique. Oxygen was released steadily from the polymeric oxygen generating (POG) film during the first 24 hours, after which it decreased until it reached complete conversion at roughly 70 hours. Using a skin flap model in nude mice to study the effects of the POG film, it was shown that necrosis was initially delayed for two days compared to control models with PLGA-only films, yet after seven days the POG and control groups were comparable. On a tissue level, exposure to the POG film resulted in significantly less degradation, visible by a reduced amount of skin discolouration. This was further supported by lower levels of lactate observed in POG groups, indicating that the cells were receiving adequate oxygen to prevent anaerobic metabolism, as well as improved tissue strength as

determined by biomechanical testing, indicating decreased degradation of ECM proteins. It is logical that the beneficial effects are limited to the first two days as the majority of the oxygen generation occurs during the first 24 hours. Evaluating oxygen delivery in an *in vivo* model is crucial because the role that oxygen plays in tissue regeneration is complex and varies between *in vitro* and clinical data.

The method of incorporating oxygen generating compounds, such as CPO and SPO, into 3D porous scaffolds shows potential for enhancing oxygen delivery to seeded cells. However, calcium hydroxide and hydrogen peroxide are a strong base and oxidizing agent, respectively which could be detrimental to cells seeded on the scaffolds. Inclusion of catalase or ascorbic acid to protect against oxidative stress and remove potentially harmful by-products could help to alleviate these effects. Based on the inconsistency in the reported cytotoxicity of the by-products of the decomposition of CPO and SPO, further studies are required to determine the amount of cell protector required to fully prevent toxic effects. In addition, incorporating oxygen generating compounds delivers oxygen for a limited time, until the oxygen generating compound is completely consumed. Further studies must be done to determine if this is enough time to extend cell viability until tissue maturation is established and if the amount of oxygen delivered could support larger constructs with higher densities of cells.[61]

Clearly, one major drawback of directly incorporating the oxygen generating compound into the tissue engineering construct is the rapid burst release resulting in enhanced oxygen delivery over a short period as well as toxic amounts of hydrogen peroxide. In order to overcome this limitation, the solid peroxide can be encapsulated within a hydrophobic, biostable polymer that will restrict interaction with water, thereby modulating oxygen generation. In one study, polydimethylsiloxane (PDMS) disks containing 25 % (w/w) CPO powder were fabricated with the intent of enhancing cell viability within 3D tissue engineered constructs.[62] In an open system at 0.05 mM oxygen, the PDMS-CPO disks were able to generate oxygen for approximately 40 days. The oxygen delivery potential of the PDMS-CPO disks was tested by centrally incorporating the PDMS-CPO disks within 3D agarose constructs containing varying cell densities of a β cell line, MIN6 cells, and

culturing them under normoxic or hypoxic oxygen conditions (0.20 or 0.05 mM oxygen, respectively) for three days. The cell viability was improved under hypoxic conditions with the inclusion of the PDMS-CPO disk to the extent that the results were not statistically significant to the corresponding normoxic group. It is likely that this improvement is not as drastic under normoxic conditions because oxygen is no longer the limiting factor, rather glucose availability or contact inhibition are preventing further increases in cell proliferation. It was determined that the PDMS-CPO disks were most beneficial, in terms of metabolic activity, at high cell loading densities, likely owing to the higher total rate of oxygen consumption. As expected, a rim of live cells surrounding a core of dead cells was evident on control constructs from live/dead confocal imaging. On the contrary, the live and dead cells were intermingled throughout the CPO-containing construct and the necrotic core was absent. Interestingly, when measurements were made three days after removing the PDMS-CPO disk, results were statistically equivalent to the control group, reinforcing the hypothesis that the observed improvement to cell viability was due solely to the released oxygen.

A recent study in our laboratory tested the oxygen delivery capability of fluorinated porous zeolite Y particles embedded into a 3D poly(carbonate urethane) (PCU) scaffold.[61] The zeolite Y particles were prepared and then fluorinated with 1*H*,1*H*,2*H*,2*H*-perfluorodecyltriethoxysilane resulting in fluorinated-zeolite (FZ) particles with particle diameters between 850-1000 nm. Three dimensional PCU scaffolds containing 2 wt. % embedded FZ particles were fabricated by the solvent casting and particulate leaching method with NH_4Cl porogens. Inclusion of greater than 2 wt. % FZ particles was not possible due to insufficient mechanical integrity. Data confirmed that the FZ particles were not leached out during the fabrication process. In addition, results showed open and well-defined pores with high interconnectivity, uniform distribution of FZ particles throughout the scaffold, and that the FZ particles were contained mostly at the surface of the scaffold which is crucial for oxygen extraction by cells. This was important for efficient cell infiltration and nutrient transport. To test the effect of the FZ particles on oxygen delivery, human coronary artery smooth muscle cells (HCASMC) were seeded onto the FZ modified and control scaffolds and were cultured for 4, 7, and 14 days. Cell

number increased significantly after 4 and 7 days of culture on the PCU-FZ scaffolds compared with control scaffolds likely attributed to increased oxygen delivery. Although the HCASMC attached and spread on both control scaffolds, the infiltration depth was double on the FZ modified scaffolds suggesting enhanced availability of oxygen at greater depths in the scaffold.

Alternatively, oxygen delivery vectors can be prepared from cyclodextrin, cyclic oligosaccharides made up of six to eight glucose units with a unique shape that allows them to readily form inclusion complexes. Perfluorocarbon nanocapsules (PFC-NC) with a mean diameter of 350 nm have been synthesized from perfluorodecalin and 2,3-di-O-decafluorooctanoylcyclomaltooctaose (β-CD-C_8^F) as vehicles for oxygen solubilization and delivery.[63] The liberation of oxygen from the nanocapsules was evaluated over a period of 24 hours following oxygenation of the PFC-NC suspension with pure oxygen at 1 mL/min for 5 minutes. Compared to pure water oxygenized under the same conditions, the PFC-NC showed both a delayed and prolonged release of oxygen. However, no cell or scaffold studies have been carried out to date utilizing this biomaterial. In comparison, PFC-NC must be oxygenated prior to use whereas FZ particles are able to solubilize the oxygen when necessary according to Henry's law. Since oxygen supply is facilitated by the unloading of the oxygen molecule from the nanocapsule, the delivery is not indefinite. Theoretically, however, the PFC-NC could be reloaded with oxygen, though this is difficult to imagine as a realistic tissue engineering approach. PFC-NC require less oxygenation than PFC emulsions and have the additional benefit of improved stability, with the ability to be conserved for three months at 4 or 25 °C, thus overcoming one of the main drawbacks of PFC emulsions, their lack of stability and resultant stringent storage conditions.[57] Since the particles are significantly smaller than the FZ particles, it can reasonably be assumed that these molecules could be embedded in a 3D scaffold without adversely affecting its properties.

As mentioned above, the delivery of oxygen to cells seeded on scaffolds is vital for successfully developing tissues of clinical relevance. The preceding cited studies have provided platforms to incorporate oxygen delivery vectors into 3D scaffolds without

adversely affecting the porosity or morphology. An important factor is the length of the oxygen delivery time provided by these vectors. Oxygen must be delivered to the cells seeded on the scaffold in sufficient quantities until the engineered tissue matures. Development of an improved method for oxygen delivery to cells, thereby preventing cell necrosis would allow for enhanced tissue structures, ultimately leading to the fabrication of clinically relevant tissues. Although the supply of oxygen to thick tissue constructs *in vitro* (such as muscle and bone) can, in part, be addressed by strategies discussed above, combination of these with prevascularization before transplantation is conceptually an attractive approach. Such an approach relies on the seeding of endothelial cells to form primitive capillary-like tubes within the constructs that may improve the vascularization, blood perfusion, and survival of the tissue constructs after transplantation.[64, 65] Both naturally occurring and synthetic scaffolds that were prevascularized appeared to have better host integration and vascularization in animal experiments compared with control scaffolds.[65-67] It is, however, not clear if the *in vivo* vascular networks formed are nascent with invested pericytes and/or smooth muscle cells. Despite this, it is likely that these emerging data and shared strategies accelerate functional tissue fabrication and host integration.

2.3 The Chemistry of Perfluorocarbon Compounds

The search for alternative oxygen binding chemicals has been and remains to be an active area of research.[68] From a clinical standpoint, this search has been fuelled by increasing negative public perceptions about blood safety coupled with the potential risk of transmitting diseases through transfusion.[69, 70] There are two general categories of current approaches for developing alternative oxygen binding chemicals, those based on hemoglobin and those based on perfluorinated compounds. Products based on hemoglobin include modified hemoglobin derived from either human or animal sources, or genetically engineered recombinant microorganisms and plants.[71-73] Perfluorinated compounds, on the other hand, have been synthesized as emulsions because PFC liquids are immiscible with aqueous systems, including blood and other body fluids.[73] Oxygent™ (Alliance Pharmaceutical Corp., San Diego, CA), for example, is an improved second-generation perfluorocarbon emulsion based on perflubron (perfluorooctylbromide, $C_8F_{17}Br$) that is

highly stable and can carry over twenty times more oxygen than plasma.[74] Perfluorocarbons are organic molecules where the carbon network is surrounded entirely by fluorine atoms. Because fluorine has a much denser electron cloud, a significantly larger electron affinity, and a lower polarizability than hydrogen, in addition to being the most electronegative atom, the resulting perfluorinated molecules are quite different than their hydrogen analogues. The larger, electronically denser fluorine atoms cover and protect the carbon backbone much more effectively than hydrogen atoms. The extreme electron attracting character of fluorine enhances the C—C bond energy in the skeleton by shrinking the orbitals of the carbons. Moreover, the match between the carbon and fluorine orbitals is superior to that of carbon and hydrogen; in fact, it is the strongest single bond found in molecular compounds (approximately 530 kJ/mol).[68, 75] The larger fluorine atom is space demanding, forcing the carbon skeleton to adopt a helical rather than zig-zag arrangement. As well, the bulkiness makes the perfluorinated chains more rigid and allows for fewer kinks. This steric shielding results in PFCs being inert as there are no low energy molecular orbitals accessible for reaction.[76] Overall, the excellent steric and electronic protection the fluorine atoms confer on the carbon skeleton make PFCs both chemically and thermodynamically stable.[76]

2.3.1   Oxygen Solubility in PFCs

PFCs do not chemically bind to gases, but they have the ability to dissolve large quantities of non-polar gases such as oxygen and carbon dioxide. This ability is due to the extremely low polarizability of fluorine which translates into low van der Waals forces within the PFC liquid because van der Waals interactions depend on fluctuations in polarity of the electronic cloud. As van der Waals interactions are the only intermolecular forces that keep non-polar molecules together, in PFCs they are weak, in sharp contrast with the strong intramolecular bonds. Gas dissolution, therefore, is a passive process whereby the gas molecules occupy "cavities" within the intermolecular spaces of the PFC liquid.[76, 77]

Oxygen carrying by PFCs is dissimilar to that of hemoglobin where the oxygen is chemically bound via a strong, localized chemical coordination bond between the dioxygen molecule and the iron atom of the hemoglobin molecule.[78] Therefore, oxygen unloading

from PFCs is enhanced significantly by the lack of chemical fixation and occurs roughly twice as fast as from hemoglobin,[70] providing immediate availability to tissues. The difference in the interactions of oxygen with hemoglobin and PFCs is reflected in the difference in oxygen uptake profiles as a function of partial pressure (pO$_2$) which is sigmoid for hemoglobin and linear for PFCs. The linearity of the oxygen uptake profile for PFCs is the result of Henry's law in which solubility (c) is directly proportional to the gas partial pressure (p),[73] shown in the following equation where k_H is a Henry's law constant.

$$p = k_H c \tag{2-6}$$

Linear PFCs, such as perflubron, dissolve oxygen more effectively than cyclic molecules, such as perfluorodecalin. In general, oxygen solubility in a PFC is inversely proportional to the molecular weight and directly proportional to the number of fluorine atoms, with a typical value of 45 mL/100 mL at standard conditions,[75] roughly 20-25 times greater than in either water or blood plasma under the same conditions.

2.3.2   PFCs for Enhanced Oxygen Delivery

In addition to being chemically unreactive, PFCs are also biologically inert. This is enabled by both their hydrophobicity and lipophobicity, such that they are not soluble in either the aqueous phase or lipids, and are therefore immiscible with body fluids and do not diffuse into interstitial fluids.[78] Furthermore, they are not metabolized in the body as there are no enzymes capable of recycling them thus they do not present any metabolite-related toxicity, and are excreted primarily as a vapour through the lungs.[77] Intravenous-administered PFC droplets are also cleared from the circulation by phagocytic cells of the monocyte-macrophage system.[73] Pure PFCs do not have any negative effects on cell cultures, simply benefits resulting from their ability to enhance oxygen delivery, but PFC emulsions can have toxic effect due to the emulsifiers used.[76] The lack of toxicity and negative side effects of liquid PFCs on living cells has been confirmed by *in vitro* experiments and also in clinical investigations.[79-82] Other characteristics that make PFCs suitable for biological applications is that they are sterilizable, for example by autoclaving, and carry no risks of infection.[57] In order to be utilized for oxygen delivery, they must have rapid excretion,

preferably a few days and no longer than a few weeks,[57] and the ability to be easily synthesized on a large scale in a highly pure form at a reasonable price.[78] The greatest disadvantage of using PFC emulsions is their lack of stability, resultant stringent storage requirements, and overall lack of user-friendliness.[57]

In order to utilize PFCs as oxygen vectors *in vivo*, they must be emulsified into a stable, injectable, and small emulsion. They can then be injected intravascularly, increasing the oxygen solubility in the plasma phase. Perflubron and perfluorodecalin are the two compounds most widely evaluated as the principal constituents of injectable PFC emulsions. Both compounds have molecular weights within the range 460-500 g/mol, which is recognized as giving acceptable tissue retention times, and can be manufactured to a high degree of purity.[77] Clark and Gollan[83] were the first to demonstrate that mice could live while breathing an O_2-saturated liquid PFC without any harm to the animals. The first preparation of a physiologically adjusted PFC emulsion was reported by Sloviter and Kamimoto using bovine serum albumin as a surfactant.[84] There is also growing interest in the use of PFCs for regulating oxygen supply to cultured cells with the potential to reduce or eliminate cellular damage caused by conventional, vigorous aeration methods.[85] PFCs are especially advantageous for use in cell and tissue culture systems since they are heat stable, readily sterilized, and can be recovered from aqueous systems with the potential for recycling, thus making them economically viable, and have been used as oxygen vectors for both mammalian and insect cells grown *in vitro*.[73, 85, 86] Specifically, in cardiac and tracheal tissue engineering, PFCs have been shown to improve oxygenation of tissue engineered constructs without adverse effects.[50, 52, 87] The major limitation in this area of application, however, is droplet settling in culture wells or medium reservoirs due to their high density.[57]

2.4 Cyclodextrin Inclusion Complexes

2.4.1 Cyclodextrins

Cyclodextrins, also known as cycloamyloses, cyclomaltoses, or Shardinger dextrins, are cyclic oligosaccharides containing six (α-CD), seven (β-CD), or eight (γ-CD) linked

glucopyranose units. Due to steric factors, cyclodextrins built from less than six glucopyranose units do not exist; however, cyclodextrins with greater than eight glucopyranose units have been synthesized.[88, 89] Due to their molecular structure and the lack of free rotation about the bonds connecting the glucopyranose units, CDs have a unique toroid or truncated cone shape (shown in **Figure 2-4**). The hydrophilic hydroxyl groups are located on the outer surface, with the primary and secondary hydroxyl groups located on the narrow and wide side, respectively.[90] This structure renders the CDs water-soluble and concurrently generates a hydrophobic inner cavity.[89, 91] CDs are capable of accommodating a variety of molecules entirely or partially within their cavity, forming a non-covalent host-guest system known as an inclusion complex.

CDs are produced by the enzymatic degradation of starch, a renewable material derived from potatoes, corn, rice, etc.[39, 89] When the amylose fraction of starch is degraded by glucosyltransferases, one or several turns of the amylose helix are hydrolyzed off and their ends are joined together, thereby producing the cyclic oligosaccharides.[91] CDs are produced in amounts of thousands of tons per year using environmentally friendly technologies, with prices at levels acceptable for most industrial purposes.[88] CDs are widely accepted as having low toxicity both orally and intravenously. Orally administered CDs have been shown to be harmless because only insignificant amounts are absorbed;[92, 93] and unmodified CDs are completely resistant towards β-amylase, and α-amylase is capable of hydrolyzing CDs only at a slow rate.[94] After intravenous injections, CDs are mainly excreted in their intact form by renal filtration as they are minimally susceptible to hydrolytic cleavage or degradation by human enzymes.[89] In general, CDs are only able to permeate lipophilic biological membranes with considerable difficulty.[95] Although tests showed that cyclodextrins cannot be considered toxic due to extremely high LD_{50} values, at very high concentrations CDs can extract cholesterol and other lipid membrane components from cells, leading to the disruption of cell membranes.[89, 92, 96]
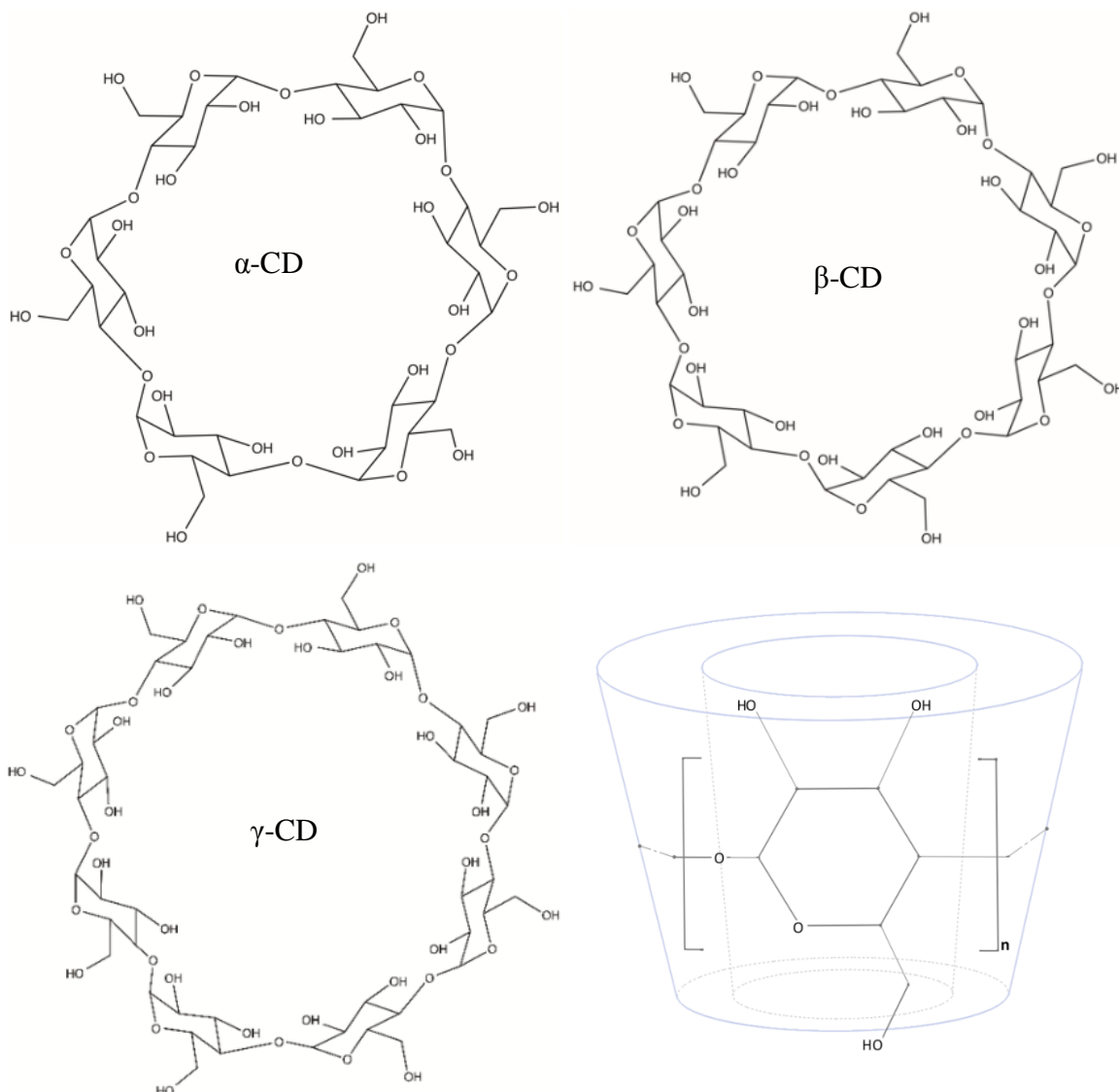
Figure 2-4: Molecular structure and toroidal shape of cyclodextrin molecules

Because they are natural and relatively non-toxic, have a low price and are commercially available, and possess the ability to form inclusion complexes with a wide range of guest molecules, CDs have been applied to many areas including but not limited to pharmaceutical,[97, 98] food,[40, 99] cosmetic,[100, 101] and textile industries.[102, 103] Their significance in pharmaceuticals alone is well evidenced by the increasing number of marketed or approved medicinal products containing CDs.[104] Furthermore, the functionalization of fibers with CD and/or its inclusion complexes leads to fibrous mats

with unique characteristics, potentially broadening the application areas of both cyclodextrins and nanofibers.[29]

2.4.2 Inclusion Complexes

Arguably the most interesting property of CDs is their ability to form inclusion complexes, a unique form of chemical complex, with a variety of solid, liquid, and gaseous guest molecules.[95] The formation of cyclodextrin inclusion complexes (CD:ICs) depends largely on the agreement between the dimensions of the cyclodextrin cavity and the guest molecule, with the guest molecule apparently striving to fill up the cyclodextrin cavity.[92, 105] If the guest is the wrong size, it will not fit properly into the cyclodextrin cavity.[95] Molecules of a very small size will not form stable complexes with cyclodextrins as they will slip out of the cavity. Moreover, molecules that are too large or bulky will also not form inclusion complexes with cyclodextrins. Nevertheless, if certain functional groups or side chains of the molecule can penetrate the CD cavity then partial complex formation is possible. Most frequently, complexes are formed at a 1:1 CD:guest ratio, although if a guest is too long to be completely enclosed by one CD cavity, multiple CDs can be threaded onto the guest creating 2:1, 3:1, etc. (CD:guest) ratios[92, 94] Furthermore, in the case of some low molecular weight molecules, more than one guest may fit into the cavity.[95] The mechanism of complex formation is depicted in **Figure 2-5** for CD:ICs formed at 1:1 and 2:1 CD:guest ratios. Due to the steric requirement of complexation, the different cyclodextrins show different capabilities to form inclusion complexes with the same guest molecules. The naturally occurring cyclodextrins have the same cavity depth (~7.8 Å), but the number of glucose units determines the internal diameter of the cavity and its volume: α-CD, β-CD, and γ-CD are roughly 6 Å, 7 Å, and 9 Å in diameter, respectively.[29, 41, 95, 106] Some properties and dimensions of CDs are shown in **Table 2-1**. The spatial requirements for inclusion complex formation can be compared to the "lock and key" mechanism of enzyme catalysis, where the substrate must be oriented properly with respect to the active centers of the enzyme.[106] Moreover, complex (CS) formation between the cyclodextrin (C) and guest (substrate, S) components occurs according to the following equation, and can be quantitatively described by the dissociation constant K_D.[92]

$$C+S \overset{K_D}{\leftrightarrow} C \cdot S \qquad\qquad (2\text{-}7)$$

$$K_D = \frac{[C] \cdot [S]}{[C \cdot S]} \qquad\qquad (2\text{-}8)$$

In solution, the process by which an inclusion complex is formed occurs according to a number of distinct steps.[94, 107] Initially, the guest approaches the CD molecule and the water structure breaks down, both inside the CD ring and around the guest, with the water molecules entering the bulk solution. Next, the interactions between the guest molecule and groups on the inner rim of the CD cavity are formed, including possibly hydrogen bonds. Finally, the water structure is reconstructed around the complex and any exposed parts of the guest. The thermodynamic interactions between the components of the system are favourable for complex formation, creating a positive energetic driving force that pulls the guest into the cyclodextrin cavity. Firstly, repulsive forces are decreased as the polar water molecules are displaced from the apolar cyclodextrin cavity to join the larger pool, and the number of hydrogen bonds formed increases. Secondly, there is a reduction in
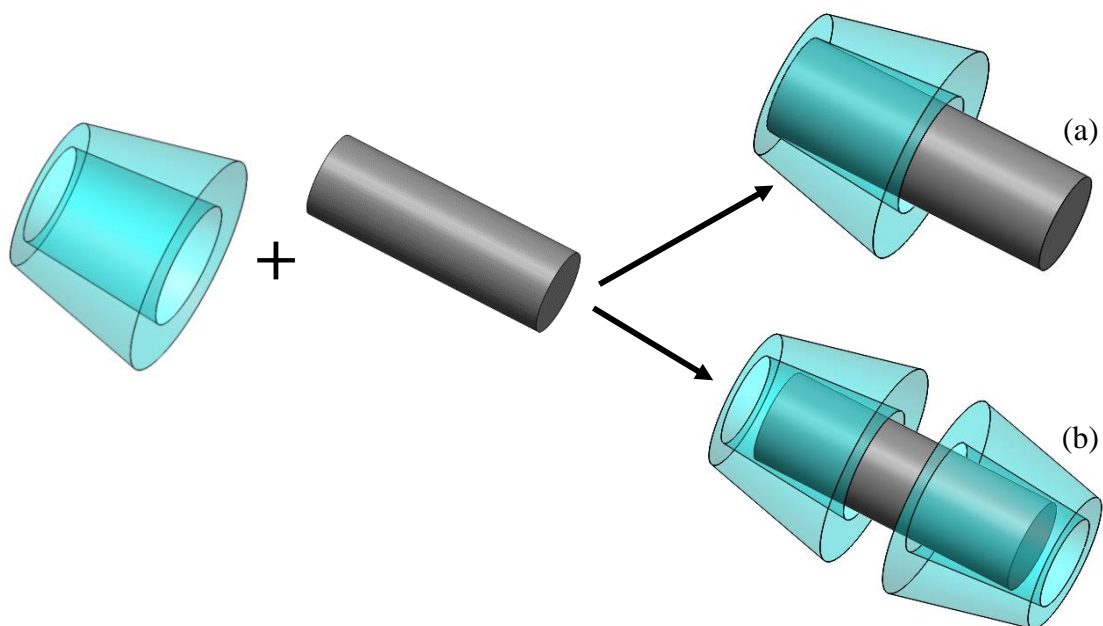
Figure 2-5: Inclusion complex formation between cyclodextrin host and a guest molecule (a) 1:1 CD:guest (b) 2:1 CD:guest

repulsive interactions between the hydrophobic guest molecule and the aqueous environment as it enters the cavity and increases the hydrophobic interactions.[95] These driving forces do not exist in the dry, crystalline state, thus, isolating a product in solid state is difficult.[88]

Table 2-1: Properties and dimensions of the naturally occurring cyclodextrins

| | Gluco-pyranose Units | Molecular Weight (g/mol) | Dimensions (Å) | | | | | Cavity Volume (Å^3) |
			a	b	c	d	e	
α	6	972.84	14.6	5.3	4.7	13.2	7.9	174
β	7	1134.98	15.4	6.5	6.0	14.9	7.9	262
γ	8	1297.12	17.5	8.3	7.5	16.1	7.9	427
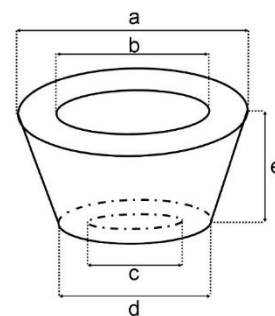
The inclusion complex is characterized by the absence of ordinary chemical bonds; the interactions between the guest molecule and surrounding cyclodextrin are non-covalent and generally weak. The interactions can be van der Waals, hydrophobic interactions, dispersion forces, hydrogen bonding, electrostatic interaction, and steric effects.[92, 105, 106, 108, 109] In general, van der Waals forces predominate and include both permanent induced-dipole-dipole interactions and London dispersion forces.[92, 94, 95] Once inside the cavity, the guest molecule may adjust its conformation in order to take maximum advantage of the weak van der Waals forces that exist.[95] Hydrophobic effects are involved because the guest molecule replaces the enthalpy-rich, energetically unfavoured water molecules present in the slightly apolar cyclodextrin cavity. If the complex is formed in solution, the liberated water molecules are taken up by the bulk water where they can form more hydrogen bonds than when contained in the cavity, and therefore gain degrees of freedom and contribute to the stability of the complex owing to the resulting increase in entropy.[92, 94] Moreover, this leads to a decrease of cyclodextrin ring strain, from the high energy conformation of the CD-water complex to the lower energy conformation of the CD-guest complex, and an apolar-apolar association, resulting in a more stable lower energy state overall.[94, 95] Depending on the guest molecule, the formation of hydrogen bonds with the CD hydroxyl

groups can be involved.[89, 94] The ion-dipole type of electrostatic interaction, between undistorted charge distributions of the two molecules, can take place in CD complexation because CDs are polar molecules, with modestly large dipole moments.[109]

Once a complex has been formed and dried, it is stable and exhibits a long shelf life when stored in dry conditions at or below ambient temperature.[95] Complex dissociation is typically driven by a large increase in the number of water molecules in the surrounding environment, frequently by dissolving a dried complex in water.[95] The resulting concentration gradient shifts the equilibrium in **Equation 2-7** to the left. Therefore, in highly dilute and dynamic systems, such as the body, once the guest dissociates it has difficulty finding another cyclodextrin to re-complex with and is left free in solution. For this reason, the guest availability in the body is not hampered by slow release, but in fact, it has been shown that the rates of formation/dissociation are close to diffusion controlled limits.[110] Moreover, complex dissociation can be triggered by an increase in temperature which weakens the complex.[92, 93] Because the normal body tissue temperature is roughly 37°C, the difference in temperature can contribute to guest dissociation *in vivo*.[93] Furthermore, if the guest is lipophilic and has access to tissue but not cyclodextrin, the tissue acts as a sink and causes dissociation of the complex based on simple mass action principles.[93]

Inherent in the formation of a cyclodextrin inclusion complex is the covering of the guest molecule either partially or entirely by cyclodextrin. This provides stabilization and protection of the guest from evaporation, degradation, oxidation, etc., as well as alters many of the physiochemical properties of the molecule.[41, 90] These physiochemical changes facilitate the use of characterization techniques to confirm that the guest is indeed contained within the cyclodextrin cavity. Cyclodextrin maintains some of its ability to form hydrogen bonds with other molecules enabling them to remain at least partially water soluble in the form of an inclusion complex.[105] In fact, the ability to enhance the aqueous solubility of highly insoluble drugs is one of the most studied applications of cyclodextrin inclusion complexes along with controlled and/or delayed release of the drug.[40, 41, 95]

Complexes can be formed via a variety of techniques, and the selection is dependent on the characteristic properties of each specific guest molecule and the equipment available. One of the most commonly utilized techniques in the laboratory is co-precipitation, where the guest is added to an aqueous solution of cyclodextrin with stirring. The inclusion complex either precipitates out immediately or upon slow cooling and/or evaporation. The collected precipitate may be washed, though this step is frequently detrimental to the complex. Although the co-precipitation method works for a variety of guest molecules, it is difficult to scale up due to the large quantity of water required. The main advantage is that complex formation is visible by the disappearance of the guest.[92, 93, 95, 105, 111] Slurry complexation involves less water than co-precipitation, suspending cyclodextrin at a 50-60% solids concentration. The aqueous phase becomes saturated with cyclodextrin in solution and, as guest molecules complex with the dissolved cyclodextrin, the complex will precipitate out of the aqueous phase. More cyclodextrin dissolves, continuing to saturate the aqueous phase, form the complex, and precipitate out of solution.[93, 95, 111] Using even less water, paste complexation involves adding a small amount of water to the cyclodextrin to form a paste. The guest is added and they are mixed using a device such as a mortar in pestle, or on a large scale using a kneader. This method is most suitable for industrial synthesis. The resulting complex can be dried directly and milled to obtain a powder if a hard mass is formed.[92, 93, 95, 105, 111] Dry complexation, on the other hand, does not involve the use of any water, the guest and cyclodextrin are simply mixed together. This method works best with oils or other liquid guests. There is a risk of the mixing not being sufficiently thorough, resulting in incomplete complexation.[93, 95, 111] Less frequently used methods include damp mixing and heating,[93, 95] extrusion,[93, 95] and layering.[92]

It is necessary to optimize the amount of water, degree and time of mixing, temperature and heating time for each specific guest and complexation technique. Heat can be used to increase the amount of CD dissolved, therefore increasing the probability of complexation, providing the guest can tolerate the increased temperature. Additionally, heat can also destabilize the complex, with most complexes beginning to decompose at 50-60 °C, though heat stability varies with differing guests and some can be highly thermally stable.[95] For this reason, if a solid complex is desired, care must be taken so as not to destroy the

complex with heat during the drying process. For extremely delicate complexes, a desiccator or freeze dryer may be used to dry the complexes in order to minimize the loss of the volatile guest.[95] Water is usually the preferred solvent for complexation techniques due to the solubility of cyclodextrin, and also because water is easily displaced from the cavity to make room for the guest molecule. However, not all guests are readily solubilized in water and as a result, complexation can be very slow or impossible. In these cases, an organic solvent can be used to dissolve the guest, but the solvent must not complex preferentially with the cyclodextrin or have increased affinity for the guest, and must be easily removed by evaporation.[93] Furthermore, the use of too much solvent can cause the guest to be so dilute that it does not come in contact with the cyclodextrin in a sufficient amount to facilitate complexation. Moreover, some guest molecules, such as high molecular weight oils, can preferentially associate with themselves rather than interact with cyclodextrin. To counter this, the amount of solvent is increased, accompanied by sufficient mixing in order to disperse and separate the guest molecules from each other.[95] Different complexation techniques, such as paste or dry mixing could be more efficient for these types of guest molecules.

Based on the complexation techniques, CD:ICs can exist in both solution and solid state, with their structures differing significantly in each state. In solution, the formation of inclusion complexes is not a fixed state but rather a dynamic equilibrium between complexed and non-complexed guest molecules where the guest molecule continuously associates and dissociates from the host.[90, 93, 95] The guest is contained within the cavity, and the entire complex is solvated by water molecules. On the other hand, in the crystal state the guest may not be included within the cyclodextrin cavity but rather be enclosed in a void space of a lattice or merely aggregate to the outside of the cyclodextrin, forming a microcrystalline or amorphous powder.[88, 90, 92] This arrangement can lead to the formation of nonstoichiometric inclusion complexes.[106] One of the benefits of preparing inclusion complexes in solution is that more cyclodextrin molecules become available for complexation whereas in the crystalline form only the surface molecules of the cyclodextrin crystal are available for complexation.[95]

2.5 Rationale and Objectives of Study

Scaffold-guided tissue engineering continues to emerge as a strategy for the repair and regeneration of diseased or damaged tissues and organs as an alternative to current therapies.[1] However, one of the major factors hindering the success of scaffold-guided tissue engineering is the inability to deliver sufficient oxygen to the growing constructs. Although numerous strategies have been developed to overcome this limitation, they have been riddled with drawbacks; thus delivering sufficient oxygen remains a fundamental consideration for fabricating engineered tissues.[51-53] One approach to improve oxygen delivery to constructs is the use of perfusion bioreactors whereby oxygen dissolved in the culture medium diffuses to the scaffold material. However, the flow rate required to maintain an adequate oxygen concentration for cell viability often surpasses the shear stress tolerance of cells.[56] Alternatively, perfluorocarbons have been extensively explored as oxygen carriers due to their high dissolving power for oxygen, though the focus has been on fabricating perfluorocarbon emulsions which lack stability and are overall user-unfriendly.[57] Moreover, the high density of the emulsions causes them to settle in the culture well or medium reservoir.[50]

By shifting the focus from PFC emulsions to alternative oxygen delivery strategies, some of the drawbacks of first generation approaches can be remedied. A promising strategy involves embedding oxygen generating compounds, such as calcium peroxide[58] or sodium percarbonate[60] which decompose in water to produce oxygen, directly into the tissue engineering scaffold. This approach has the advantage of providing oxygen throughout the construct, notably in the center which is difficult to reach by diffusion alone, but it is limited as the oxygen generating compound is eventually depleted. Tissue engineering scaffolds incorporating fluorinated porous zeolite particles provide an alternative to this approach whereby the embedded compound does not generate oxygen but enhances oxygen delivery using the principles of oxygen solubility in PFCs.[61]

Cyclodextrins, cyclic oligosaccharides, have a unique shape that enables them to include a wide range of guest molecules within their cavity forming an inclusion complex. In addition, they are natural and relatively non-toxic, making them suitable for biological

applications, and have a low price and are commercially available.[112] Because inclusion of a guest molecule within the cyclodextrin cavity provides stabilization, it may serve to overcome some of the shortcomings of PFC emulsions. Moreover, cyclodextrin inclusion complexes have been incorporated into three-dimensional scaffolds via electrospinning;[41, 42, 113] this immobilization of the CD:IC within the scaffold would impart enhanced oxygen delivery throughout the construct, and delay or prevent settling of the PCFs in the culture well or medium reservoir. Ultimately, the benefits of this approach would serve to enhance oxygen delivery to the cells seeded on the construct, potentially facilitating the development of thick constructs suitable for clinical applications.

It was hypothesized that cyclodextrin/perfluorocarbon inclusion complexes incorporated into three-dimensional tissue engineering scaffolds would enhance oxygen delivery to seeded cells. In view of the above rationale, the following objectives were formulated:

- Prepare and characterize (FTIR, TGA, XRD) an inclusion complex from cyclodextrin and a perfluorocarbon

- Fabricate a three-dimensional scaffold containing the cyclodextrin inclusion complex

- Evaluate the ability of the cyclodextrin inclusion complex to act as an oxygen carrier both on its own and when embedded in a scaffold

2.6 References

1.   Langer, R.; Vacanti, J. P., Tissue engineering. *Science* **1993,** 260, (5110), 920-6.

2.   L'Heureux, N.; Stoclet, J. C.; Auger, F. A.; Lagaud, G. J.; Germain, L.; Andriantsitohaina, R., A human tissue-engineered vascular media: a new model for pharmacological studies of contractile responses. *FASEB J* **2001,** 15, (2), 515-24.

3.   Katare, R. G.; Ando, M.; Kakinuma, Y.; Sato, T., Engineered heart tissue: a novel tool to study the ischemic changes of the heart in vitro. *PLoS One* **2010,** 5, (2), e9275.

4.   Hansen, A.; Eder, A.; Bönstrup, M.; Flato, M.; Mewe, M.; Schaaf, S.; Aksehirlioglu, B.; Schwoerer, A. P.; Schwörer, A.; Uebeler, J.; Eschenhagen, T., Development of a drug screening platform based on engineered heart tissue. *Circ Res* **2010,** 107, (1), 35-44.

5.   Laflamme, M. A.; Murry, C. E., Heart regeneration. *Nature* **2011,** 473, (7347), 326-35.

6.   Fisher, M. B.; Mauck, R. L., Tissue engineering and regenerative medicine: recent innovations and the transition to translation. *Tissue Eng Part B Rev* **2013,** 19, (1), 1-13.

7.   Gauvin, R.; Ahsan, T.; Larouche, D.; Lévesque, P.; Dubé, J.; Auger, F. A.; Nerem, R. M.; Germain, L., A novel single-step self-assembly approach for the fabrication of tissue-engineered vascular constructs. *Tissue Eng Part A* **2010,** 16, (5), 1737-47.

8.   L'Heureux, N.; Pâquet, S.; Labbé, R.; Germain, L.; Auger, F. A., A completely biological tissue-engineered human blood vessel. *FASEB J* **1998,** 12, (1), 47-56.

9.   Norotte, C.; Marga, F. S.; Niklason, L. E.; Forgacs, G., Scaffold-free vascular tissue engineering using bioprinting. *Biomaterials* **2009,** 30, (30), 5910-7.

10.   Niklason, L. E.; Gao, J.; Abbott, W. M.; Hirschi, K. K.; Houser, S.; Marini, R.; Langer, R., Functional arteries grown in vitro. *Science* **1999,** 284, (5413), 489-93.

11.   Engelmayr, G. C.; Cheng, M.; Bettinger, C. J.; Borenstein, J. T.; Langer, R.; Freed, L. E., Accordion-like honeycombs for tissue engineering of cardiac anisotropy. *Nat Mater* **2008,** 7, (12), 1003-10.

12.   Grenier, S.; Sandig, M.; Holdsworth, D. W.; Mequanint, K., Interactions of coronary artery smooth muscle cells with 3D porous polyurethane scaffolds. *J Biomed Mater Res A* **2009,** 89, (2), 293-303.

13.   Grenier, S.; Sandig, M.; Mequanint, K., Smooth muscle alpha-actin and calponin expression and extracellular matrix production of human coronary artery smooth muscle cells in 3D scaffolds. *Tissue Eng Part A* **2009,** 15, (10), 3001-11.

14.   Lee, K. W.; Stolz, D. B.; Wang, Y., Substantial expression of mature elastin in arterial constructs. *Proc Natl Acad Sci U S A* **2011,** 108, (7), 2705-10.

15.   Williamson, M. R.; Black, R.; Kielty, C., PCL-PU composite vascular scaffold production for vascular tissue engineering: attachment, proliferation and bioactivity of human vascular endothelial cells. *Biomaterials* **2006,** 27, (19), 3608-16.

16.   Cukierman, E.; Pankov, R.; Stevens, D. R.; Yamada, K. M., Taking cell-matrix adhesions to the third dimension. *Science* **2001,** 294, (5547), 1708-12.

17.   Dubey, G.; Mequanint, K., Conjugation of fibronectin onto three-dimensional porous scaffolds for vascular tissue engineering applications. *Acta Biomater* **2011,** 7, (3), 1114-25.

18.   Martin, T. A.; Caliari, S. R.; Williford, P. D.; Harley, B. A.; Bailey, R. C., The generation of biomolecular patterns in highly porous collagen-GAG scaffolds using direct photolithography. *Biomaterials* **2011,** 32, (16), 3949-57.

19.   Sanghvi, A. B.; Miller, K. P.; Belcher, A. M.; Schmidt, C. E., Biomaterials functionalization using a novel peptide that selectively binds to a conducting polymer. *Nat Mater* **2005,** 4, (6), 496-502.

20.   Weinberg, C. B.; Bell, E., A blood vessel model constructed from collagen and cultured vascular cells. *Science* **1986,** 231, (4736), 397-400.

21.   Hoemann, C. D.; Sun, J.; Légaré, A.; McKee, M. D.; Buschmann, M. D., Tissue engineering of cartilage using an injectable and adhesive chitosan-based cell-delivery vehicle. *Osteoarthritis Cartilage* **2005,** 13, (4), 318-29.

22.   Ramamurthi, A.; Vesely, I., Evaluation of the matrix-synthesis potential of crosslinked hyaluronan gels for tissue engineering of aortic heart valves. *Biomaterials* **2005,** 26, (9), 999-1010.

23.   Madurantakam, P. A.; Cost, C. P.; Simpson, D. G.; Bowlin, G. L., Science of nanofibrous scaffold fabrication: strategies for next generation tissue-engineering scaffolds. *Nanomedicine (Lond)* **2009,** 4, (2), 193-206.

24.   Hutmacher, D. W., Scaffold design and fabrication technologies for engineering tissues--state of the art and future perspectives. *J Biomater Sci Polym Ed* **2001,** 12, (1), 107-24.

25.   Peltola, S. M.; Melchels, F. P.; Grijpma, D. W.; Kellomäki, M., A review of rapid prototyping techniques for tissue engineering purposes. *Ann Med* **2008,** 40, (4), 268-80.

26.   Carletti, E.; Motta, A.; Migliaresi, C., Scaffolds for tissue engineering and 3D cell culture. *Methods Mol Biol* **2011,** 695, 17-39.

27.   Agarwal, S.; Wendorff, J. H.; Greiner, A., Progress in the field of electrospinning for tissue engineering applications. *Adv Mater* **2009,** 21, (32-33), 3343-51.

28.   Sill, T. J.; von Recum, H. A., Electrospinning: applications in drug delivery and tissue engineering. *Biomaterials* **2008,** 29, (13), 1989-2006.

29.   Uyar, T.; Nur, Y.; Hacaloglu, J.; Besenbacher, F., Electrospinning of functional poly(methyl methacrylate) nanofibers containing cyclodextrin-menthol inclusion complexes. *Nanotechnology* **2009,** 20, (12), 125703.

30.   Wang, S.; Bai, J.; Li, C.; Zhang, J., Functionalization of electrospun beta-cyclodextrin/polyacrylonitrile (PAN) with silver nanoparticles: Broad-spectrum antibacterial property. *Applied Surface Science* **2012,** 261, 499-503.

31.   Uyar, T.; Havelund, R.; Hacaloglu, J.; Zhou, X.; Besenbacher, F.; Kingshott, P., The formation and characterization of cyclodextrin functionalized polystyrene nanofibers produced by electrospinning. *Nanotechnology* **2009,** 20, (12), 125605.

32.   Doshi, J.; Reneker, D. H., Electrospinning process and applications of electrospun fibers. *Journal of Electrostatics* **1995,** 35, 151-160.

33.   Xie, J.; Li, X.; Xia, Y., Putting Electrospun Nanofibers to Work for Biomedical Research. *Macromol Rapid Commun* **2008,** 29, (22), 1775-1792.

34.   Bai, J.; Yang, Q.; Li, M.; Zhang, C.; Yiaoxian, L., Synthesis of poly(N-vinylpyrrolidone)/beta-cyclodextrin composite nanofibers using electrospinning techniques. *Journal of Materials Processing Technology* **2008,** 208, 251-254.

35.   Anandharamakrishnan, C., Electrospraying and Electrospinning Techniques for Nanoencapsulation. In *Techniques for Nanoencapsulation of Food Ingredients*, SpringerBriefs: 2014; Vol. Food, Health, and Nutrition, p 24.

36.   Pham, Q. P.; Sharma, U.; Mikos, A. G., Electrospinning of polymeric nanofibers for tissue engineering applications: a review. *Tissue Eng* **2006,** 12, (5), 1197-211.

37.   Akhyari, P.; Kamiya, H.; Haverich, A.; Karck, M.; Lichtenberg, A., Myocardial tissue engineering: the extracellular matrix. *Eur J Cardiothorac Surg* **2008,** 34, (2), 229-41.

38.   Shin, H.; Jo, S.; Mikos, A. G., Biomimetic materials for tissue engineering. *Biomaterials* **2003,** 24, (24), 4353-64.

39.   Celebioglu, A.; Uyar, T., Cyclodextrin nanofibers by electrospinning. *Chem Commun (Camb)* **2010,** 46, (37), 6903-5.

40.   Uyar, T.; Hacaloglu, J.; Besenbacher, F., Electrospun polystyrene fibers containing high temperature stable volatile fragrance/flavor facilitated by cyclodextrin inclusion complexes. *Reactive & Functional Polymers* **2009,** 69, 145-150.

41.   Kayaci, F.; Uyar, T., Encapsulation of vanillin/cyclodextrin inclusion complex in electrospun polyvinyl alcohol (PVA) nanowebs: Prolonged shelf-life and high temperature stability of vanillin. *Food Chemistry* **2012,** 133, 641-649.

42.   Uyar, T.; Havelund, R.; Hacaloglu, J.; Besenbacher, F.; Kingshott, P., Functional electrospun polystyrene nanofibers incorporating α-, β-, and γ-cyclodextrins: comparison of molecular filter performance. *ACS Nano* **2010,** 4, (9), 5121-30.

43.   Celebioglu, A.; Uyar, T., Electrospinning of polymer-free nanofibers from cyclodextrin inclusion complexes. *Langmuir* **2011,** 27, (10), 6218-26.

44.   Rappaport, C., Review-progress in concept and practice of growing anchorage-dependent mammalian cells in three dimension. *In Vitro Cell Dev Biol Anim* **2003,** 39, (5-6), 187-92.

45.   Seifu, D. G. Oxygen delivery strategies in tissue-engineered constructs. University of Western Ontario, Electronic Thesis and Dissertation Repository, 2012.

46.   Sutherland, R. M.; Sordat, B.; Bamat, J.; Gabbert, H.; Bourrat, B.; Mueller-Klieser, W., Oxygenation and differentiation in multicellular spheroids of human colon carcinoma. *Cancer Res* **1986,** 46, (10), 5320-9.

47.   Wendt, D.; Stroebel, S.; Jakob, M.; John, G. T.; Martin, I., Uniform tissues engineered by seeding and culturing cells in 3D scaffolds under perfusion at defined oxygen tensions. *Biorheology* **2006,** 43, (3-4), 481-8.

48.   Malda, J.; Klein, T. J.; Upton, Z., The roles of hypoxia in the in vitro engineering of tissues. *Tissue Eng* **2007,** 13, (9), 2153-62.

49.   Semenza, G. L., Life with oxygen. *Science* **2007,** 318, (5847), 62-4.

50.   Radisic, M.; Park, H.; Chen, F.; Salazar-Lazzaro, J. E.; Wang, Y.; Dennis, R.; Langer, R.; Freed, L. E.; Vunjak-Novakovic, G., Biomimetic approach to cardiac tissue engineering: oxygen carriers and channeled scaffolds. *Tissue Eng* **2006,** 12, (8), 2077-91.

51.   Malda, J.; Rouwkema, J.; Martens, D. E.; Le Comte, E. P.; Kooy, F. K.; Tramper, J.; van Blitterswijk, C. A.; Riesle, J., Oxygen gradients in tissue-engineered PEGT/PBT cartilaginous constructs: measurement and modeling. *Biotechnol Bioeng* **2004,** 86, (1), 9-18.

52.   Radisic, M.; Deen, W.; Langer, R.; Vunjak-Novakovic, G., Mathematical model of oxygen distribution in engineered cardiac tissue with parallel channel array perfused with culture medium containing oxygen carriers. *Am J Physiol Heart Circ Physiol* **2005,** 288, (3), H1278-89.

53.   Radisic, M.; Malda, J.; Epping, E.; Geng, W.; Langer, R.; Vunjak-Novakovic, G., Oxygen gradients correlate with cell density and cell viability in engineered cardiac tissue. *Biotechnol Bioeng* **2006,** 93, (2), 332-43.

54.   Malda, J.; Rouwkema, J.; Martens, D. E.; le Comte, E. P.; Kooy, F. K.; Tramper, J.; van Blitterswijk, C. A.; Riesle, J., Oxygen gradients in tissue-engineered PEGT/PBT cartilaginous constructs: Measurement and modeling. *Biotechnol Bioeng* **2004,** 86, (1), 9-18.

55.   Radisic, M.; Malda, J.; Epping, E.; Geng, W. L.; Langer, R.; Vunjak-Novakovic, G., Oxygen gradients correlate with cell density and cell viability in engineered cardiac tissue. *Biotechnol Bioeng* **2006,** 93, (2), 332-343.

56.   Yu, X.; Botchwey, E. A.; Levine, E. M.; Pollack, S. R.; Laurencin, C. T., Bioreactor-based bone tissue engineering: the influence of dynamic flow on osteoblast phenotypic expression and matrix mineralization. *Proc Natl Acad Sci U S A* **2004,** 101, (31), 11203-8.

57.   Riess, J. G., Highly fluorinated systems for oxygen transport, diagnosis and drug delivery. *Colloids Surf., A* **1994,** 84, 33-48.

58.   Oh, S. H.; Ward, C. L.; Atala, A.; Yoo, J. J.; Harrison, B. S., Oxygen generating scaffolds for enhancing engineered tissue survival. *Biomaterials* **2009,** 30, (5), 757-62.

59.   Wang, J.; Zhu, Y.; Bawa, H. K.; Ng, G.; Wu, Y.; Libera, M.; van der Mei, H. C.; Busscher, H. J.; Yu, X., Oxygen-generating nanofiber cell scaffolds with antimicrobial properties. *ACS Appl Mater Interfaces* **2011,** 3, (1), 67-73.

60.   Harrison, B. S.; Eberli, D.; Lee, S. J.; Atala, A.; Yoo, J. J., Oxygen producing biomaterials for tissue regeneration. *Biomaterials* **2007,** 28, (31), 4628-34.

61.   Seifu, D. G.; Isimjan, T. T.; Mequanint, K., Tissue engineering scaffolds containing embedded fluorinated-zeolite oxygen vectors. *Acta Biomater* **2011,** 7, (10), 3670-8.

62.   Pedraza, E.; Coronel, M. M.; Fraker, C. A.; Ricordi, C.; Stabler, C. L., Preventing hypoxia-induced cell death in beta cells and islets via hydrolytically activated, oxygen-generating biomaterials. *Proc Natl Acad Sci U S A* **2012,** 109, (11), 4245-50.

63.   Skiba, M.; Skiba-Lahiani, M.; Arnaud, P., Design of nanocapsules based on novel fluorophilic cyclodextrin derivatives and their potential role in oxygen delivery. *Journal of Inclusion Phenomena and Macrocyclic Chemistry* **2002,** 44, 151-154.

64.   Finkenzeller, G.; Torio-Padron, N.; Momeni, A.; Mehlhorn, A. T.; Stark, G. B., In vitro angiogenesis properties of endothelial progenitor cells: a promising tool for vascularization of ex vivo engineered tissues. *Tissue Eng* **2007,** 13, (7), 1413-20.

65.   Levenberg, S.; Rouwkema, J.; Macdonald, M.; Garfein, E. S.; Kohane, D. S.; Darland, D. C.; Marini, R.; van Blitterswijk, C. A.; Mulligan, R. C.; D'Amore, P. A.; Langer, R., Engineering vascularized skeletal muscle tissue. *Nat Biotechnol* **2005,** 23, (7), 879-84.

66.   Bach, A. D.; Arkudas, A.; Tjiawi, J.; Polykandriotis, E.; Kneser, U.; Horch, R. E.; Beier, J. P., A new approach to tissue engineering of vascularized skeletal muscle. *J Cell Mol Med* **2006,** 10, (3), 716-26.

67.   Asakawa, N.; Shimizu, T.; Tsuda, Y.; Sekiya, S.; Sasagawa, T.; Yamato, M.; Fukai, F.; Okano, T., Pre-vascularization of in vitro three-dimensional tissues created by cell sheet engineering. *Biomaterials* **2010,** 31, (14), 3903-9.

68.   Riess, J. G., Oxygen carriers ("blood substitutes")--raison d'etre, chemistry, and some physiology. *Chem Rev* **2001,** 101, (9), 2797-920.

69.   Finucane, M. L.; Slovic, P.; Mertz, C. K., Public perception of the risk of blood transfusion. *Transfusion* **2000,** 40, (8), 1017-22.

70.   Lowe, K. C., Engineering blood: synthetic substitutes from fluorinated compounds. *Tissue Eng* **2003,** 9, (3), 389-99.

71.   Jahr, J. S.; Akha, A. S.; Holtby, R. J., Crosslinked, polymerized, and PEG-conjugated hemoglobin-based oxygen carriers: Clinical safety and efficacy of recent and current products. *Curr Drug Discov Technol* **2011**.

72.   Zuckerman, S. H.; Doyle, M. P.; Gorczynski, R.; Rosenthal, G. J., Preclinical biology of recombinant human hemoglobin, rHb1.1. *Artif Cells Blood Substit Immobil Biotechnol* **1998,** 26, (3), 231-57.

73.   Lowe, K. C., Perfluorinated blood substitutes and artificial oxygen carriers. *Blood Rev* **1999,** 13, (3), 171-84.

74.   Keipert, P. E., Perflubron emulsion (Oxygent(tm)): a temporary intravenous oxygen carrier. *Anasthesiol Intensivmed Notfallmed Schmerzther* **2001,** 36 Suppl 2, S104-6.

75.   Lowe, K. C., Perfluorochemical respiratory gas carriers: applications in medicine and biotechnology. *Sci Prog* **1997,** 80 (Pt 2), 169-93.

76.   Riess, J. G., Understanding the fundamentals of perfluorocarbons and perfluorocarbon emulsions relevant to in vivo oxygen delivery. *Artif Cells Blood Substit Immobil Biotechnol* **2005,** 33, (1), 47-63.

77.   Lowe, K. C., Fluorinated blood substitutes and oxygen carriers. *J. Fluorine Chem.* **2001,** 109, (1), 59-65.

78.   Riess, J. G., Perfluorocarbon-based oxygen delivery. *Artif Cells Blood Substit Immobil Biotechnol* **2006,** 34, (6), 567-80.

79.   Castro, C. I.; Briceno, J. C., Perfluorocarbon-based oxygen carriers: review of products and trials. *Artif Organs* **2010,** 34, (8), 622-34.

80.   Krafft, M. P., Fluorocarbons and fluorinated amphiphiles in drug delivery and biomedical research. *Adv Drug Deliv Rev* **2001,** 47, (2-3), 209-28.

81.   Lowe, K. C., Perfluorochemical respiratory gas carriers: Benefits to cell culture systems. *Journal of Fluorine Chemistry* **2002,** 118, 19-26.

82.   Pilarek, M.; Brand, E.; Hillig, F.; Krause, M.; Neubauer, P., Enhanced plasmid production in miniaturized high-cell-density cultures of Escherichia coli supported with perfluorinated oxygen carrier. *Bioprocess Biosyst Eng* **2013,** 36, (8), 1079-86.

83.   Clark, L. C.; Gollan, F., Survival of mammals breathing organic liquids equilibrated with oxygen at atmospheric pressure. *Science* **1966,** 152, (3730), 1755-6.

84.   Sloviter, H. A.; Kamimoto, T., Erythrocyte substitute for perfusion of brain. *Nature* **1967,** 216, (5114), 458-60.

85.   Lowe, K. C.; Davey, M. R.; Power, J. B., Perfluorochemicals: their applications and benefits to cell culture. *Trends Biotechnol* **1998,** 16, (6), 272-7.

86.   King, A. T.; Mulligan, B. J.; Lowe, K. C., Perfluorochemicals and cell culture. *Nature Biotechnology* **1989,** 7, 1037-1042.

87.   Tan, Q.; El-Badry, A. M.; Contaldo, C.; Steiner, R.; Hillinger, S.; Welti, M.; Hilbe, M.; Spahn, D. R.; Jaussi, R.; Higuera, G.; van Blitterswijk, C. A.; Luo, Q.; Weder, W., The effect of perfluorocarbon-based artificial oxygen carriers on tissue-engineered trachea. *Tissue Eng Part A* **2009,** 15, (9), 2471-80.

88.   Szejtli, J., Introduction and General Overview of Cyclodextrin Chemistry. *Chem Rev* **1998,** 98, (5), 1743-1754.

89.   van de Manakker, F.; Vermonden, T.; van Nostrum, C. F.; Hennink, W. E., Cyclodextrin-based polymeric materials: synthesis, properties, and pharmaceutical/biomedical applications. *Biomacromolecules* **2009,** 10, (12), 3157-75.

90.   Singh, R.; Bharti, N.; Jyotsana, M.; Hiremath, S. N., Characterization of cyclodextrin inclusion complexes - A review. *Journal of Pharmaceutical Science and Technology* **2010,** 2, (3), 171-183.

91.   Saenger, W.; Jacob, J.; Gessler, K.; Steiner, T.; Hoffmann, D.; Sanbe, H.; Koizumi, K.; Smith, S. M.; Takaha, T., Structures of the Common Cyclodextrins and Their Larger Analogues-Beyond the Doughnut. *Chem Rev* **1998,** 98, (5), 1787-1802.

92.   Saenger, W., Cyclodextrin inclusion compounds in research and industry. *Angewandte Chemie International Edition* **1980,** 19, 344-362.

93.   Shimpi, S.; Chauhan, B.; Shimpi, P., Cyclodextrins: application in different routes of drug administration. *Acta Pharm* **2005,** 55, (2), 139-56.

94.   Bekers, O.; Uijtendaal, E. V.; Beijnen, J. H.; Bult, A.; Underberg, W. J. M., Cyclodextrins in the pharmaceutical field. *Drug Development and Industrial Pharmacy* **1991,** 17, (11), 1503-1549.

95.   Del Valle, E. M. M., Cyclodextrins and their uses: a review. *Process Biochemistry* **2004,** 39, 1033-1046.

96.   Bilensoy, E.; Hincal, A. A., Recent advances and future directions in amphiphilic cyclodextrin nanoparticles. *Expert Opin Drug Deliv* **2009,** 6, (11), 1161-73.

97.   Rocks, N.; Bekaert, S.; Coia, I.; Paulissen, G.; Gueders, M.; Evrard, B.; Van Heugen, J. C.; Chiap, P.; Foidart, J. M.; Noel, A.; Cataldo, D., Curcumin-cyclodextrin complexes potentiate gemcitabine effects in an orthotopic mouse model of lung cancer. *Br J Cancer* **2012,** 107, (7), 1083-92.

98.   He, H.; Chen, S.; Zhou, J.; Dou, Y.; Song, L.; Che, L.; Zhou, X.; Chen, X.; Jia, Y.; Zhang, J.; Li, S.; Li, X., Cyclodextrin-derived pH-responsive nanoparticles for delivery of paclitaxel. *Biomaterials* **2013,** 34, (21), 5344-58.

99.   Zhu, G.; Xiao, Z.; Zhou, R.; Zhu, Y., Study of production and pyrolysis characteristics of sweet orange flavor-β-cyclodextrin inclusion complex. *Carbohydr Polym* **2014,** 105, 75-80.

100.   Kfoury, M.; Auezova, L.; Fourmentin, M.; Greiges-Gerges, H., Investigation of monoterpenes complexation with hydroxypropyl-beta-cyclodextrin. *J. Incl. Phenom. Macrocycl. Chem.* **2014**.

101.   Pellegrini, M.; De Orsi, D.; Guarino, C.; Rotolo, M. C.; di Giovannandrea, R.; Pacifici, R.; Pichini, S., Ultra-performance liquid chromatography tandem mass spectrometry measurement of caffeine in caffeine-laced pants and in urine and skin of a pants user. *Cosmetics* **2014,** 1, (2), 82-93.

102.   Abdel-Halim, E. S.; Al-Deyab, S. S.; Alfaifi, A. Y., Cotton fabric finished with β-cyclodextrin: Inclusion ability toward antimicrobial agent. *Carbohydr Polym* **2014,** 102, 550-6.

103.   Hebeish, A.; El-Shafei, A.; Sharaf, S.; Zaghloul, S., In situ formation of silver nanoparticles for multifunctional cotton containing cyclodextrin. *Carbohydr Polym* **2014,** 103, 442-7.

104.   Giordano, F.; Novak, C.; Moyano, J. R., Thermal analysis of cyclodextrins and their inclusion compounds. *Thermochimica Acta* **2001,** 380, 123-151.

105.   Khan, N. A.; Durakshan, M., Cyclodextrin: An Overview. *International Journal of Bioassays* **2013,** 2, (6), 858-865.

106.   Frank, S. G., Inclusion compounds. *J Pharm Sci* **1975,** 64, (10), 1585-604.

107.   Cramer, F.; Saenger, W.; Spatz, H.-C., Inclusion Compounds. The Formation of Inclusion Compounds of Alpha-Cyclodextrin in Aqueous Solutions. Thermodynamics and Kinetic. *J. Am. Chem. Soc.* **1967,** 89, (1), 14-20.

108.   Rekharsky, M. V.; Inoue, Y., Complexation Thermodynamics of Cyclodextrins. *Chem Rev* **1998,** 98, (5), 1875-1918.

109.   Liu, L.; Guo, Q.-X., The driving forces in the inclusion complexation of cyclodextrins. *Journal of Inclusion Phenomena and Macrocyclic Chemistry* **2002,** 42, 1-14.

110.   Loftsson, T.; Duchêne, D., Cyclodextrins and their pharmaceutical applications. *Int J Pharm* **2007,** 329, (1-2), 1-11.

111.   Hedges, A. R., Industrial applications of cyclodextrins. *Chem. Rev.* **1998,** 98, 2035-2044.

112.   Lo Nostro, P.; Santoni, I.; Bonini, M.; Baglioni, P., Inclusion compound from a semifluorinated alkane and beta-cyclodextrin. *Langmuir* **2003,** 19, 2313-2317.

113.   Canbolat, M. F.; Celebioglu, A.; Uyar, T., Drug delivery system based on cyclodextrin-naproxen inclusion complex incorporated in electrospun polycaprolactone nanofibers. *Colloids Surf B Biointerfaces* **2013,** 115C, 15-21.

3 PREPARATION AND CHARACTERIZATION OF CYCLODEXTRIN INCLUSION COMPLEXES WITH PERFLUOROPERHYDROPHENANTHRENE

Overview: This chapter discusses the preparation of a cyclodextrin inclusion complex from alpha-cyclodextrin and perfluoroperhydrophenanthrene. A number of different complexation techniques were employed and the products were characterized by Fourier transform infrared spectroscopy, thermogravimetric analysis, and X-ray diffraction. Following analysis, the most effective preparation technique was identified for application as an oxygen carrier for tissue engineering.

Keywords: cyclodextrin, inclusion complex, perfluorocarbon

3.1 Introduction

Cyclodextrins are cyclic oligosaccharides with a unique toroidal shape which allows them to accommodate a variety of guest molecules within their cavity, forming non-covalent host-guest systems known as inclusion complexes. Cyclodextrins are natural and relatively non-toxic materials, making them suitable for biological applications, they have a low price, and are commercially available.[1] Perfluorocarbons are organic molecules where the carbon network is surrounded entirely by fluorine atoms and they have the ability to dissolve large quantities of non-polar gases such as oxygen. Perfluorocarbons have been extensively explored as oxygen carriers to enhance the delivery of oxygen to cells in scaffold-guided tissue engineering applications. However, previous approaches involving PFCs have focused on fabricating PFC emulsions which lack stability and are not overall user-friendly.[2] Moreover, the high density of the emulsions causes them to settle in the culture well or medium reservoir.[3] This study explores the preparation and characterization of a cyclodextrin inclusion complex with a perfluorocarbon as a novel oxygen carrier for application in tissue engineering. Because inclusion of a guest molecule within the cyclodextrin cavity can provide stabilization, it may serve to overcome some of the shortcomings of PFC emulsions. Moreover, cyclodextrin inclusion complexes have been

incorporated into 3D scaffolds via electrospinning;[4-6] this immobilization of the CD:IC within the scaffold would impart enhanced oxygen delivery throughout the construct, and delay or prevent settling of the PCFs in the culture well or medium reservoir.

Table 3-1: Comparison of the dimensions of potential cyclodextrin host molecules to those of perfluorocarbon guest molecules. Sizes of guest molecules are approximated from a computer simulation.

Cyclodextrin	Cavity Diameter (Å)	Cavity Height (Å)
α-CD	4.7-5.3	7.9
β-CD	6.0-6.5	7.9
γ-CD	7.5-8.3	7.9
Guest Molecule	Diameter (Å)	Height (Å)
PFD	3	6-7
PFP	5	11-12

The formation of a cyclodextrin inclusion complex depends largely on the agreement between the dimensions of the cyclodextrin cavity and the guest molecule. **Table 3-1** shows the dimensions of the cyclodextrins and the guest molecules considered in this study. Perfluorodecalin (PFD) and perfluoroperhydrophenanthrene (PFP) were the PFC guest molecules considered in this study and their molecular structures are shown in **Figure 3-1**. PFD dissolves a high level of oxygen (100 mL of PFD dissolves roughly 40 mL of O_2 at 37 °C) and has a longer tissue retention time than the most widely used perflubron which suggests potential for clinical application.[7] Furthermore, the feasibility of PFD as an oxygen carrier has been studied previously in our lab with promising results.[8,9] PFP, on the other hand, has been used as a perfluorinated, high molecular weight high boiling point oil additive to help prevent instability and retard phase separation in emulsions of PFD.[10,11] From **Table 3-1**, it is clear that the best match of host and guest dimensions is between α-CD and PFP, with the 5 Å diameter PFC able to fit snugly inside the α-CD cavity. For this reason, PFP and α-CD were the components used to prepare the inclusion complex in this study. In fact, consistent with the internal cavity diameter, Druliner and Wasserman[12] reported that among a group of perfluoroalkanes studied, PFP was the only case in which any evidence of inclusion complex formation with α-CD was found. It should be noticed that considering that the depth of the CD cavity is roughly 8 Å, it is possible that two CD

rings can be threaded onto a single chain of the PFP.[1] Therefore, both 1:1 and 2:1 α-CD:PFP molar ratios were explored in the methodology.

Complexes can be formed via numerous techniques, and the selection is dependent on the characteristic properties of the specific guest molecule and the equipment available.[13] Three complexation techniques were tested for optimal results in the preparation of the PFP/α-CD complexes: co-precipitation, paste mixing, and dry mixing, as reviewed in Section 2.4.2. When the cyclodextrin covers the guest molecule, either partially or entirely, it provides stabilization and protection, and alters many of the physiochemical properties of the guest.[5, 14] These physiochemical changes are the basis for the characterization techniques used to confirm that the guest is indeed contained within the cyclodextrin cavity.
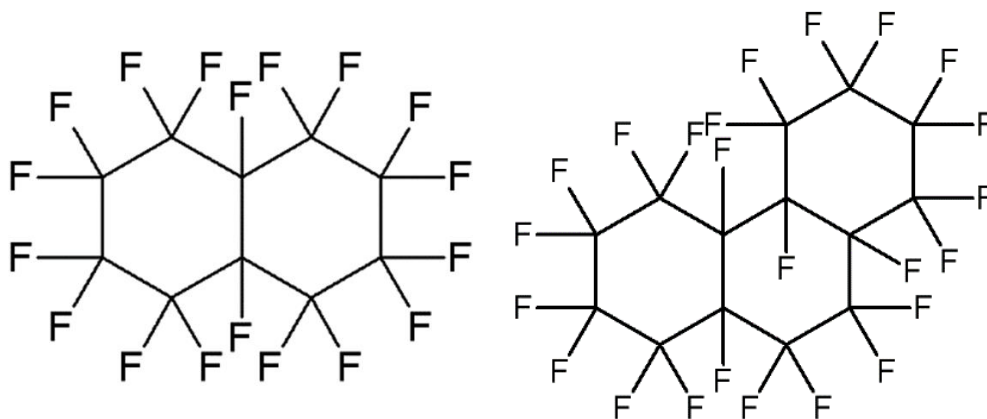
Figure 3-1: Molecular structure of perfluorodecalin (PFD, left) and perfluoroperhydrophenanthrene (PFP, right)

3.2 Materials

Perfluoroperhydrophenanthrene ($C_{14}F_{24}$) was obtained as a mixture of isomers (83 % purity) from Alfa Aesar (Ward Hill, MA). Perfluorodecalin ($C_{10}F_{18}$) was obtained as a mixture of cis and trans isomers (99.9 % purity) from Sigma Aldrich (Milwaukee, WI) Alpha-cyclodextrin (α-CD, 100 % purity) and beta-cyclodextrin (β-CD, 10.8 % moisture) were obtained commercially from Alfa Aesar. Solvents were purchased from Caledon Labs

(Georgetown, ON). All other chemicals were purchased from Sigma Aldrich. Unless noted otherwise, all chemicals were used as received without any further modification.

3.3 Methods

3.3.1 Preliminary Studies

Initial complexation studies were carried out using PFD as the guest molecule with both α-CD and β-CD as hosts. The co-precipitation technique was carried out at both a 1:1 and 2:1 CD:PFD molar ratio.

Alpha- or beta-cyclodextrin was added to de-ionized (d.i.) water to create a saturated aqueous solution. Weighed amounts of PFD were added to the α-CD solution at a ratio of 1:1 or 2:1 CD to PFC. The solution was stirred continuously and vigorously (1000 rpm) at room temperature (RT) in a sealed vial. After 72 hours of mixing, the solvent (water) was evaporated over 2-3 days in an open system in order to obtain a solid product. The solid product was dried and stored in a desiccator with potassium hydroxide used as a desiccant.

3.3.2 Preparation of Cyclodextrin Inclusion Complexes with Perfluoroperhydrophenanthrene

Throughout this chapter, α-CD is referred to as the "host" and PFP is referred to as the "guest". Three complexation techniques were studied to obtain an inclusion complex between α-CD and PFP: co-precipitation, paste mixing, and dry mixing. All complexation techniques were carried out at both 1:1 and 2:1 molar ratios of α-CD to PFP (host to guest). Following complexation the product was not washed because the washing process is often detrimental to the complex.

3.3.2.1 Co-precipitation

The solid α-CD/PFP complexes were prepared using a co-precipitation method modified from a previously reported method also utilizing a PFC.[15] Heating can be used to increase the amount of CD dissolved, thus increasing the probability of complexation. Therefore, in addition to RT, co-precipitation was carried out at the mild temperature of 40 °C, as most

complexes begin to decompose at 50-60 °C.[16] The amount of solvent required was minimized, to prevent the guest molecule from becoming too dilute that it does not come in contact with the CD in sufficient amounts to facilitate complexation. Moreover, because the guest molecule is a high molecular weight fluorocarbon, it may preferentially associate with itself as opposed to interact with the CD, so a vigorous amount of stirring was utilized in order to disperse and separate the guest molecules from each other.[16]

Alpha-cyclodextrin was added to d.i. water to create a saturated aqueous solution. Weighed amounts of PFP were added to the α-CD solution at a ratio of 1:1 or 2:1 α-CD to PFP. The solution was stirred continuously at 1000 rpm at either RT or 40 °C in a sealed vial. After 72 hours of stirring, the solvent (water) was evaporated over 2-3 days in an open system at RT in order to obtain a solid product. The solid product was dried and stored in a desiccator with potassium hydroxide used as a desiccant.

3.3.2.2 Paste Mixing

Weighed amounts of α-CD and a minimal amount of d.i. water were combined to form a paste. Weighed amounts of PFP were added to the α-CD paste at a 1:1 or 2:1 α-CD to PFP molar ratio. The paste was thoroughly mixed using a ceramic mortar and pestle for ten minutes. The product was collected in a glass vial, dried and stored in a desiccator with potassium hydroxide used as a desiccant.

3.3.2.3 Dry Mixing

Weighed amounts of α-CD and PFP were combined at a 1:1 or 2:1 α-CD to PFP molar ratio. The dry mixture was thoroughly mixed with a ceramic mortar and pestle for ten minutes. The solid product was collected and stored in a desiccator with potassium hydroxide used as a desiccant.

3.3.3   Fourier Transform Infrared Spectroscopy

The products obtained in the preliminary studies were characterized by Fourier transform infrared (FTIR) spectrometry using a Bruker Vector 22 (Bruker Optics, Billerica, MA)

equipped with a MIRacle Attenuated Total Reflectance (ATR) diamond crystal plate sample cell (PIKE Technologies, Madison, WI). In the follow-up studies, FTIR characterization of the α-CD/PFP complexes was carried out on a Bruker Tensor 27 spectrometer equipped with an ATR attachment using a ZnSe crystal.

In all cases, the samples were run as fine powders or a liquid (in the case of PFP) for 32 scans with a resolution of 4 cm^{-1} over the scan range 600 to 4000 cm^{-1}. All spectra were collected and processed with the OPUS software version 6.5. Absorption frequencies are reported in wavenumbers (cm^{-1}).

3.3.4 Thermogravimetric Analysis

Thermogravimetric analysis (TGA) was performed using an SDT Q600 Thermal Analyzer (TA Instruments, USA). Experiments were performed under nitrogen at a heating rate of 10 °C/min up to 600 °C. The real time weight loss as a function of temperature was recorded during the experiment using the Universal Analysis 2000 data acquisition system.

3.3.5 X-ray Diffraction

X-ray diffraction (XRD) spectra were collected with a Rigaku Ultima IV X-ray Diffraction Generator (Rigaku, Japan). The patterns were measured in the continuous mode, applying a CuKα X-ray source at a range of $2\theta = 2 - 60°$ with a scan rate of 2 °/min. The applied voltage and current were set to 40 kV and 40 mA, respectively.

3.4 Results

3.4.1 Preliminary Studies

Preliminary studies were carried out with PFD as the guest molecule for inclusion complexation with cyclodextrin. PFD was readily available and had been used previously in our lab as an oxygen carrier with promising results.[8, 9] The products of the co-precipitation complexation technique between both α- and β-CD and PFD were analyzed with FTIR spectroscopy. The FTIR spectra are shown in **Figure 3-2** and **Figure 3-3** for α-CD and β-CD, respectively. The FTIR spectra of the products are compared to those of the

native CDs and as-received PFD. Peaks characteristic of the PFD guest are not evident in the FTIR spectra of the products. In fact, the spectra of the products are virtually identical to those of the respective parent CDs. Therefore, there is a lack of evidence of complexation with PFD in the FTIR spectra for either α-CD or β-CD. It is likely that an inclusion complex did not form between these specific host and guest molecules because of an unsuitable match between the dimensions of PFD and the CD cavity. The diameter of PFD is much smaller than the width of both the α- and β-CD cavity. Molecules of a very small size do not form stable complexes with cyclodextrins as they slip out of the cavity. As demonstrated in **Table 3-1**, the best match of host and guest dimensions is between α-CD and PFP. As such, the focus of further studies was complexation between α-CD and PFP. Furthermore, the number of complexation techniques explored was expanded in order to test for optimal results of complexation between α-CD and PFP.

Furthermore, the complexes were initially dried in a vacuum oven at RT. However, it became apparent that this procedure likely compromised the product because most complexes start to decompose at 50-60°C.[16] Thus, the procedure was altered and the complexes were dried in a desiccator as suggested in the literature for extremely delicate complexes in order to minimize the loss of the guest.[16]
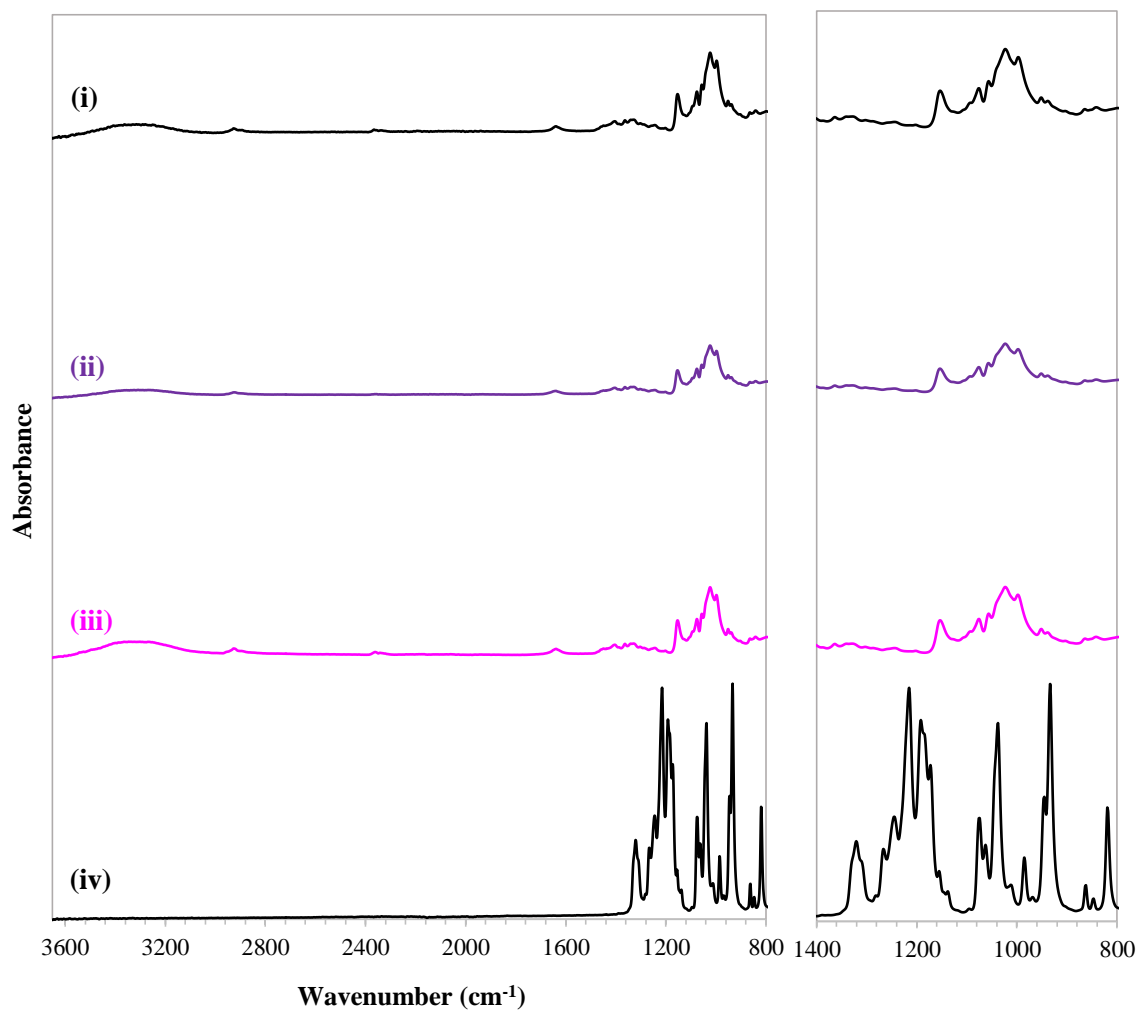
Figure 3-2: FTIR spectra of (i) unmodified α-CD, products of RT co-precipitation at a (ii) 2:1 and (iii) 1:1 molar ratio, and (iv) as-received PFD
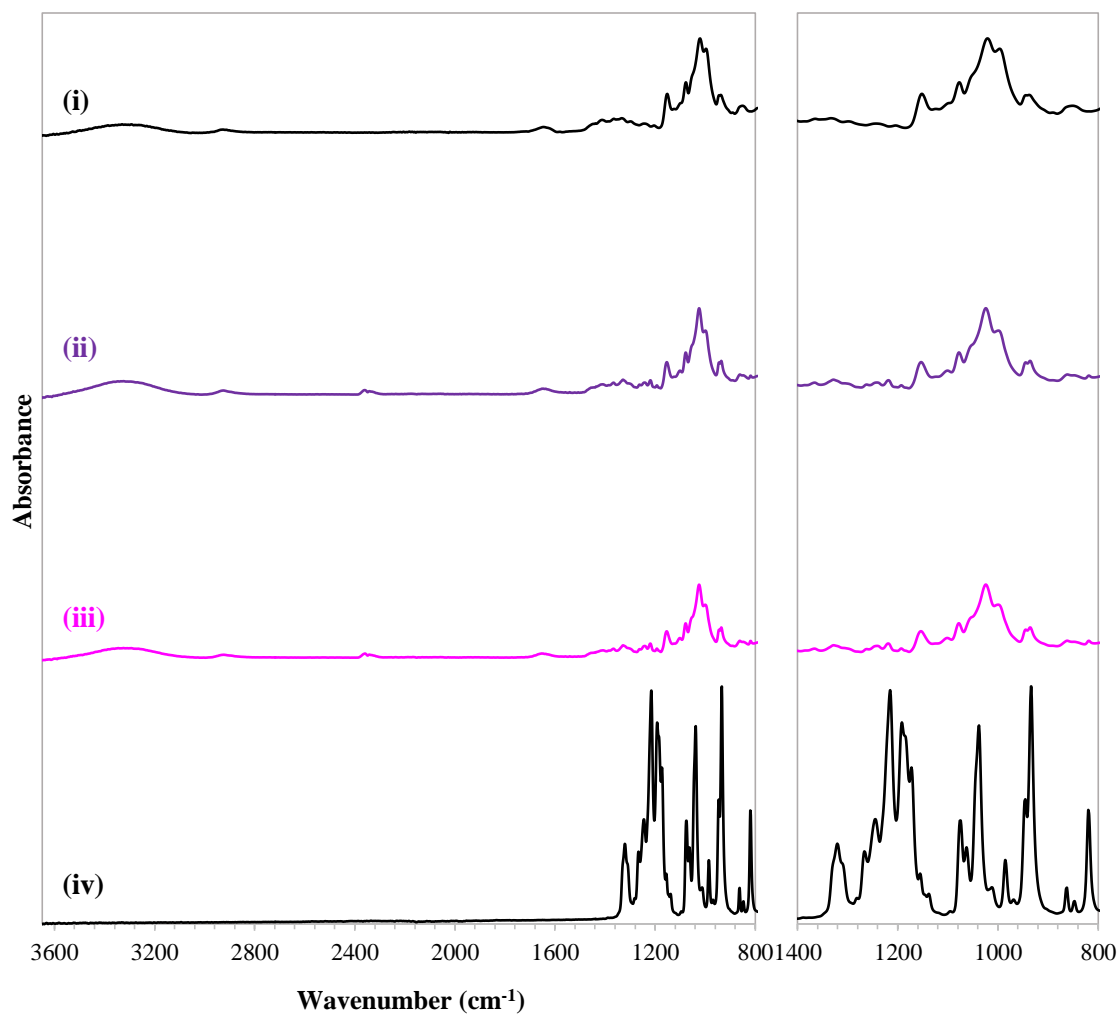
Figure 3-3: FTIR spectra of (i) unmodified β-CD, products of RT co-precipitation at a (ii) 2:1 and (iii) 1:1 molar ratio, and (iv) as-received PFD

3.4.2   Fourier Transform Infrared Spectroscopy

FTIR spectroscopy was carried out on the products obtained from each of the complexation techniques: co-precipitation, paste mixing, and dry mixing. FTIR spectroscopic techniques are not generally suitable for conclusively confirming the formation of an inclusion complex because there are only slight shifts and changes upon complexation.[17] There are interferences in the spectra from the cyclodextrin, and some of the changes are very subtle, requiring careful interpretation of the spectrum.[13] Moreover, if the fraction of the guest molecule included within the cyclodextrin cavity is less than 25 %, the bands which could be assigned to the guest molecule can be masked by the bands of the cyclodextrin and the water of crystallization.[14, 17, 18] Nevertheless, changes in the fingerprint region (below 1300 cm^{-1}) can confirm that the products are different from each parent molecule as they possess new spectroscopic signals. Thus, FTIR was used in this study as an initial characterization technique because it is both inexpensive and readily available. The slight changes in the spectra of the products were used to identify the complexation techniques that were most effective.

The various complexation techniques utilized in this study were carried out at both 1:1 and 2:1 host to guest (α-CD:PFP) molar ratios; the FTIR spectra for these products are shown in **Figure 3-4** and **Figure 3-5**, respectively. The FTIR spectra of the products are compared to those of the native α-CD, as-received PFP, and 1:1 or 2:1 physical mixtures of the two parent molecules. The spectrum for the unmodified α-CD shows peaks at 1024 and 1076 cm^{-1} corresponding to coupled C-C/C-O stretching vibrations, and at 1153 cm^{-1} corresponding to the anti-symmetric stretching vibration of the C-O-C glucosidic bridge, in agreement with the literature.[19, 20] Furthermore, a broad band at roughly 3300 cm^{-1} is attributed to the symmetric and anti-symmetric OH stretching, and a peak at roughly 2900 cm^{-1} is attributed to C-H vibrations.[21, 22] When complex formation occurs, there is frequently a slight shift in the hydroxyl band which is usually ascribed to hydrogen bonding or other intermolecular interactions between the CD and guest molecule.[23, 24]
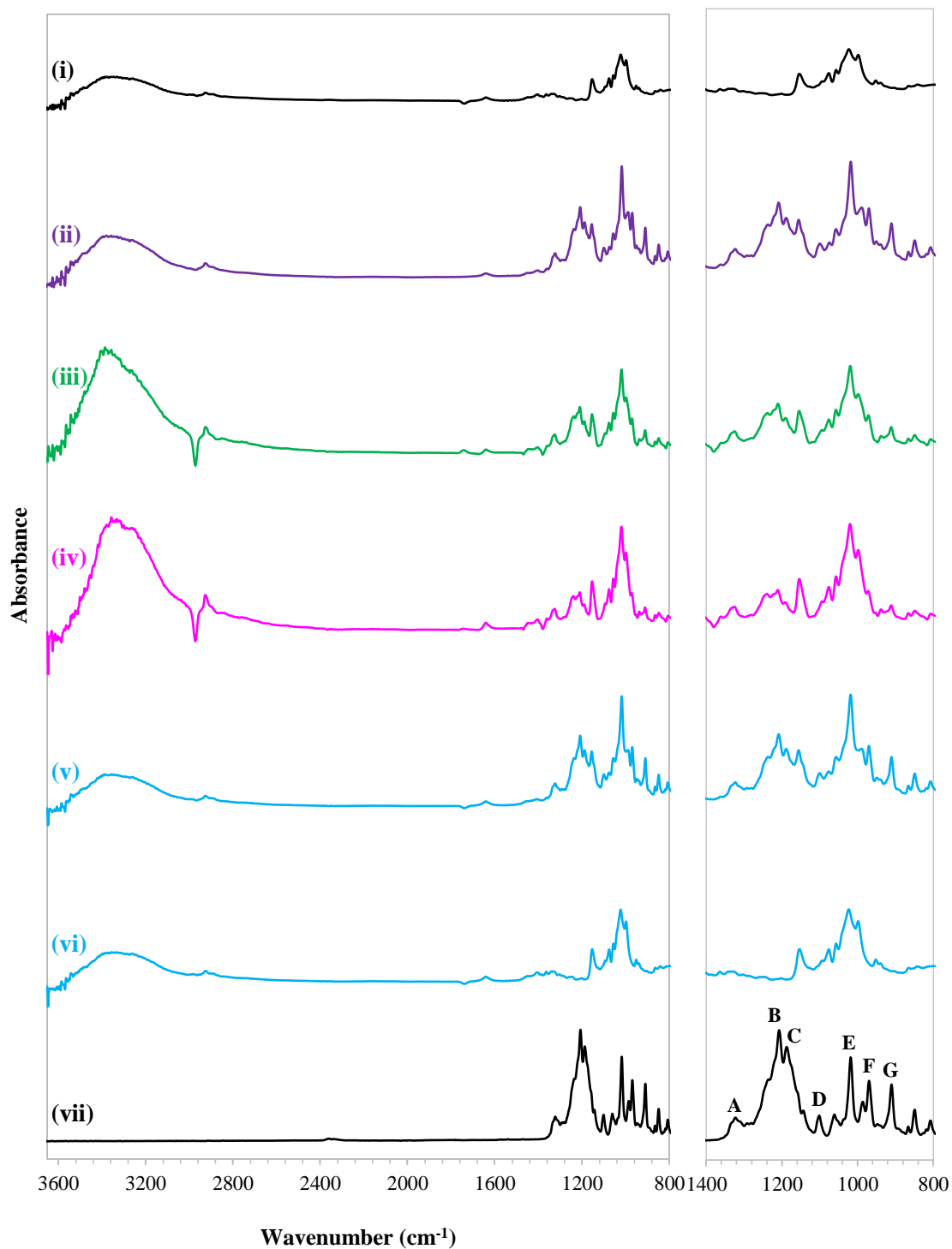
Figure 3-4: FTIR spectra of (i) unmodified α-CD, (ii) physical mixture of α-CD and PFP at a 1:1 molar ratio, inclusion complexes formed at a 1:1 (CD:PFP) molar ratio via (iii) dry mixing, (iv) paste mixing, (v) co-precipitation at 40°C, (vi) co-precipitation at RT(vii) and as-received PFP
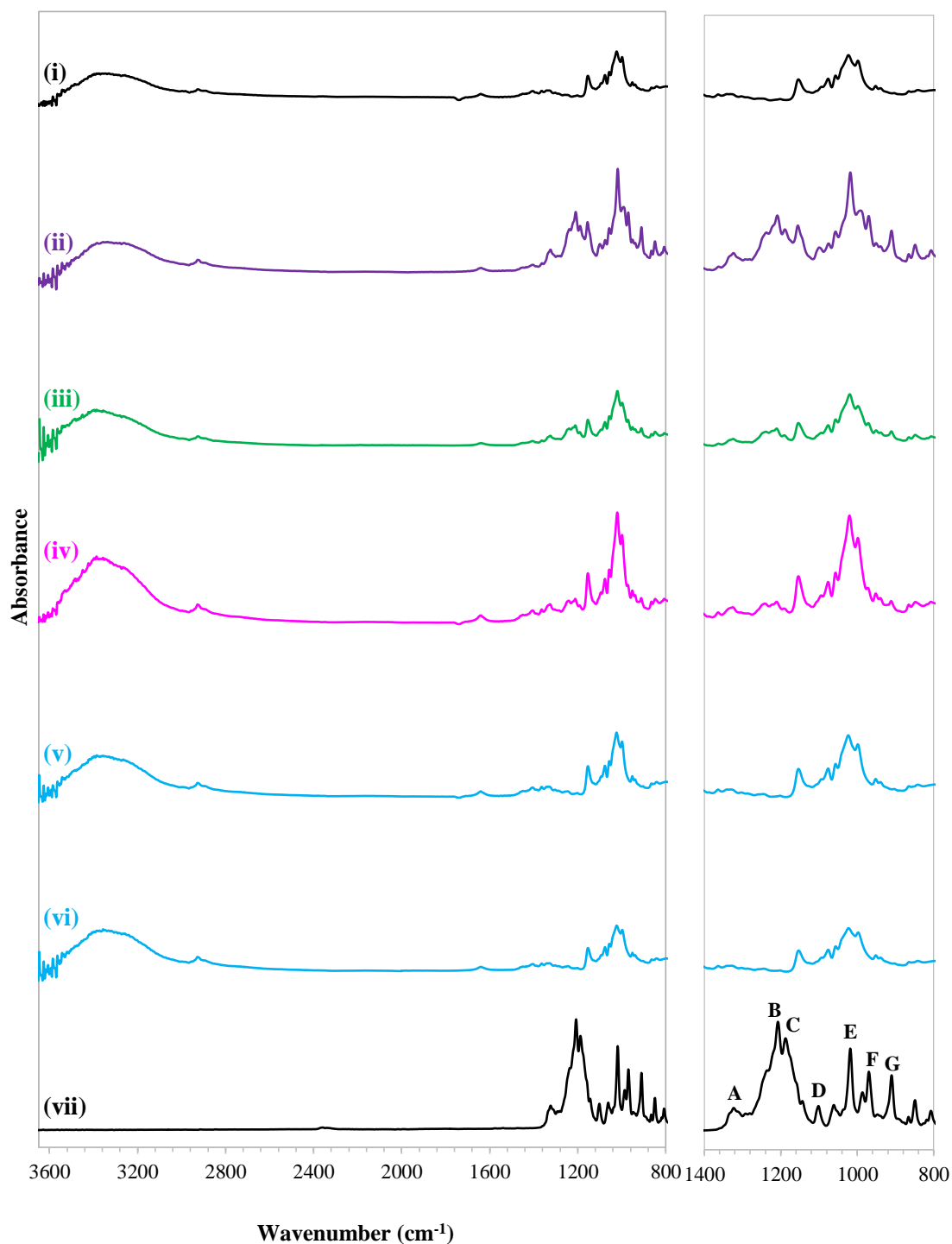
Figure 3-5: FTIR spectra of (i) unmodified α-CD, (ii) physical mixture of α-CD and PFP at a 2:1 molar ratio, inclusion complexes formed at a 2:1 (CD:PFP) molar ratio via (iii) dry mixing, (iv) paste mixing, (v) co-precipitation at 40°C, (vi) co-precipitation at RT(vii) and as-received PFP

Table 3-2: Characteristic peaks (cm^{-1}) of PFP and the corresponding peaks observed in the products of various complexation techniques at both 1:1 and 2:1 molar ratios of α-CD and PFP. A double dash indicates that a peak was not observed at that wavenumber.

Peak	PFP	1:1 Physical Mixture	1:1 Co-precipitation RT	1:1 Co-precipitation 40	1:1 Paste Mixing	1:1 Dry Mixing
A	1323	1323	1329	1323	1325	1325
B	1207	1209	--	1209	1211	1211
C	1188	1188	--	1188	1192	1190
D	1101	1099	1094	1101	1094	1094
E	1018	1018	--	1018	1020	1018
F	970	970	--	970	972	972
G	910	910	905	910	910	910

Peak	PFP	2:1 Physical Mixture	2:1 Co-precipitation RT	2:1 Co-precipitation 40	2:1 Paste Mixing	2:1 Dry Mixing
A	1323	1323	1329	1331	1325	1325
B	1207	1209	--	--	1211	1211
C	1188	1190	--	--	1192	1192
D	1101	1099	--	1094	1094	1093
E	1018	1018	1022	1024	1020	1020
F	970	970	--	--	972	972
G	910	910	904	905	912	910

Peaks characteristic of the PFC guest are evident in the spectra of the products (**Figure 3-4** and **Figure 3-5**). Unequivocal assignment of the FTIR bands of PFP is beyond the scope of the present work. Nonetheless, a number of these characteristic peaks were selected such that they did not overlap with strong absorption bands for the α-CD and are denoted by the letters A-G**.** The wavenumbers at which these peaks occur shifts slightly upon complexation; the shifts observed in this study for the selected peaks are tabulated in **Table 3-2**. A more thorough and quantitative characterization of the complexes was carried out by further analyzing the absorbance at these characteristic peaks. First, the absorbance value at each characteristic peak was divided by the absorbance values at the equivalent peak in the corresponding physical mixture, serving as an external standard. Secondly, the resulting values were divided by their average, acting as an internal standard. Finally, the

standard deviation of these normalized values was calculated and they are presented in **Table 3-3**. The standard deviation quantitatively demonstrates the difference between the peaks observed in the product and those observed in the physical mixture. Simply put, a larger standard deviation signifies a larger chemical shift (complexation), relative to the physical mixture.

Table 3-3: Absorbance values at peaks characteristic of PFP, normalized to physical mixture (external standard) and concentration (internal standard) for products prepared via various complexation techniques at both a 1:1 and 2:1 ratio of α-CD and PFP

Peak	1:1 Co-precipitation RT	1:1 Co-precipitation 40	1:1 Paste Mixing	1:1 Dry Mixing
A	0.96	0.95	1.29	1.23
B	--	1.02	0.80	1.03
C	--	1.03	0.70	0.92
D	1.55	1.09	1.32	1.08
E	--	1.01	1.38	1.17
F	--	0.93	0.85	0.84
G	0.50	0.98	0.67	0.74
St. Dev.	**0.53**	**0.05**	**0.31**	**0.18**

Peak	2:1 Co-precipitation RT	2:1 Co-precipitation 40	2:1 Paste Mixing	2:1 Dry Mixing
A	1.09	0.91	1.15	1.11
B	--	--	0.57	0.79
C	--	--	0.54	0.72
D	--	1.41	1.51	1.34
E	1.22	1.20	1.54	1.15
F	--	--	0.91	0.98
G	0.69	0.49	0.78	0.92
St. Dev.	**0.27**	**0.40**	**0.41**	**0.22**

Inclusion complex formation is characterized by weak, non-covalent interactions between the host and guest molecules. In addition to van der Waals forces, hydrophobic interactions are predicted to be involved in the inclusion of the PFP molecule within the α-CD cavity. During the co-precipitation technique, there are strong repulsions between the water molecules and the hydrophobic PFC. PFP can avoid contact with the water molecules by

entering the CD cavity and forming an inclusion complex. In addition, this results in the expulsion of enthalpy-rich, energetically unfavoured water molecules present in the slightly apolar cyclodextrin cavity. The expelled water molecules are taken up by the bulk solution where they can form more hydrogen bonds than when contained in the cyclodextrin cavity, and therefore gain degrees of freedom and contribute to the stability of the complex owing to the increase in entropy.[17, 18] In a 1:1 conformation the guest would partially stick out of the α-CD cavity. Since the main driving force of this complexation is the minimization of the contact between the PFC and the aqueous environment, it can reasonably be expected that each PFP molecule would prefer to be totally covered by CDs. Consequently a 2:1 α-CD:PFP complex is more likely. However, it is evident from the FTIR spectra of the products obtained via the co-precipitation complexation technique at both 1:1 and 2:1 at RT, as well as at 2:1 and 40 °C, that salient peaks characteristic of PFP at 1207 and 1188 cm^{-1} (B and C, respectively in **Figure 3-4** and **Figure 3-5**) were not observed. In fact, these spectra are almost identical to that of the un-modified α-CD and it can be concluded that these techniques are not effective in preparing an inclusion complex from these specific host and guest molecules. In contrast, the product prepared via 1:1 co-precipitation at 40 °C does show the peaks characteristic of the PFP guest. However, when compared to the corresponding physical mixture the standard deviation of the normalized absorbance values is exceptionally low (**Table 3-3**). This demonstrates that the product from this technique is actually only a physical mixture of the two parent components and inclusion of the PFP within the α-CD cavity did not occur.

Overall, the FTIR spectra of the products prepared via both the dry and paste mixing techniques indicate successful inclusion complex formation as the characteristic peaks of PFP, A-G in **Figure 3-4** and **Figure 3-5**, are visible. In fact, it is evident that these characteristic peaks have shifted slightly (**Table 3-2**). For example, the characteristic bands of PFP at 1207 and 1188 cm^{-1} shifted to 1211 and 1192 cm^{-1}, respectively for both the 2:1 paste and dry mixing techniques. These peaks are also different than those observed in the 2:1 physical mixture, at 1209 and 1190 cm^{-1}, respectively. This suggests that host-guest interactions were formed in the product and is in agreement with the literature where similar shifts were reported.[1, 15, 25] Further evidence of the effectiveness of the mixing

techniques is that the characteristic peaks were suppressed when compared to both PFP and the physical mixture. The attenuation of the absorption bands of guest molecules is typically observed for CD:IC systems because the inclusion of the guest molecules in the CD cavity hinders their molecular vibrations, and therefore the intensity of their absorption bands is diminished.[26] Furthermore, the standard deviations of the absorbance values obtained for these products indicate significant differences from their corresponding physical mixtures (**Table 3-3**). It is likely that the mixing techniques were more successful than co-precipitation in preparing an inclusion complex with this specific guest due to its liquid form. The PFP may not have associated with the CD in solution in an amount sufficient to facilitate complexation for two reasons: it is possible that the PFP was too dilute in the aqueous solvent, and because PFP is a high molecular weight compound, it may preferentially associate with itself even with vigorous stirring. However, one of the limitations of the mixing techniques is the inability to guarantee homogeneous mixing; thus, the product may be a mixture of host, guest, and complex. In fact, the complexes prepared via the mixing technique at a 1:1 molar ratio show a larger hydroxyl vibrational band (roughly 3300 cm^{-1}), potentially due to an amount of uncomplexed CD remaining in the product. Although this could be remedied by washing the product, there is a risk of destroying the complex or decreasing the product yield.

The complexes prepared at a 2:1 molar ratio of the α-CD host to the PFP guest appeared to be the most successful overall. This corresponds with the α-CD cavity height being smaller than that of the PFP so that in order for the PFP to be fully covered, two α-CD molecules must be threaded onto one PFP molecule. Further characterization techniques were only carried out on the samples prepared at a 2:1 molar ratio.

3.4.3   Thermogravimetric Analysis

TGA was carried out on the products of the co-precipitation, paste mixing, and dry mixing complexation techniques carried out at a 2:1 molar ratio (α-CD:PFP) for further confirmation of the formation of an inclusion complex. Thermal characterization techniques involve analyzing the broadening, shifting, and disappearance of existing peaks, as well as the appearance of new peaks, when compared to the parent molecules and/or the

physical mixture of the parent molecules. The thermograms for the parent molecules, α-CD and PFP, their 2:1 physical mixture, and complexes prepared from co-precipitation (at RT), paste mixing, and dry mixing are shown in **Figure 3-6**. The TGA data is presented as weight percent, and both derivative weight and derivative heat flow (with respect to temperature) versus temperature.

The thermogram for α-CD shows two mass losses centered at 60 and 90 °C, corresponding to a loss of absorbed water and water of crystallization, and a third at 320 °C corresponding to its decomposition.[27] PFP, with a reported boiling point of 214-216 °C,[28] shows a mass loss centered at 165 °C, corresponding to its complete vaporization. The difference with the literature data may be due different isomeric composition or the relatively low purity of the PFP molecule used in this study. The thermogram for the 2:1 physical mixture of α-CD and PFP appears to be almost identical to that obtained for pure α-CD. This is potentially due to incomplete mixing of the parent molecules with the result that the fraction used for TGA analysis did not contain any PFP. It was not possible to remedy this by more thoroughly mixing the components as this would, in effect, be carrying out the dry mixing complexation technique.

The thermograms for the products prepared by different complexation techniques all show two mass losses which occur at approximately 100 and 320 °C. The latter peak clearly corresponds to the degradation of α-CD. The loss of PFP overlaps with the loss of water at 100 °C, and it was therefore difficult to elucidate differences in the thermograms by looking solely at weight loss and derivative weight. Comparing the derivative heat flow for the product prepared via co-precipitation (at RT) to that for α-CD, some differences are observed; however, the same basic shape of the thermogram of CD is maintained. For example, there are still two peaks around 100 °C, and although they have shifted slightly, the shifts are not sufficient to confirm complex formation. These results are in agreement with the FTIR results discussed previously (Section 3.4.2).

The derivative heat flow (with respect to temperature) for the product prepared via dry mixing shows a very similar pattern to that of α-CD around 100 °C, indicating a large mass

loss at this temperature corresponds to the release of water. There are noticeable differences, however, starting at 300 °C when the α-CD begins to decompose. This provides evidence that some PFP was in fact included within the CD cavity, such that it was thermally stabilized and did not evaporate until the CD began to decompose, in agreement with results reported in the literature.[29] The product prepared via paste mixing, on the other hand, shows a different derivative heat flow at both 100 and 320 °C. This indicates that this technique was more effective, with more PFP included within the cavity. Around 100 °C, there is only one endothermic peak, indicating that there was some degree of displacement of water molecules from the host CD cavity, which corresponds to the inclusion of PFP within that cavity.[26]

If PFP molecules escape from the α-CD cavities at temperatures below 300 °C when α-CD begins to decompose, the weight loss should correspond to the mass fraction of PFP in the complexes. In the case that the CD:IC contains no water of crystallization, the calculated mass fraction of PFP approaches 25 %. However, it is clear from the thermograms, specifically those showing derivative heat flow, that there is some water remaining in the complexes, and therefore the calculated mass fraction of PFP is overestimated. The amount of water bound to the complex could likely be further decreased by using a more effective drying technique, such as heat-drying, however, this could be detrimental to the complex. The calculated mass loss below 123 °C for the complex prepared via paste mixing is less than the calculated expected mass loss. Taking into consideration that the observed mass loss also includes water loss, this is further evidence that some PFP was included within the α-CD cavity and was not thermally altered until the temperature at which the α-CD began to decompose. It is possible that some of the product of paste complexation is an inclusion complex and some is simply a physical mixture of the parent molecules. Increasing the mixing time for paste complexation could serve to reduce the amount of uncomplexed α-CD in the product.
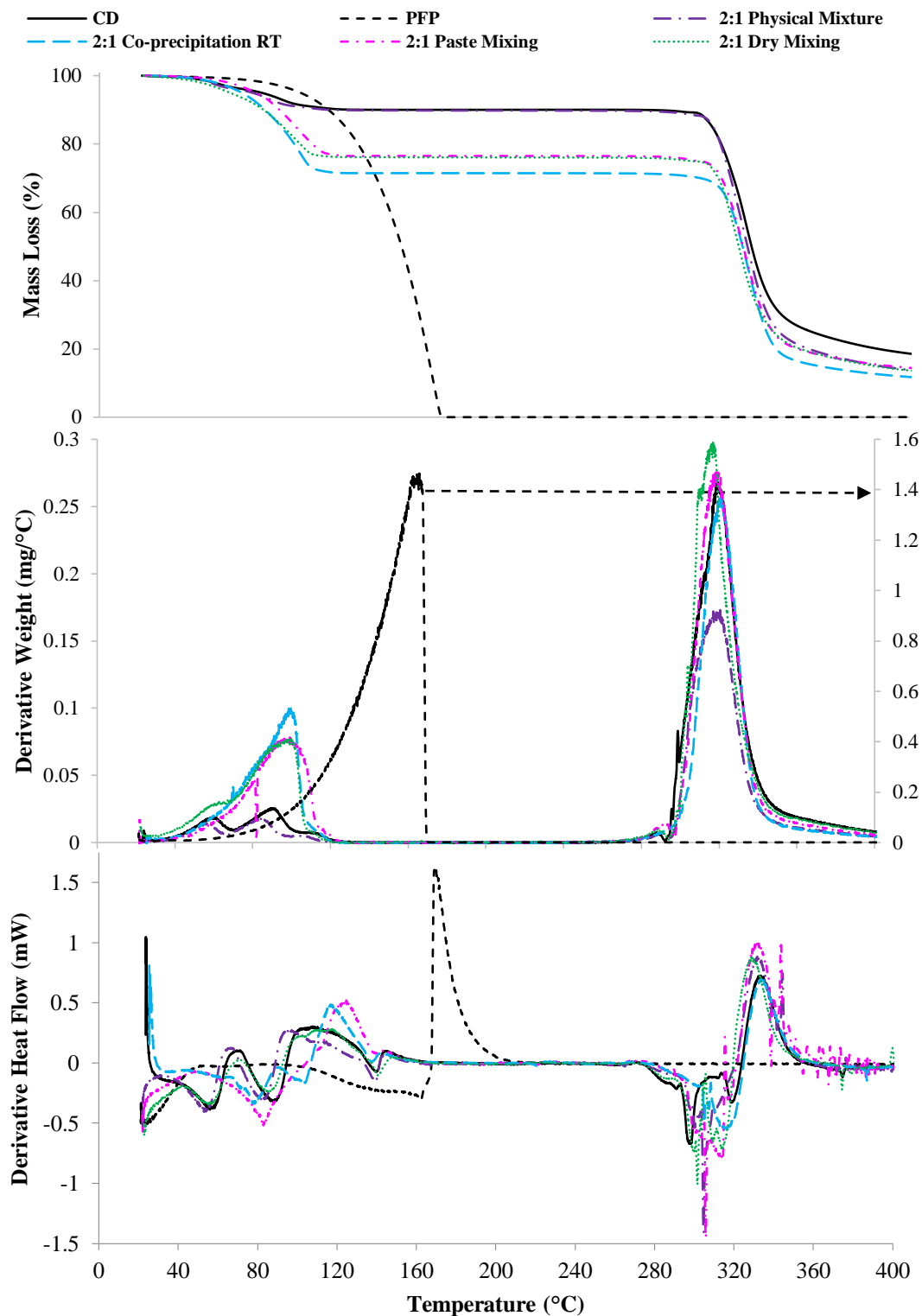
Figure 3-6: TGA thermograms of unmodified α-CD and PFP, their 2:1 physical mixture, and complexes prepared via co-precipitation (at RT), paste mixing, and dry mixing at a 2:1 molar ratio

Unfortunately, the main thermal event for PFP in the complexes was not increased as is the case most reported in the literature for evidence supporting the formation of a stable inclusion complex.[15, 25, 30] Interaction of the guest with the cyclodextrin provides a higher energy barrier to overcome for volatilization resulting in an increase in boiling temperature of about 10 °C.[13] On the other hand, the inclusion complexes prepared with volatile guests often do not have substantially higher thermal decomposition temperatures.[26] In this case, it was actually observed that the PFP in the products evaporated at a lower temperature than the unmodified PFP. Although inclusion within the cyclodextrin cavity can provide stability for the guest molecule, in this case the interactions with the CD cavity are weaker than those formed in the bulk solution between the liquid PFP molecules. It is also possible that the guest is not completely included within the cyclodextrin cavity, but rather is closed in a void space of a lattice or aggregated to the outside of the cyclodextrin, forming a microcrystalline or amorphous powder.[14, 17, 31] This type of complex would have a much lower stability than if the guest was included entirely within the cyclodextrin cavity. Nevertheless, it was observed that some of the PFP was not removed until the CD began to decompose which has also been reported in the literature as evidence supporting the formation of an inclusion complex.[5, 29]

Overall, thermal characterization using TGA did not prove to be an effective technique for confirming complex formation between the host and guest molecules used in this study. This was mainly due to the similarity of the guest vaporization temperature to that for water. Nonetheless, it was possible to further ascertain the effectiveness of the different complexation techniques, specifically providing the opportunity to further distinguish the differences between the paste and dry mixing complexation techniques, which showed similar efficacy when analyzed using FTIR. Overall, the TGA data suggests that the paste mixing technique was the most effective whereas co-precipitation (at RT) was the least effective, which is in agreement with the data obtained from FTIR characterization. The paste mixing technique is likely more effective due to the small amount of water utilized in this preparation technique which acts as a driving force for the PFP molecule to enter the hydrophobic CD cavity in order to reduce contact with the aqueous environment.

3.4.4 X-ray Diffraction

After initial characterization with FTIR, it was determined that inclusion complex formation occurred preferentially at a 2:1 α-CD:PFP molar ratio. XRD was carried out on complexes prepared at this ratio using co-precipitation (at RT), paste mixing, and dry mixing techniques. When an inclusion complex is formed with a solid substance as a guest, a comparison has to be made between the diffractogram of the product and that of the physical mixture of the two parent molecules. However, in the case of a liquid guest, as with PFP, no comparison is necessary because liquids do not have diffraction patterns of their own. Therefore, if the diffraction pattern of the product clearly differs from that of the unmodified cyclodextrin, the difference indicates complex formation. Complex formation leads to the sharpening and/or shifting of existing peaks, as well as the appearance of a few new peaks.[14, 18]

CDs are crystalline and have crystal structures referred to as cage or channel type.[32] The as-received CDs have a cage type packing structure characteristic of a random packing arrangement. In cage type packing, the CDs are arranged in a herringbone pattern (**Figure 3-7c**) where both openings of each CD unit are closed by adjacent CD molecules. CDs take this form when small molecules, such as water, are included in its cavity. In general, CD molecules form the channel type arrangement when they are in an inclusion complex conformation. In this arrangement the CDs are aligned and stacked on top of each other in a head-to-head (**Figure 3-7b**) or head-to-tail fashion (**Figure 3-7a**), forming cylindrical channels.[5] Depending on the nature and dimension of the guest, a variety of conformations can be adopted, from perfectly aligned to more or less displaced, possibly forming, in the most favourable case, endless channels.[33] The two salient peaks in X-ray diffractograms most commonly reported as corresponding to the channel type packing structure for α-CD are centered at $2\theta \approx 13°$ and $20°$.[19] These peaks have also been reported as $2\theta \approx 19.6°$ and $22.3°$.[19]
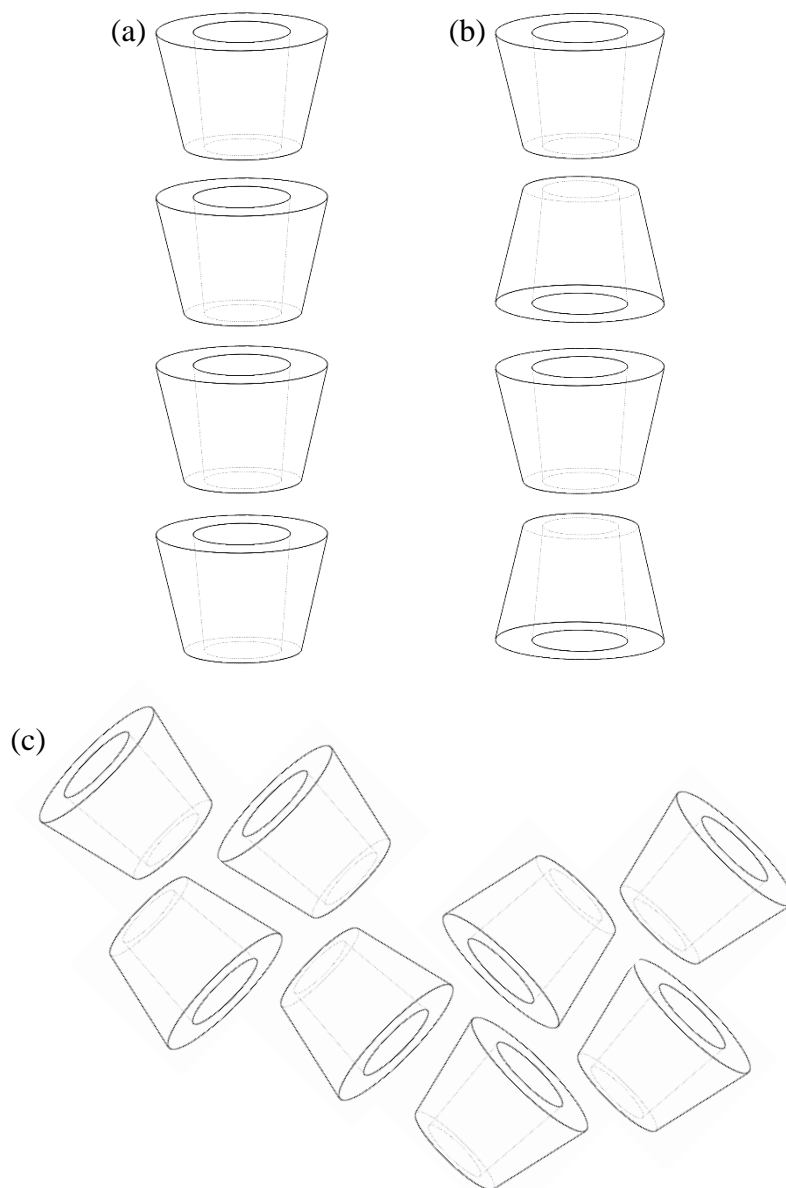
Figure 3-7: Possible cyclodextrin conformations (a) head-to-tail channel structure (b) head-to-tail channel structure (c) cage structure

XRD spectra for the host, α-CD, and products of the 2:1 co-precipitation (at RT), paste mixing, and dry mixing complexation techniques are shown in **Figure 3-8**. Salient peaks at 9.72°, 12.13°, 14.32°, and 21.67° previously reported as characteristic of cage-type packing in α-CD were observed and are denoted in **Figure 3-8** by an asterisk.

The diffractogram for the product obtained via co-precipitation (at RT) shows a spectrum very different from that of the host α-CD. It can be seen that not only is there disappearance of characteristic peaks from the parent spectra, there is both sharpening and shifting of existing peaks. Furthermore, the peaks at 19.64° and 22.34° (A and B, respectively in **Figure 3-8**) can be attributed to the α-CD adopting a channel structure due to the formation of an inclusion complex.[21, 34] It is possible that some of these changes can be attributed to recrystallization of the α-CD from the aqueous solvent used in the co-precipitation technique.
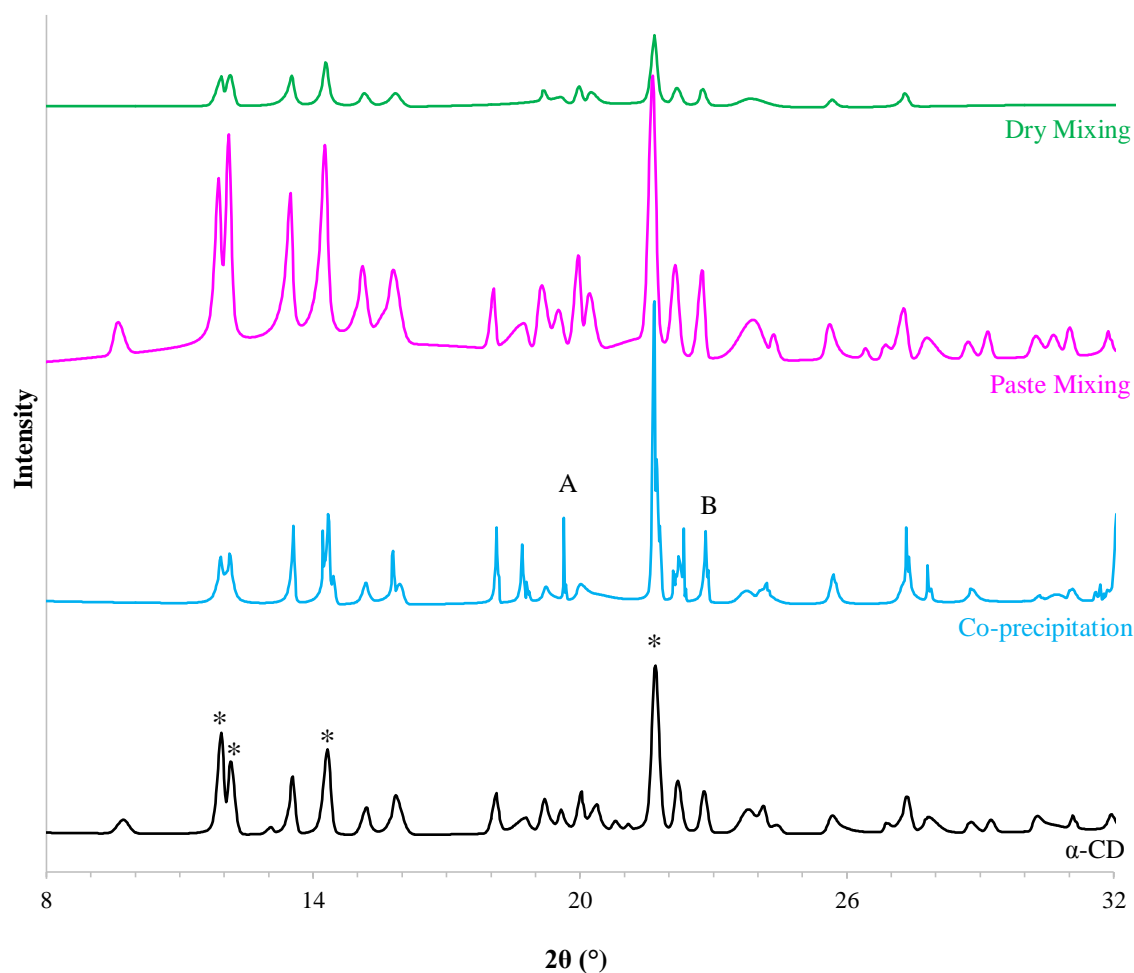
Figure 3-8: XRD comparison of CD:ICs prepared from α-CD and PFP via different complexation techniques at a 2:1 host:guest ratio and that of the unmodified α-CD

The diffractogram for the product obtained via paste mixing shows a very similar spectrum to that of α-CD but with increased intensity. This can be attributed to a large amount of uncomplexed CD remaining in the product, possibly owing to the contribution of 1:1 complexes in the product, resulting in an overall stoichiometric ratio less than 2:1.[22] The XRD results for the product obtained via dry mixing, on the other hand, show a severely diminished structure when compared to the host diffractogram. Specifically, the peaks previously identified as being characteristic of a cage type structure in the host have either disappeared, in the case of the peak at 9.72°, or noticeably dwarfed, especially with the peak at 21.67°.

Overall, because the diffraction patterns do not correspond exactly to those of the unmodified parent molecule, a true inclusion complex may exist. Products obtained by the three different complexation techniques all show unique features when compared to the diffractogram for α-CD.

3.5 Conclusion

Taken together, the results of the FTIR, TGA, and XRD characterization techniques confirm that inclusion complexation did in fact occur between the selected host and guest molecules, α-CD and PFP respectively. Following characterization with FTIR, it was possible to narrow down the complexation techniques and conditions to those most effective at yielding true complex formation. It was evident that a 2:1 molar ratio of the α-CD host to PFP guest was preferred. This corresponds with the α-CD cavity height being smaller than that of the PFP so that in order for the CD to be fully covered, two α-CD molecules must be threaded onto one PFP molecule. From the FTIR spectra, it was also apparent that the mixing techniques were more effective than co-precipitation. Peaks characteristic of the PFP guest molecule were visible in the spectra for the mixing techniques, and in fact the peaks were both shifted and suppressed when compared to the FTIR spectra of the as-received PFP. These spectral features are evidence of host-guest interactions and the cavity hindering the vibrations of the PFP, ultimately indicating successful complex formation. Finally, a comparison of the standard deviations of

normalized absorbance values at the characteristic peaks indicated that the products prepared via the mixing technique were sufficiently different than the corresponding physical mixtures.

TGA was subsequently carried out on the products of 2:1 co-precipitation (at RT), paste mixing, and dry mixing. This characterization technique was difficult with the specific guest molecule used in this study due to the similarity of its main thermal event to that of water. Nevertheless, the differences in the derivative heat flow thermograms for the products were sufficiently large compared to the thermogram of the unmodified α-CD to demonstrate successful complexation. Overall, TGA analysis indicated that the paste mixing technique was the most effective in preparing an inclusion complex in this study.

Finally, XRD was carried out on the products of the 2:1 co-precipitation (at RT), paste mixing, and dry mixing. Differences in the diffractograms of the three products when compared to that of the unmodified α-CD show differences including the disappearance, sharpening, and shifting of existing peaks, as well as the occurrence of new peaks which all suggest successful complexation. Further analysis indicated that the dry mixing technique may be the most effective in preparing inclusion complexes between α-CD and PFP. In summary, characterization of the products prepared via the different complexation techniques utilized indicate that the mixing techniques were overall more effective than co-precipitation. Although TGA provided evidence that paste mixing was the best technique, characterization with XRD indicated that dry mixing may be more effective. Nevertheless, the paste mixing technique was selected for preparing an inclusion complex with α-CD and PFP due to its proven ability to produce the desired complex and the fact that it allowed for simple handling and preparation of the complex.

3.6 References

1. Lo Nostro, P.; Santoni, I.; Bonini, M.; Baglioni, P., Inclusion compound from a semifluorinated alkane and beta-cyclodextrin. *Langmuir* **2003,** 19, 2313-2317.

2. Riess, J. G., Highly fluorinated systems for oxygen transport, diagnosis and drug delivery. *Colloids Surf., A* **1994,** 84, 33-48.

3. Radisic, M.; Park, H.; Chen, F.; Salazar-Lazzaro, J. E.; Wang, Y.; Dennis, R.; Langer, R.; Freed, L. E.; Vunjak-Novakovic, G., Biomimetic approach to cardiac tissue engineering: oxygen carriers and channeled scaffolds. *Tissue Eng* **2006,** 12, (8), 2077-91.

4. Canbolat, M. F.; Celebioglu, A.; Uyar, T., Drug delivery system based on cyclodextrin-naproxen inclusion complex incorporated in electrospun polycaprolactone nanofibers. *Colloids Surf B Biointerfaces* **2013,** 115C, 15-21.

5. Kayaci, F.; Uyar, T., Encapsulation of vanillin/cyclodextrin inclusion complex in electrospun polyvinyl alcohol (PVA) nanowebs: Prolonged shelf-life and high temperature stability of vanillin. *Food Chemistry* **2012,** 133, 641-649.

6. Uyar, T.; Havelund, R.; Hacaloglu, J.; Besenbacher, F.; Kingshott, P., Functional electrospun polystyrene nanofibers incorporating α-, β-, and γ-cyclodextrins: comparison of molecular filter performance. *ACS Nano* **2010,** 4, (9), 5121-30.

7. Lowe, K. C., Fluorinated blood substitutes and oxygen carriers. *J. Fluorine Chem.* **2001,** 109, (1), 59-65.

8. Seifu, D. G.; Mequanint, K., Experimental and modeling studies of oxygen tension in vascular tissue engineering with and without an oxygen carrier. *Journal of Biomaterials and Tissue Engineering* **2011,** 1, 49-59.

9. Seifu, D. G.; Isimjan, T. T.; Mequanint, K., Tissue engineering scaffolds containing embedded fluorinated-zeolite oxygen vectors. *Acta Biomater* **2011,** 7, (10), 3670-8.

10. Sharma, S. K.; Lowe, K. C.; Davis, S. S., Novel compositions of emulsified perfluorochemicals for biological uses. *Biomater Artif Cells Artif Organs* **1988,** 16, (1-3), 447-50.

11. Bollands, A. D.; Lowe, K. C.; Sharma, S. K.; Davis, S. S., Biocompatibility studies with a novel perfluorochemical emulsion. *Biomater Artif Cells Artif Organs* **1988,** 16, (1-3), 451-3.

12. Druliner, J. D.; Wasserman, E., Synthesis and characterization of cyclodextrin/perfluoroalkane inclusion compounds. *Journal of Fluorine Chemistry* **1995,** 72, 75-78.

13. Hedges, A. R., Industrial applications of cyclodextrins. *Chem. Rev.* **1998,** 98, 2035-2044.

14. Singh, R.; Bharti, N.; Jyotsana, M.; Hiremath, S. N., Characterization of cyclodextrin inclusion complexes - A review. *Journal of Pharmaceutical Science and Technology* **2010,** 2, (3), 171-183.

15.   Karoyo, A. H.; Sidhu, P.; Wilson, L. D.; Hazendonk, P., Characterization and dynamic properties for the solid inclusion complexes of β-cyclodextrin and perfluorooctanoic acid. *J Phys Chem B* **2013,** 117, (27), 8269-82.

16.   Del Valle, E. M. M., Cyclodextrins and their uses: a review. *Process Biochemistry* **2004,** 39, 1033-1046.

17.   Saenger, W., Cyclodextrin inclusion compounds in research and industry. *Angewandte Chemie International Edition* **1980,** 19, 344-362.

18.   Bekers, O.; Uijtendaal, E. V.; Beijnen, J. H.; Bult, A.; Underberg, W. J. M., Cyclodextrins in the pharmaceutical field. *Drug Development and Industrial Pharmacy* **1991,** 17, (11), 1503-1549.

19.   Rusa, C. C.; Bullions, T. A.; Fox, J.; Porbeni, F. E.; Wang, X.; Tonelli, A., Inclusion compound formation with a new columnar cyclodextrin host. *Langmuir* **2002,** 18, (25), 10016-10023.

20.   Uyar, T.; Kingshott, P.; Besenbacher, F., Electrospinning of cyclodextrin-pseudopolyrotaxane nanofibers. *Angew Chem Int Ed Engl* **2008,** 47, (47), 9108-11.

21.   Zhan, J.; Singh, A.; Zhang, Z.; Huang, L.; Elisseeff, J. H., Multifunctional aliphatic polyester nanofibers for tissue engineering. *Biomatter* **2012,** 2, (4), 202-12.

22.   Karoyo, A. H.; Borisov, A. S.; Wilson, L. D.; Hazendonk, P., Formation of host-guest complexes of β-cyclodextrin and perfluorooctanoic acid. *J Phys Chem B* **2011,** 115, (31), 9511-27.

23.   Huang, L.; Allen, E.; Tonelli, A. E., Study of the inclusion compounds formed between alpha-cyclodextrin and high molecular weight poly(ethylene oxide) and poly(caprolactone). *Polymer* **1998,** 39, (20), 4857-4865.

24.   Harada, A.; Takashima, Y.; Yamaguchi, H., Cyclodextrin-based supramolecular polymers. *Chem Soc Rev* **2009,** 38, (4), 875-82.

25.   Celebioglu, A.; Uyar, T., Electrospinning of polymer-free nanofibers from cyclodextrin inclusion complexes. *Langmuir* **2011,** 27, (10), 6218-26.

26.   Koontz, J. L.; Marcy, J. E.; O'Keefe, S. F.; Duncan, S. E., Cyclodextrin inclusion complex formation and solid-state characterization of the natural antioxidants alpha-tocopherol and quercetin. *J Agric Food Chem* **2009,** 57, (4), 1162-71.

27.   Trotta, F.; Cavalli, R.; Martina, K.; Biasizzo, M.; Vitillo, J.; Bordiga, S.; Vavia, P.; Ansari, K., Cyclodextrin nanosponges as effective gas carriers. *J Incl Phenom Macrocycl Chem* **2011,** 71, 189-194.

28.   Harrison, D.; Stacey, M., Polycyclic fluoroaromatic compounds - III. *Tetrahedron* **1963,** 19, 1893-1901.

29.   Tatsuno, H.; Ando, S., Structure and dynamics of perfluoroalkane/beta-cyclodextrin inclusion compounds as studied by solid-state 19F MAS and 1H -->19F CP/MAS NMR spectroscopy. *J Phys Chem B* **2006,** 110, (51), 25751-60.

30.   Uyar, T.; Hacaloglu, J.; Besenbacher, F., Electrospun polystyrene fibers containing high temperature stable volatile fragrance/flavor facilitated by cyclodextrin inclusion complexes. *Reactive & Functional Polymers* **2009,** 69, 145-150.

31.   Szejtli, J., Introduction and General Overview of Cyclodextrin Chemistry. *Chem Rev* **1998,** 98, (5), 1743-1754.

32.   Saenger, W.; Jacob, J.; Gessler, K.; Steiner, T.; Hoffmann, D.; Sanbe, H.; Koizumi, K.; Smith, S. M.; Takaha, T., Structures of the Common Cyclodextrins and Their Larger Analogues-Beyond the Doughnut. *Chem Rev* **1998,** 98, (5), 1787-1802.

33.   Giordano, F.; Novak, C.; Moyano, J. R., Thermal analysis of cyclodextrins and their inclusion compounds. *Thermochimica Acta* **2001,** 380, 123-151.

34.   Harada, A.; Kamachi, M., Complex formation between poly(ethylene glycol) and alpha-cyclodextrin. *Macromolecules* **1990,** 23, 2823-2824.

4 FABRICATION OF TISSUE ENGINEERED SCAFFOLDS INCORPORATING CYCLODEXTRIN INCLUSION COMPLEXES WITH PERFLUOROPERHYDROPHENANTHRENE

Overview: This chapter discusses the incorporation of an inclusion complex from alpha-cyclodextrin and perfluoroperhydrophenanthrene in 3D tissue engineering constructs. Scaffold fabrication was carried out via electrospinning and the inclusion complexes were incorporated in both biodegradable (PCL) and stable (PCU) materials. Optimized concentrations were identified and the effect of adding cyclodextrin explored. The resulting fibrous mats were imaged with scanning electron microscopy and the surface content was analyzed with X-ray photoelectron spectroscopy.

Keywords: 3D scaffold, electrospinning, tissue engineering, cyclodextrin, inclusion complex, perfluorocarbons

4.1 Introduction

Tissue engineering involves the assembly of cells and their support structures for the repair and regeneration of diseased or damaged tissues and organs as an alternative to current therapies.[1] One strategy of tissue engineering involves seeding cells onto a porous 3D scaffold that supports *in vitro* tissue formation and maturation. One of the major factors hindering the success of scaffold-guided tissue engineering is the inability to deliver sufficient oxygen to the growing constructs. A number of strategies to improve oxygen delivery have focused on the development of PFC emulsions. Although PFC emulsions show excellent oxygen carrying capacity, they lack stability causing overall user-unfriendliness and they have a high density causing them to settle in the culture well or medium reservoir.[2, 3] Another approach for improving oxygen delivery involves embedding oxygen generating compounds, such as calcium peroxide[4] or sodium percarbonate[5] which decompose in water to produce oxygen, directly into the tissue engineering scaffold. This approach has the advantage of providing oxygen throughout the

construct, notably in the center where it is difficult to reach by diffusion alone, but it is restricted because the oxygen generating compound is eventually depleted. Tissue engineering scaffolds incorporating fluorinated porous zeolite particles provide an alternative to this approach whereby the embedded compound does not generate oxygen but enhances its delivery using the principles of oxygen solubility in perfluorocarbons.[6] Cyclodextrin inclusion complexes with perfluorocarbons have been prepared previously for application as novel oxygen carriers. Because inclusion of a guest molecule within the cyclodextrin cavity can provide stabilization, it may serve to overcome some of the shortcomings of PFC emulsions. The goal of this study was to incorporate α-CD/PFP inclusion complexes into 3D fibrous scaffolds. Embedding the CD/PFC complexes in the scaffold would impart enhanced oxygen delivery throughout the construct, and delay or prevent settling of the PCFs in the culture well or medium reservoir.

One of the most commonly utilized methods for scaffold fabrication is electrospinning. Electrospinning is a versatile technique that enables the production of multi-functional fibers in the nano- to micrometer range from a wide variety of materials and it is generally a relatively simple, versatile, and cost-effective method. Because electrospinning allows for the fabrication of scaffolds that closely mimic the scale and fibrous nature of the native ECM, electrospinning was selected as the scaffold fabrication technique for this study. It has been demonstrated that cyclodextrin inclusion complexes can be incorporated into three-dimensional scaffolds via electrospinning.[7-9] In fact, cyclodextrin has been shown to positively affect the electrospinning of polymer solutions. The addition of CD increases the conductivity of the polymer solution, allowing for successful electrospinning of bead-free fibers from lower polymer concentrations.[10, 11] This is because the polymer solution is subjected to higher stretching under the high electric field.[12] Moreover, it was reported that preparation of a homogenous film from polymer/cyclodextrin solutions via other fabrication techniques, such as spin coating or solvent casting methods, failed because the CD molecules phase separated and formed crystal aggregates either immediately or upon solvent evaporation.[9, 12]

Depending on the intended application, scaffolds may be designed to be biodegradable so that only the neo-tissue will remain after a given period of culture time or following implantation, or they may be biostable such that a composite tissue that provides long-term support could be fabricated.[13-16] In the case of biodegradable scaffolds, cells will remodel the scaffold with their own ECM proteins creating the intended tissue without compromising tissue structural integrity. This, however, requires strict coordination of the scaffold biodegradation rate with the biosynthetic rate and is one of the major obstacles in the field today. In addition, a scaffold must have several required characteristics: biocompatibility, appropriate mechanical strength and compliance, optimal porosity for cell seeding, *in vitro* nutrient and oxygen transport, and the ability to bind to cells and release growth factors when needed. PCU and PCL were selected as polymer materials because they have previously been utilized as polymers for scaffold fabrication in our lab and have been shown to have acceptable cell compatibility.[17, 18] These polymer materials present the opportunity for a proof of concept study showing that the CD/PFC inclusion complex can be incorporated in both biostable (PCU) and biodegradable (PCL) tissue engineering scaffolds.

4.2 Materials

Perfluoroperhydrophenanthrene (PFP, mixture of isomers, 83 % purity) and alpha-cyclodextrin (α-CD, 100 % purity) were obtained commercially from Alfa Aesar (Ward Hill, MA). Medical grade poly(carbonate urethane) (PCU) (Bionate® 55D) was obtained from DSM Biomedical (Berkeley, CA). Polycaprolactone (PCL), M_n 70,000-90,000, was purchased from Sigma Aldrich (Milwaukee, WI). Solvents were purchased from Caledon Labs (Georgetown, ON). All other chemicals were purchased from Sigma Aldrich. Unless noted otherwise, all chemicals were used as received without any further purification.

4.3 Methods

4.3.1 Preparation of Inclusion Complex

Weighed amounts of α-CD and a minimal amount of d.i. water were combined to form a paste. Weighed amounts of PFP were added to the α-CD paste at a 2:1 α-CD to PFP molar

ratio. The paste was thoroughly mixed using a ceramic mortar and pestle for ten minutes. The product was collected in a glass vial, dried and stored in a desiccator with potassium hydroxide as a desiccant. The products were analyzed with FTIR as discussed previously (Section 3.3.3) to ensure successful complexation consistent with previous results (Section 3.4.2)

4.3.2   Fabrication of 3D Scaffolds

4.3.2.1 Electrospinning of Poly(carbonate urethane)

The polymer solution was prepared by varying concentrations of PCU in *N*,*N*-dimethylformamide (DMF), and also varying the amount of CD:IC added. The concentration of PCU ranged from 5-10 % (v/v) with respect to the solvent, and the concentration of CD:IC ranged from 5-60 % (w/w) with respect to PCU. First, the PCU was added to the corresponding amount of DMF and stirred until it was fully dissolved. Then the corresponding amount of CD:IC was added and stirred until it was fully dispersed in the polymer solution.

The electrospinning conditions used were based on those previously optimized in our lab.[17] The viscous polymer solution was transferred to a 0.5 mL glass syringe equipped with a 22 gauge stainless steel needle. The syringe was fixed horizontally on a syringe pump (KD101, KD Scientific, USA) which maintained the flow rate at 0.1 mL/h and was connected to a high voltage supply (ES30P, Gamma High Voltage, USA) which applied a voltage of 15 kV. The fibers were collected on a grounded stationary metal collector covered in aluminum foil, 8 cm from the needle tip. Following electrospinning, the scaffolds were removed from the electrospinning assembly and the solvent was allowed to evaporate in the fume hood.

4.3.2.2 Electrospinning of Polycaprolactone

The electrospinning of PCL was based on conditions obtained from literature, where a cyclodextrin/naproxen inclusion complex was incorporated into electrospun PCL fibers.[7] The polymer solution was prepared in a co-solvent mixture at a ratio of 3:1 or 1:1 DMF to

dichloromethane (DCM). The concentration of PCL ranged from 5-10 % (v/v) with respect to the total amount of solvent, and the concentration of CD:IC ranged from 15-50 % (w/w) with respect to PCL. First, the PCL was added to the corresponding amount of DMF and DCM solvents and stirred until it was fully dissolved. Then the corresponding amount of CD:IC was added, with stirring and vortexing used in order to fully disperse the CD:IC in the polymer solution.

The viscous polymer solution was then transferred to a 0.5 mL glass syringe equipped with an 18, 20, or 22 gauge stainless steel needle. The syringe was fixed horizontally on a syringe pump (KD101, KD Scientific, USA) which maintained the flow rate at 0.1 mL/h and connected to a high voltage supply (ES30P, Gamma High Voltage, USA) which applied a voltage of 15 kV. The fibers were collected on a grounded stationary metal collector covered in aluminum foil, 8 or 10 cm from the needle tip. Following electrospinning, the scaffolds were removed from the electrospinning assembly and the solvent was allowed to evaporate in the fume hood.

4.3.3   Scanning Electron Microscopy

Fiber morphology of the electrospun fibrous mats was visualized using scanning electron microscopy (SEM, 3400S, Hitachi, Ltd., Tokyo, Japan). The samples were mounted on aluminum stubs with carbon tape and sputtered with osmium prior to analysis (courtesy of the Nanofab facility, Filgen OPC80T, Japan). The stub was then placed in the SEM and scanned at a working distance of 5 mm at a constant accelerating voltage of 5 kV. Images were captured at various magnifications. The fiber diameters were measured using ImageJ software (NIH, USA), analyzing a total of 100 fibers from three different fields of view at 10,000x magnification. Average fiber diameters were compared using the Student's t-test with significance assigned to $p < 0.05$.

4.3.4   X-Ray Photoelectron Spectroscopy

X-ray photoelectron spectroscopy (XPS) was carried out on the CD:IC and 3D scaffolds using a Kratos Axis Ultra Spectrometer (Kratos Analytical Ltd. Manchester, UK) using a

monochromatic Al Kα X-ray source (15 mA, 14 kV). The instrument work function was calibrated to give a binding energy (BE) of 83.96 eV for the Au 4f7/2 line for metallic gold and the spectrometer dispersion was adjusted to give a BE of 932.62 eV for the Cu 2p3/2 line of metallic copper. The Kratos charge neutralizer system was used on all samples, which were analyzed to a depth of 5-7 nm, with detection limits ranging from 0.1 to 0.5 atomic percent depending on the element. Survey scans were carried out on an analysis area of 300-700 μm at a pass energy of 160 eV. Spectra have been charge corrected to the main line of the carbon 1s spectrum (adventitious carbon) set to 284.8 eV. Spectra were analyzed using CasaXPS software version 2.3.14.

4.4 Results and Discussion

4.4.1 Three-dimensional Electrospun Fibrous Mats

Incorporating the inclusion complex prepared from α-CD and PFP into a 3D tissue engineering scaffold affords the possibility of enhancing cell viability within the construct due to the enhanced oxygen availability. In this study, electrospinning was used as a scaffold fabrication technique because it allows for the fabrication of fibrous structures that closely mimic the scale and fibrous nature of the native ECM, it is a relatively simple, cost-effective, and versatile technique, and it has been reported that CD:ICs can be successfully incorporated into scaffolds with this technique.

The method for preparing the electrospinning solution required optimization. Initially, the solution components, PCU, CD:IC, and DMF, were added concurrently and stirred until the polymer was fully dissolved and a homogeneous solution was produced. However, it was observed that the PFP separated as liquid drops at the bottom of the mixture and was displaced from the α-CD cavity, likely because the inclusion complex was destroyed during solvation in DMF. The resolution to this problem was to first fully dissolve the polymer in the solvent, and then add the CD:IC until it was thoroughly dispersed in the polymer solution. As a result, no displaced PFP was observed. It is possible that this was due to the non-ideality of the polymer solution, and that because the PCU is solvated in the DMF, the DMF molecules are not able to displace the PFP from the CD cavity.

Functionalized fibers were fabricated by electrospinning a PCU solution incorporating an inclusion complex prepared from α-CD and PFP. The PCU concentration was varied, testing the amounts 5, 7.5, 8, and 10 % (v/v) with respect to the DMF solvent. The amount of CD:IC incorporated was also varied, from 5-60 % (w/w) with respect to PCU. The concentration of CD:IC depended upon the specific PCU concentration being used, such that when the CD:IC concentration was increased, the polymer concentration was decreased. The sample nomenclature is based on the volume percentage of PCU and the weight percentage of CD:IC used in the sample preparation. For example, 10PCU-20CD:IC refers to an electrospun fibrous mat prepared from 10 % (v/v) PCU with respect to the DMF solvent and 20 % (w/w) CD:IC with respect to PCU. **Table 4-1** summarizes the different PCU/CD:IC concentrations tested and the resulting fiber morphology.

Table 4-1: Concentrations of PCU/CD:IC electrospinning solutions and characteristics of the resulting fibers

% (v/v) PCU	% (w/w) CD:IC	Fiber Morphology
5	35	Heavily beaded nanofibers
7.5	50	Bead-free nanofibers
8	30	Bead-free nanofibers
8	35	Fused nanofibers
8	45	Not uniform, heavily beaded, nanofibers
8	50	Bead-free nanofibers
8	60	Not uniform, fused, beaded nanofibers
10	5	Thick, fused microfibers
10	20	Bead-free nanofibers
10	25	Bead-free nanofibers
10	30	Slightly beaded nanofibers

Interestingly, with the incorporation of cyclodextrin it was possible to produce uniform, bead-free fibers from concentrations lower than 10 % (v/v) PCU. Our lab previously reported that electrospinning concentrations lower than 10 % (v/v) PCU was not achievable because the fibers were still wet when they reached the collector and fused with beading.[17] This ability to electrospin bead-free fibers from low polymer concentrations clearly demonstrates the positive effect of cyclodextrin on electrospinning. The addition of CD

increases the conductivity of the polymer solution, causing it to be subjected to greater stretching under the high electric field.[10, 12, 11] Bead-free, uniform fibers were obtained at both 7.5 and 8 % PCU with the incorporation of various amount of cyclodextrin (**Table 4-1**). However, when the PCU concentration was reduced to 5 %, vastly beaded fibers were obtained (see **Figure 4-1A**) because there was not enough chain entanglement and overlapping to create a stable jet.[19]
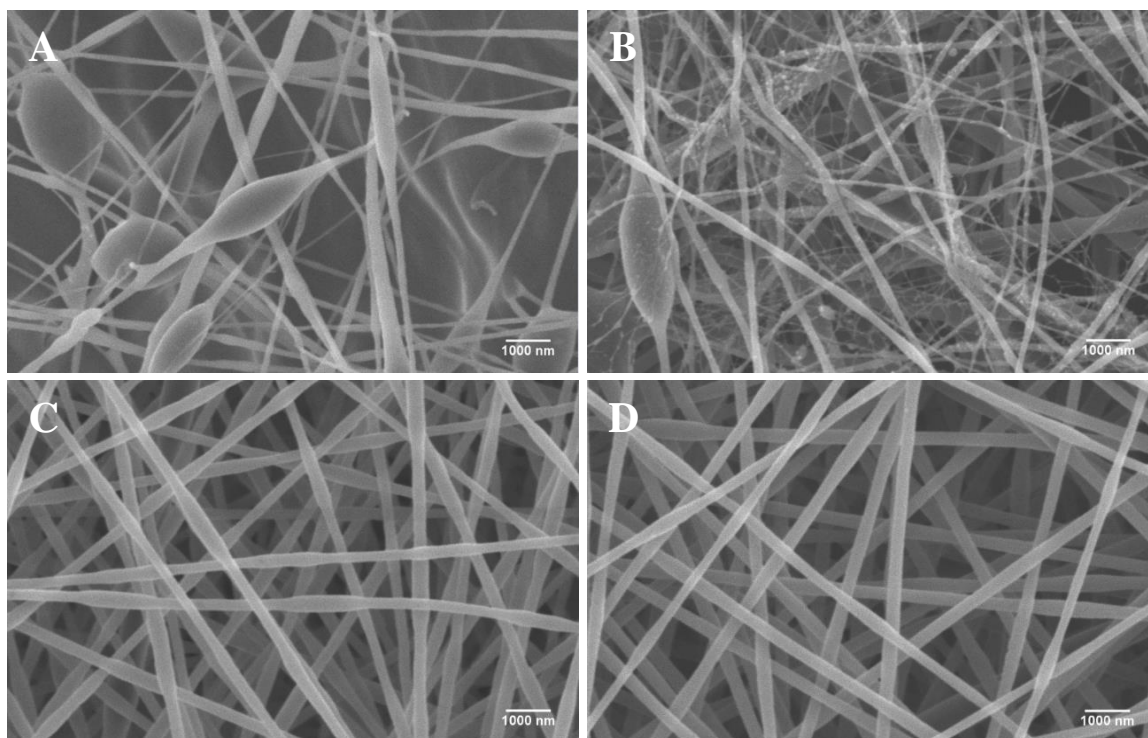
Figure 4-1: Representative SEM images of electrospun mats at 10,000x magnification (A) 5 % (v/v) PCU, 35 % (w/w) CD:IC (B) 8 % (v/v) PCU, 60 % (w/w) CD:IC (C) 8 % (v/v) PCU, 50 % (w/w) CD:IC (D) 8 % (v/v) PCU, 50 % (w/w) α-CD

Even though uniform, bead-free fibers were obtained at the initial tested concentrations of 10PCU-20CD:IC and 10PCU-25CD:IC, the ultimate objective of this work was to enhance oxygen delivery to the cells eventually seeded onto these scaffolds; thus the goal was to maximize the amount of CD:IC incorporated in the electrospun fibers. In order for the solution to be electrospinnable and to produce uniform bead-free fibers, it was necessary to decrease the polymer concentration as the amount of CD:IC incorporated was increased. **Figure 4-1B** shows the non-uniformity of the fibers obtained from 8PCU-60CD:IC, where the fiber diameter ranges considerably and various beads and other defects are present. After the SEM images for all of the tested concentrations tested were analyzed, the optimal concentration for the PCU/CD:IC solution was determined to be 8PCU-50CD:IC, shown in **Figure 4-1C**. In addition to the fibers being bead-free, it can be seen that the fibers are randomly oriented which is desirable for tissue engineering as it mimics the actual physiological structure of the ECM and allows for cell infiltration, nutrient and waste transport, and subsequent vascularization. Electrospinning was also carried out at the optimized concentration with unmodified α-CD (8PCU-50CD), and the resulting fibers are shown in **Figure 4-1D**. No notable differences were observed between the fibers incorporating CD:IC compared to those with unmodified α-CD.

Because PCU is a biostable polymer, further electrospinning studies were carried out using the biodegradable polymer PCL. In addition to its biodegradability, PCL was selected because it is biocompatible, it is commonly used in the field of biomedical engineering, and it is commercially available.[18] The sample nomenclature is based on the volume percentage of PCL and the weight percentage of CD:IC used in the sample preparation. For example, 10PCL-20CD:IC refers to an electrospun fibrous mat prepared from 10 % (v/v) PCL with respect to solvent and 20 % (w/w) CD:IC with respect to polymer. **Table 4-2** summarizes the different concentrations tested and the resulting fiber morphology.

Table 4-2: Concentrations of PCL/CD:IC electrospinning solutions, the corresponding electrospinning conditions employed, and characteristics of the resulting fibers

% (v/v) PCL	% (w/w) CD:IC	Solvent DMF:DCM Ratio	Distance (cm)	Needle Gauge	Fiber Morphology
5	50	3:1	10	22	Heavily beaded nanofibers
8	15	3:1	10	22	Uniform nanofibers with film formation
8	20	3:1	10	22	Not uniform, nanofibers, film formation
8	50	3:1	10	22	Not uniform, nanofibers, film formation, CD precipitation
10	10	3:1	10	22	Not uniform, nanofibers, film formation
10	15	3:1	10	22	Not uniform, mostly microfibers, film formation
10	20	3:1	10	22	Not uniform, mostly microfibers, film formation
10	25	3:1	10	22	Not uniform, mostly nanofibers, film formation
7.5	15	1:1	10	22	Not uniform, mostly nanofibers, some defects
			8	22	Mostly uniform, mostly nanofibers, few defects
8	15	1:1	10	22	Not uniform, mostly nanofibers, some defects and beading
			8	18	Mostly uniform, mostly nanofibers, no defects
			8	20	Uniform nanofibers, no defects
8	20	1:1	10	22	Not uniform, nanofibers, some defects
			10	18	Mostly uniform, mostly microfibers, few defects
			10	20	Mostly uniform, nanofibers, few defects
			8	20	Mostly uniform, nanofibers, few defects

As with the PCU-based solutions, the CD:IC had to be added to the solution after the PCL was fully dissolved in the co-solvent system to prevent the displacement of the PFP from the CD cavity. However, further difficulties were encountered as the polymer solutions were highly viscous and the CD:IC could not be homogeneously dispersed. For this reason, vortexing was added as a further step to the electrospinning solution preparation.
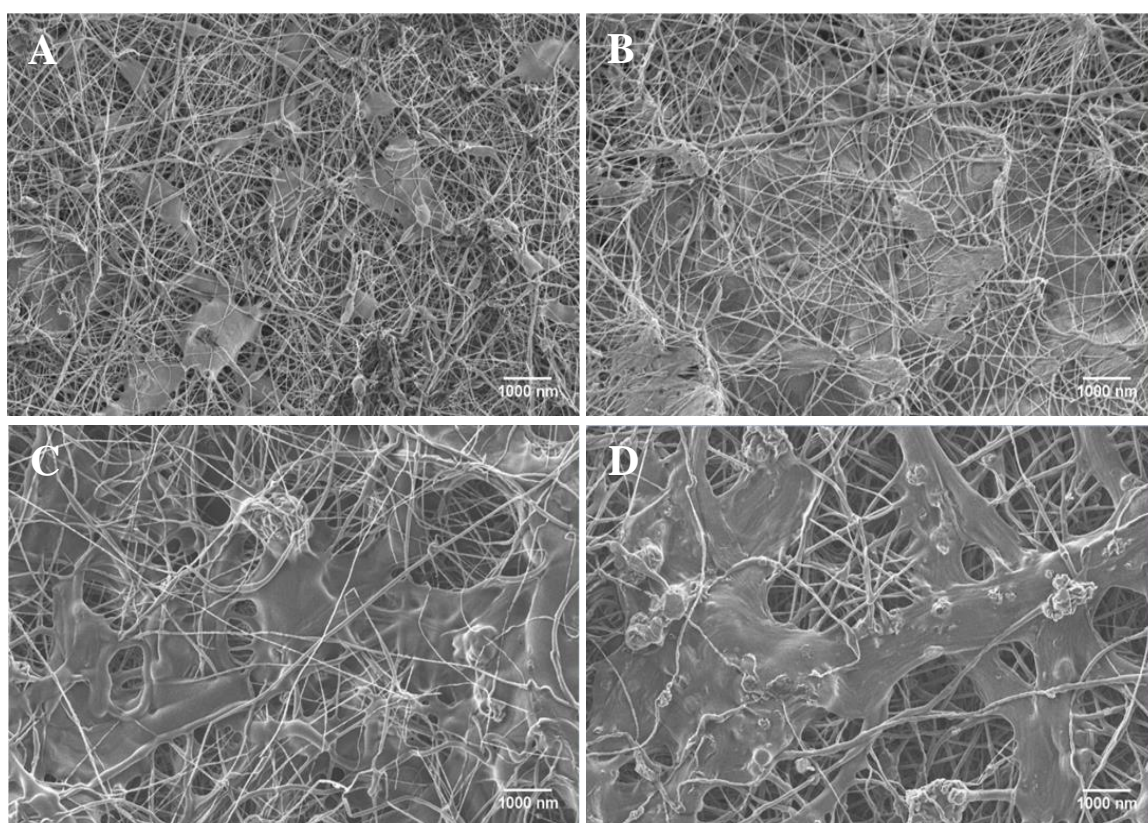
Figure 4-2: Representative SEM images of electrospun mats at 1,000x magnification highlighting the film formation on the surface of the fibrous mats when a solvent ratio of 3:1 DMF:DCM was used (A) 8 % (v/v) PCL, 15 % (w/w) CD:IC (B) 8 % (v/v) PCL, 20 % (w/w) CD:IC (C) 10 % (v/v) PCL, 10 % (w/w) CD:IC (D) 10 % (v/v) PCL, 20 % (w/w) CD:IC

1,000 x   **2,500 x**   **10,000 x**
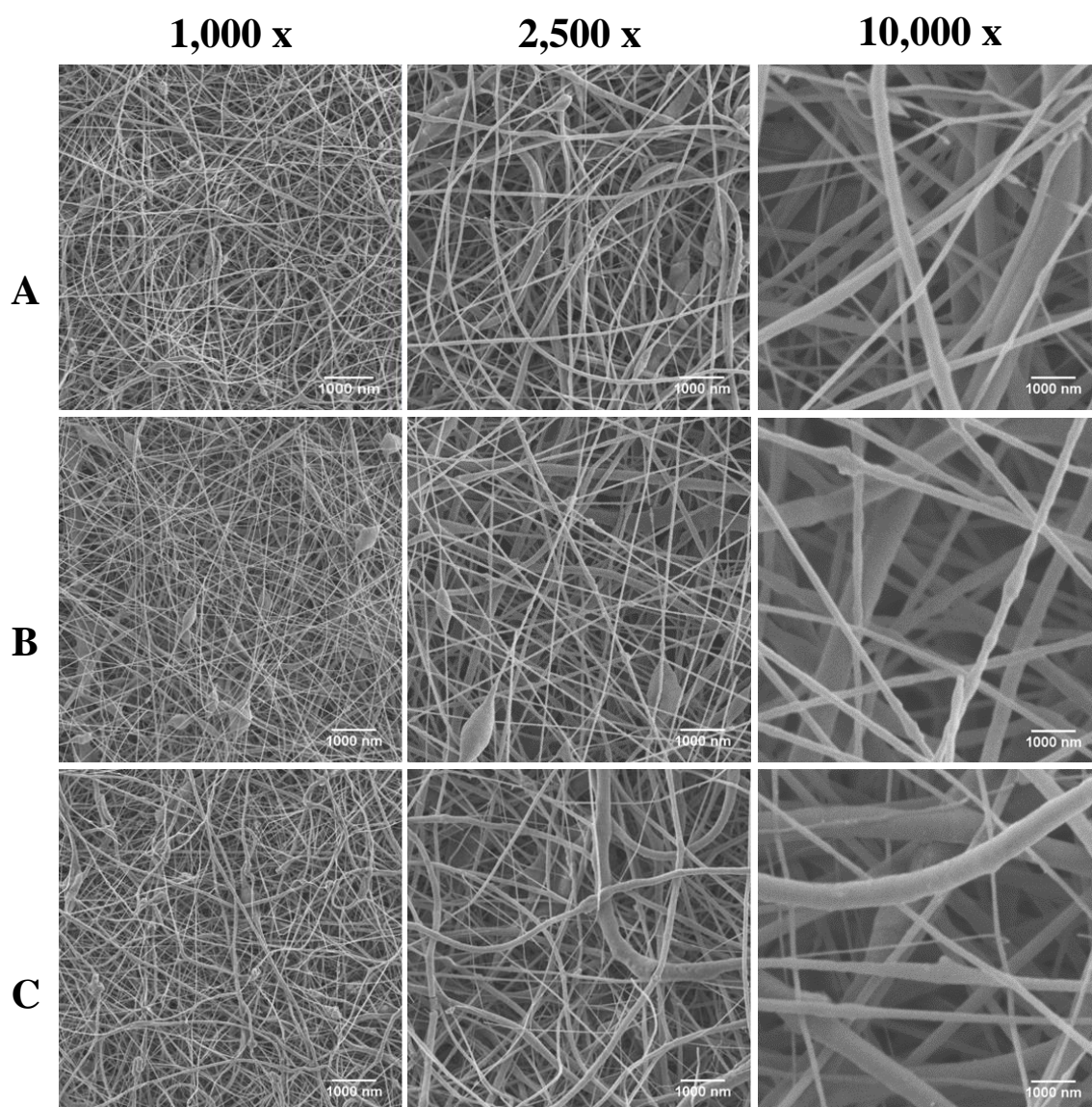
Figure 4-3: Representative SEM images of electrospun mats at multiple magnifications (A) 7.5 % (v/v) PCL, 15 % CD:IC in 1:1 DMF:DCM (B) 8 % (v/v) PCL, 15 % CD:IC in 1:1 DMF:DCM (C) 8 % (v/v) PCL, 20 % (w/w) CD:IC in 1:1 DMF:DCM

Following the conditions used by Canbolat *et al.*, the PCL electrospinning solutions were initially prepared with a co-solvent system of 3:1 (v/v) DMF:DCM, using a 22 gauge needle and a distance of 10 cm between the needle tip and collector.[7] Even after significantly varying the concentrations of both PCL and CD:IC, a film was observed on the surface of the fibrous mat at the macro scale, as can be seen in **Figure 4-2**. Then, the ratio of solvents was altered to 1:1 DMF:DCM, and the result was drastically reduced film formation (**Figure 4-3**). However, as demonstrated in **Figure 4-3**, the fiber diameter was far from uniform, and there were significant defects observed in the fibers. In an attempt to decrease the occurrence of defects and unify the fiber diameter, the electrospinning parameters were further modified, changing the needle gauge from 22 to 18 or 20, and decreasing the distance between the needle tip and collector from 10 to 8 cm. **Figure 4-4** shows representative SEM images at various concentrations of PCL and CD:IC with the variation of electrospinning conditions. Although increasing the needle inner diameter has the overall effect of increasing the fiber diameter, it was hypothesized that by increasing the thickness of the polymer jet, the CD:IC would be better encompassed in the polymer matrix, ultimately leading to a decreased occurrence of defects in the fibers. As can be seen in **Figure 4-4**, considerably reduced defects and beads on the fibers were observed and the fibers appeared to be more uniform, if thicker overall.

At this time, it was not possible to incorporate higher amounts of CD:IC into the PCL polymer matrix while maintaining the desired fiber morphology. At 8PCL-50CD:IC, it appears as though the CD:IC actually precipitated out of the polymer (**Figure 4-5A**). Decreasing the polymer concentration to 5PCL-50CD:IC resulted in a vast amount of beading (**Figure 4-5B**). These observations are similar to those made for 5PCU-35CD:IC (**Figure 4-1A**) and 8PCU-60CD:IC (**Figure 4-1B**). It is possible that with further optimization more CD:IC could be incorporated in order to increase the oxygen delivery potential of the PCL fibers. At this time, however, the optimized concentration for this study was determined to be 8PCL-15CD:IC, prepared in a co-solvent system at a 1:1 ratio of DMF:DCM and electrospun with a 20 gauge needle at a distance of 8 cm between the needle tip and collector (shown in **Figure 4-4B**).
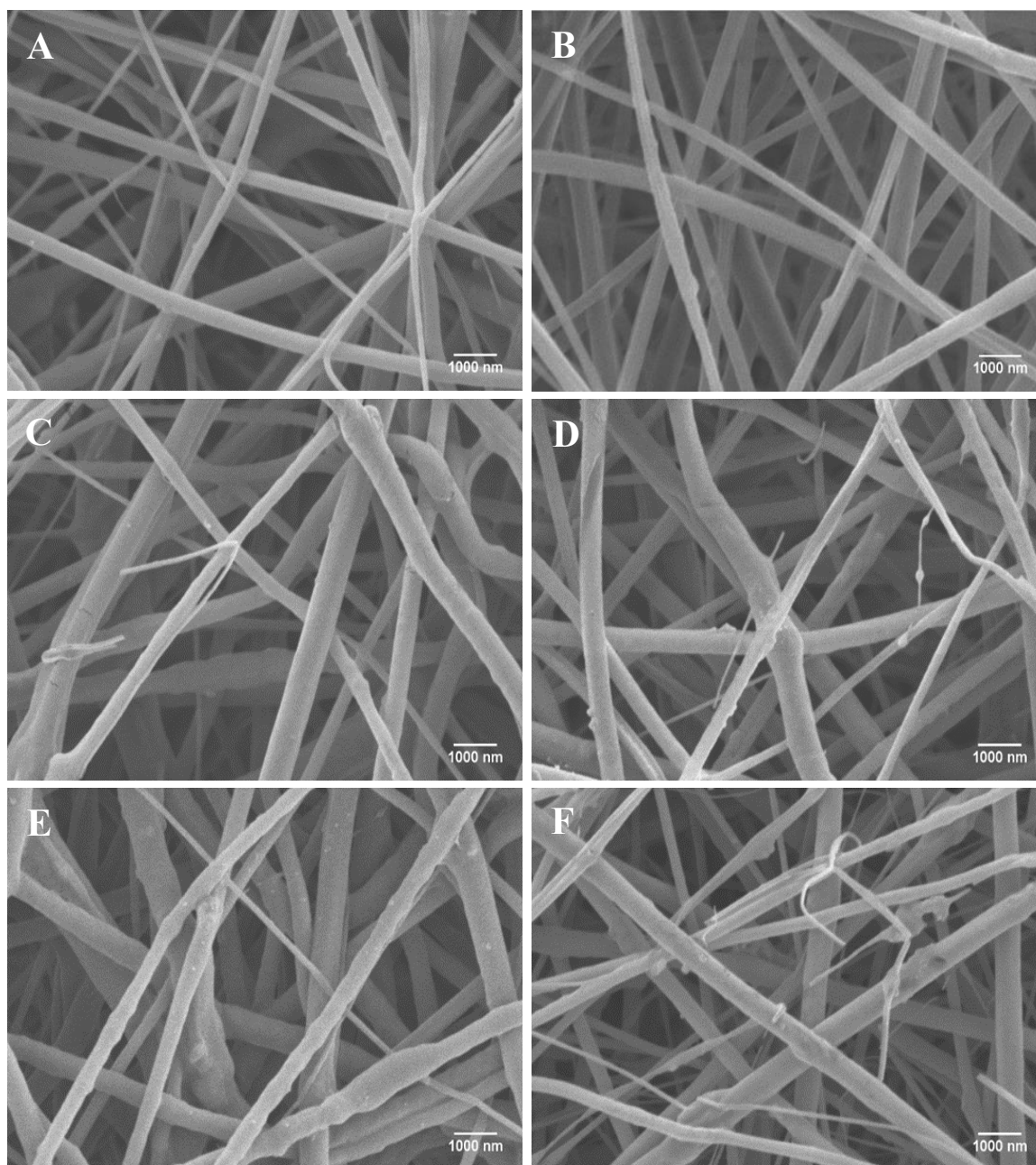
Figure 4-4: Representative SEM images at 10,000x magnification showing the reduction in defects when the electrospinning parameters were altered using 1:1 DMF:DCM co-solvent system (A) 8 % (v/v) PCL, 15 % (w/w) CD:IC with 18 gauge needle at 8 cm (B) 8 % (v/v) PCL, 15 % (w/w) CD:IC with 20 gauge needle at 8 cm (C) 8 % (v/v) PCL, 20 % (w/w) CD:IC with 20 gauge needle at 8 cm (D) 8 % (v/v) PCL, 20 % (w/w) CD:IC with 20 gauge needle at 10 cm (E) 8 % (v/v) PCL, 20 % (w/w) CD:IC with 18 gauge needle at 10 cm (F) 7.5 % (v/v) PCL, 15 % (w/w) CD:IC with 22 gauge needle at 8 cm
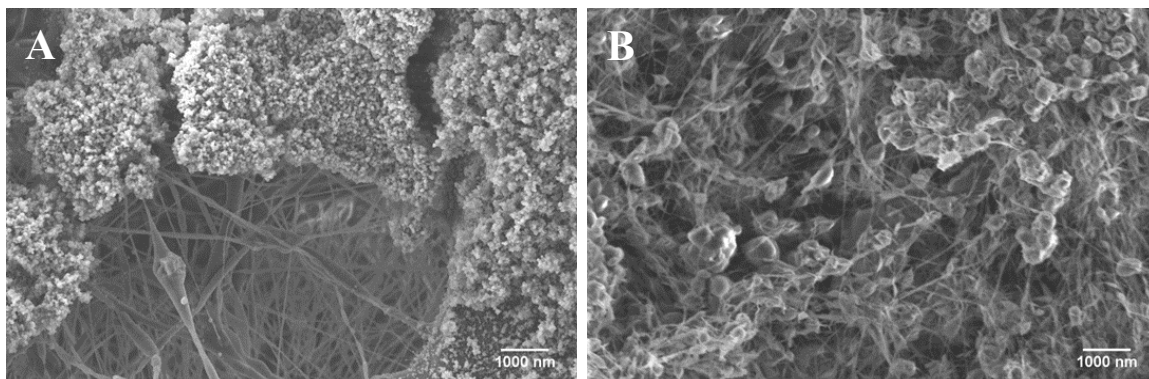
Figure 4-5: SEM images at 2,500x magnification showing the defects observed when a high concentration of CD:IC is incorporated (A) 8% (v/v) PCL, 50% (w/w) CD:IC (B) 5% (v/v) PCL, 50% CD:IC

The average fiber diameter obtained with the optimized polymer solutions was calculated using ImageJ software, measuring a total of 100 fibers from three different fields of view. For 8PCU-50CD:IC, the average fiber diameter was calculated to be (232 ± 31) nm which is within the range preferred for tissue engineering applications as they are most similar to the typical diameter of protein fibers in the native ECM.[20] The average fiber diameter for 8PCL-15CD:IC was calculated to be (342 ± 56) nm. Although significantly larger than the fibers fabricated with PCU ($p \leq 0.001$), they are still within the acceptable range for tissue engineering applications.[20] Another important feature is that the fibers obtained were uniform in diameter so that the scaffold can better recreate the functions of the native ECM.[21] **Figure 4-6A** shows the distribution of fiber diameter in the 8PCU-50CD:IC electrospun scaffold, demonstrating the relatively narrow distribution and the close fit to the normal distribution (R^2=0.97). In contrast, the fiber diameter distribution for the 8PCL-15CD:IC scaffold (**Figure 4-6B**) was not as narrow and does not follow the normal distribution as closely (R^2=0.90). This can be explained by the difficulties experienced while electrospinning the PCL-based solutions. Overall, the control over fiber morphology is important for scaffold designs that better recreate the functions of the native ECM.
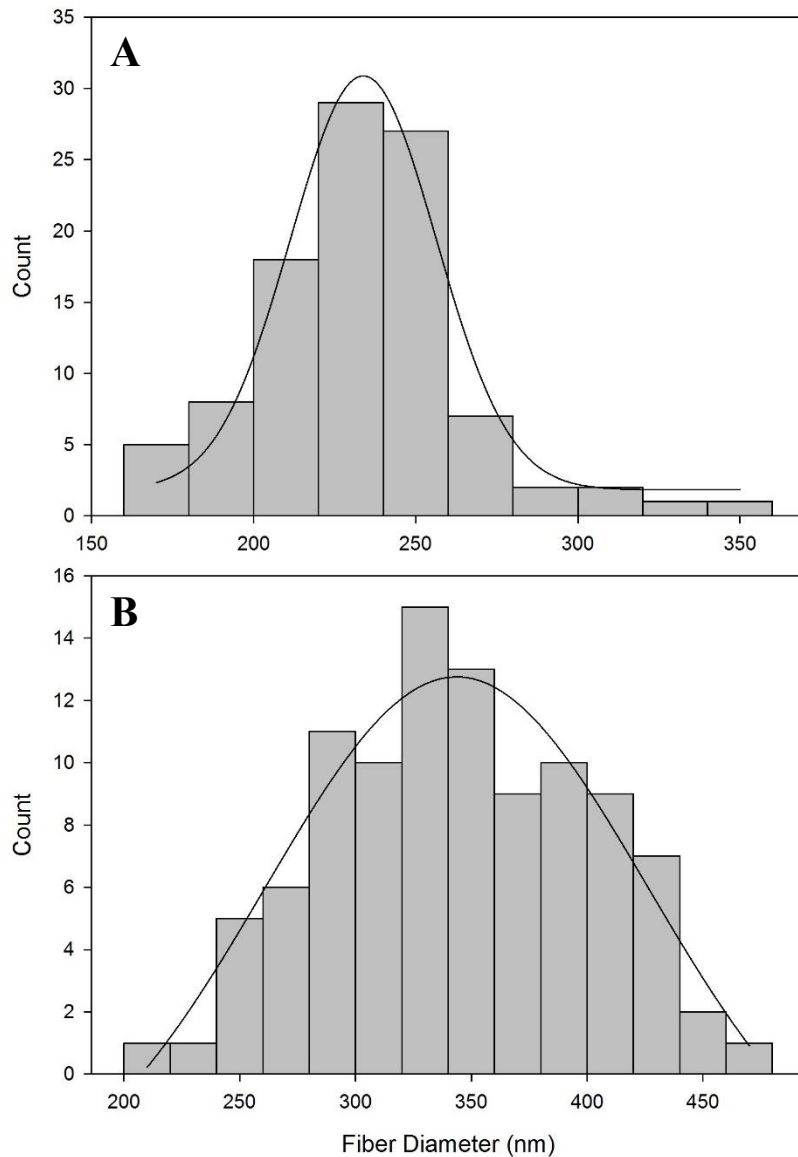
Figure 4-6: Fiber diameter distribution (N=100) of electrospun fibers and Gaussian distribution for (A) 8PCU-50CD:IC and (B) 8PCL-15CD:IC

In conclusion, it was possible to incorporate the inclusion complex prepared from α-CD and PFP in 3D scaffolds via electrospinning. Incorporating cyclodextrin in the polymer solution had a positive effect on the electrospinning process, enabling successful electrospinning at low polymer concentrations. It was possible to obtain scaffolds with acceptable fiber morphology, as determined by SEM, and there was no sign of CD:IC crystal aggregates on the surface of the fibers. This study provides confirmation of the

feasibility of incorporating the CD/PFC inclusion complexes in 3D constructs for application in tissue engineering as oxygen carriers. Arguably the most notable strength of this study is the potential of incorporating the inclusion complex in a virtually any polymer matrix through electrospinning. Successful incorporation of the CD:IC was observed with both the biostable PCU and biodegradable PCL. The optimized concentrations were determined to be 8PCU-50CD:IC and 5PCL-15CD:IC leading to fiber diameters of (232 ± 31) nm and (342 ± 56) nm, respectively.

4.4.2   Surface Characterization

The scaffolds were characterized by XPS to reveal the elemental analysis up to a depth of 5-7 nm from the surface. Characterization was carried out using polymer and CD:IC concentrations previously determined to provide fibrous mats with a morphology acceptable for tissue engineering applications. XPS of the 8PCU-50CD:IC fibrous mat was compared to that of PCU incorporating unmodified α-CD at the same concentration, that is 8 % (v/v) PCU and 50 % (w/w) α-CD, and PCU alone, electrospun from a 12 % (v/v) solution in DMF. Similarly, the 8PCL-15CD:IC fibrous mat was compared to a PCL scaffold incorporating unmodified α-CD at the same concentration, 8 % (v/v) PCL with 15 % (w/w) α-CD, as well as a PCL control scaffold electrospun from 12 % (w/v) PCL. It was necessary to electrospin the PCU and PCL control scaffolds at concentrations higher than the 8 % (v/v) concentration used in the CD:IC-modified scaffolds because the polymer concentration was too low for successful electrospinning without incorporating CD.

The elemental analysis obtained from XPS is provided in **Table 4-3** and the corresponding spectra are shown in **Appendix 6-1**. In both the PCU-CD and PCU-CD:IC fibers, a higher oxygen content is observed, confirming the presence of CD within the outer surface of the fibrous mat. However, the increase in surface content of oxygen is lower than the amount of CD incorporated. This indicates that a portion of the CD molecules are buried in the bulk of the fibers, similar to results reported in the literature for PS/CD nanofibers[9, 12] The increase in oxygen content is much less obvious for the PCL-CD and PCL-CD:IC nanofibers because only 15 % (w/w) CD or CD:IC was incorporated in the PCU fibers

compared to the 50 % (w/w) concentration of CD or CD:IC in the PCU fibers. No fluorine content is observed in the fibers containing the CD:IC because it is buried inside both the CD:IC cavity and the polymer matrix and is therefore not detected by the survey scan.

Because some of the CD:IC is buried in the bulk of the fibers, there is a benefit of using a biodegradable polymer matrix. For instance, as the PCL degrades, the CD:IC embedded within the fibrous matrix would gradually be exposed. By contrast, with a biostable polymer matrix, such as PCU, only the inclusion complexes on the surface of the fibers would be available for use as oxygen carriers and only if they are not completely covered by the polymer. Therefore, utilizing a biodegradable polymer guarantees the availability of the CD:IC over the course of an *in vitro* cell cultivation. It is also possible that the experimental parameters could be further optimized in order to obtain highly efficient fibers with a high CD content on the surface of the fibers. This may be achieved by varying the electrospinning temperature or the solvent system, for example, or by using chemically modified CD derivatives which have been reported to phase segregate to the fiber surface during solvent evaporation.[12]

Table 4-3: Elemental analysis from XPS spectra showing atomic % of each element observed

Sample	C%	O%	N%	F%
α-CD	57.6	42.4		
CD:IC	58.4	41.4		0.2
PCU	71.2	25.1	3.7	
PCU-CD	58.4	41.3	0.3	
PCU-CD:IC	60.9	38.0	1.0	
PCL	74.8	25.2		
PCL-CD	72.9	27.1		
PCL-CD:IC	74.6	25.4		

4.5 Conclusion

In this study, a CD:IC prepared from α-CD and PFP was incorporated into 3D scaffolds with the ultimate goal of improving oxygen delivery in tissue engineering applications. Electrospinning was used as the fabrication technique, and both stable and biodegradable polymer matrices were studied: PCU and PCL, respectively. Incorporating cyclodextrin in the polymer solutions showed a positive effect on electrospinning, allowing for successful electrospinning of bead-free fibers from low polymer concentrations, as expected based on previous studies.[10, 11] This is because the addition of CD increases the conductivity of the polymer solution causing the polymer solution to be subjected to higher stretching under the high electric field.[12] The CD:IC was successfully incorporated within both polymers producing bead-free, uniform fibers with suitable diameters for tissue engineering applications, as determined by SEM images. It was possible to incorporate up to 50 % (w/w) CD:IC in the PCU fibers but only 15 % (w/w) CD:IC in the PCL fibers. The average fiber diameters of the scaffolds were determined to be (232 ± 31) nm and (342 ± 56) nm for PCU-CD:IC and PCL-CD:IC, respectively, which is within the acceptable margin for most tissue engineering applications.[20]

The CD:IC-functionalized scaffolds were further characterized using XPS. An increase in oxygen content was observed when compared to PCU and PCL control scaffolds which confirms the incorporation of α-CD within the fibers. It was determined that a large amount of CD:IC was buried within the bulk of the fibers. This suggests that a biodegradable polymer matrix, such as PCL, may be better for cell culturing as the CD:IC buried within the bulk of the fibers would be exposed as the scaffold material degrades. Overall, these results provided the proof of concept necessary to support further studies on the *in vitro* ability of these functionalized fibers to enhance oxygen delivery to seeded cells.

4.6 References

1.   Langer, R.; Vacanti, J. P., Tissue engineering. *Science* **1993,** 260, (5110), 920-6.

2.   Riess, J. G., Highly fluorinated systems for oxygen transport, diagnosis and drug delivery. *Colloids Surf., A* **1994,** 84, 33-48.

3.   Radisic, M.; Park, H.; Chen, F.; Salazar-Lazzaro, J. E.; Wang, Y.; Dennis, R.; Langer, R.; Freed, L. E.; Vunjak-Novakovic, G., Biomimetic approach to cardiac tissue engineering: oxygen carriers and channeled scaffolds. *Tissue Eng* **2006,** 12, (8), 2077-91.

4.   Oh, S. H.; Ward, C. L.; Atala, A.; Yoo, J. J.; Harrison, B. S., Oxygen generating scaffolds for enhancing engineered tissue survival. *Biomaterials* **2009,** 30, (5), 757-62.

5.   Harrison, B. S.; Eberli, D.; Lee, S. J.; Atala, A.; Yoo, J. J., Oxygen producing biomaterials for tissue regeneration. *Biomaterials* **2007,** 28, (31), 4628-34.

6.   Seifu, D. G.; Isimjan, T. T.; Mequanint, K., Tissue engineering scaffolds containing embedded fluorinated-zeolite oxygen vectors. *Acta Biomater* **2011,** 7, (10), 3670-8.

7.   Canbolat, M. F.; Celebioglu, A.; Uyar, T., Drug delivery system based on cyclodextrin-naproxen inclusion complex incorporated in electrospun polycaprolactone nanofibers. *Colloids Surf B Biointerfaces* **2013,** 115C, 15-21.

8.   Kayaci, F.; Uyar, T., Encapsulation of vanillin/cyclodextrin inclusion complex in electrospun polyvinyl alcohol (PVA) nanowebs: Prolonged shelf-life and high temperature stability of vanillin. *Food Chemistry* **2012,** 133, 641-649.

9.   Uyar, T.; Havelund, R.; Hacaloglu, J.; Besenbacher, F.; Kingshott, P., Functional electrospun polystyrene nanofibers incorporating α-, β-, and γ-cyclodextrins: comparison of molecular filter performance. *ACS Nano* **2010,** 4, (9), 5121-30.

10.   Uyar, T.; Nur, Y.; Hacaloglu, J.; Besenbacher, F., Electrospinning of functional poly(methyl methacrylate) nanofibers containing cyclodextrin-menthol inclusion complexes. *Nanotechnology* **2009,** 20, (12), 125703.

11.   Uyar, T.; Hacaloglu, J.; Besenbacher, F., Electrospun polystyrene fibers containing high temperature stable volatile fragrance/flavor facilitated by cyclodextrin inclusion complexes. *Reactive & Functional Polymers* **2009,** 69, 145-150.

12.   Uyar, T.; Havelund, R.; Hacaloglu, J.; Zhou, X.; Besenbacher, F.; Kingshott, P., The formation and characterization of cyclodextrin functionalized polystyrene nanofibers produced by electrospinning. *Nanotechnology* **2009,** 20, (12), 125605.

13.   Grenier, S.; Sandig, M.; Holdsworth, D. W.; Mequanint, K., Interactions of coronary artery smooth muscle cells with 3D porous polyurethane scaffolds. *J Biomed Mater Res A* **2009,** 89, (2), 293-303.

14.   Grenier, S.; Sandig, M.; Mequanint, K., Smooth muscle alpha-actin and calponin expression and extracellular matrix production of human coronary artery smooth muscle cells in 3D scaffolds. *Tissue Eng Part A* **2009,** 15, (10), 3001-11.

15.   Lee, K. W.; Stolz, D. B.; Wang, Y., Substantial expression of mature elastin in arterial constructs. *Proc Natl Acad Sci U S A* **2011,** 108, (7), 2705-10.

16.   Williamson, M. R.; Black, R.; Kielty, C., PCL-PU composite vascular scaffold production for vascular tissue engineering: attachment, proliferation and bioactivity of human vascular endothelial cells. *Biomaterials* **2006,** 27, (19), 3608-16.

17.   Rogers, L.; Said, S.; Mequanint, K., The effects of fabrication strategies on 3D scaffold morphology, porosity, and vascular smooth muscle cell response. *Journal of Biomaterials and Tissue Engineering* **2013,** 3, (3), 300-311.

18.   Cipitria, A.; Skelton, A.; Dargaville, T. R.; Dalton, P. D.; Hutmacher, D. W., Design, fabrication and characterization of PCL electrospun scaffolds - a review. *Journal of Materials Chemistry* **2011,** 21, 9419-9453.

19.   Celebioglu, A.; Uyar, T., Cyclodextrin nanofibers by electrospinning. *Chem Commun (Camb)* **2010,** 46, (37), 6903-5.

20.   Ma, Z.; Kotaki, M.; Inai, R.; Ramakrishna, S., Potential of nanofiber matrix as tissue-engineering scaffolds. *Tissue Eng* **2005,** 11, (1-2), 101-9.

21.   Pham, Q. P.; Sharma, U.; Mikos, A. G., Electrospinning of polymeric nanofibers for tissue engineering applications: a review. *Tissue Eng* **2006,** 12, (5), 1197-211.

5 *IN VITRO* ANALYSIS OF OXYGEN DELIVERY OF CYCLODEXTRIN INCLUSION COMPLEXES WITH PERFLUOROPERHYDROPHENANTHRENE

Overview: *This chapter discusses the in vitro analysis of the effect of inclusion complexes prepared from alpha-cyclodextrin and perfluoroperhydrophenanthrene on dissolved oxygen. Studies were carried out both in solution and on 3D scaffolds incorporating the inclusion complex. Preliminary degradation studies were also carried out on the CD:IC-functionalized 3D scaffolds.*

Keywords: dissolved oxygen, oxygen delivery, tissue engineering, 3D scaffold, cyclodextrin, inclusion complex, perfluorocarbon

5.1 Introduction

Scaffold-guided tissue engineering continues to emerge as a strategy for the repair and regeneration of diseased or damaged tissues and organs as an alternative to current therapies.[1] However, one of the major factors hindering the success of scaffold-guided tissue engineering is the inability to deliver sufficient oxygen to the growing constructs. Although numerous strategies have been developed to overcome this limitation, they have been riddled with drawbacks; thus delivering sufficient oxygen remains a fundamental consideration for fabricating engineered tissues.[2-4] One approach to improve oxygen delivery to constructs is the use of perfusion bioreactors whereby oxygen dissolved in the culture medium diffuses to the scaffold material. However, the flow rate required to maintain an adequate oxygen concentration for cell viability often surpasses the shear stress tolerance of cells.[5] Alternatively, perfluorocarbons have been extensively explored as oxygen carriers due to their high dissolving power for oxygen, though the focus has been on fabricating perfluorocarbon emulsions which lack stability and are overall user-unfriendly.[6] Moreover, the high density of the emulsions causes them to settle in the culture well or medium reservoir.[7] An alternative strategy involves embedding oxygen generating compounds, such as calcium peroxide[8] or sodium percarbonate[9] which decompose in water

to produce oxygen, directly into the tissue engineering scaffold. This approach has the advantage of providing oxygen throughout the construct, specifically in the center where it is difficult to reach by diffusion alone, but it is limited as the oxygen generating compound is eventually depleted. Tissue engineering scaffolds incorporating fluorinated porous zeolite particles provide an alternative to this approach whereby the embedded compound does not generate oxygen but enhances its delivery using the principles of oxygen solubility in PFCs.[10]

In this work, cyclodextrin inclusion complexes with perfluorocarbons have been prepared for application as oxygen carriers in tissue engineering. Because inclusion of a guest molecule within the cyclodextrin cavity can provide stabilization, it may serve to overcome some of the shortcomings of PFC emulsions. Moreover, the complexes have been successfully incorporated in 3D scaffolds via electrospinning. This would impart enhanced oxygen delivery throughout the construct, and delay or prevent settling of the PCFs in the culture well or medium reservoir. It was possible to incorporate the CD/PFC complexes in both biostable (PCU) and biodegradable (PCL) polymer matrices while maintaining acceptable fiber morphology for tissue engineering. This study explores the ability of the cyclodextrin/perfluorocarbon inclusion complexes to act as oxygen carriers in terms of their ability to increase dissolved oxygen.

5.2 Materials

Perfluoroperhydrophenanthrene (PFP, mixture of isomers, 83 % purity) and alpha-cyclodextrin (α-CD, 100 % purity) were obtained commercially from Alfa Aesar (Ward Hill, MA). Solvents were purchased from Caledon Labs (Georgetown, ON). Span80 ($C_{24}H_{44}O_6$) was used as a surfactant and was purchased from Sigma Aldrich (Milwaukee, WI). All other chemicals were purchased from Sigma Aldrich. Unless noted otherwise, all chemicals were used as received without any further modification.

5.3 Methods

5.3.1   Preparation of Inclusion Complex

Weighed amounts of α-CD and a minimal amount of d.i. water were combined to form a paste. Weighed amounts of PFP were added to the α-CD paste at a 2:1 α-CD to PFP molar ratio. The paste was thoroughly mixed using a ceramic mortar and pestle for ten minutes. The product was collected in a glass vial, dried and stored in a desiccator with potassium hydroxide as a desiccant. The products were analyzed with FTIR as discussed previously (Section 3.3.3) to ensure successful complexation consistent with previous results (Section 3.4.2)

5.3.2   Fabricating 3D Scaffolds

Fibrous mats were prepared from PCU and PCL via electrospinning, at the optimized concentrations and conditions described in Section 4.4.1. PCU-CD:IC was electrospun at a concentration of 8 % (v/v) in DMF with 50 % (w/w) CD:IC incorporated, using a 22 gauge stainless steel needle at a distance of 8 cm from the needle tip to collector. A PCU control was electrospun at a concentration of 12 % (v/v) in DMF using a 22 gauge stainless steel needle at a distance of 8 cm from the needle tip to collector. PCL-CD:IC was electrospun at a concentration of 8 % (v/v) in 1:1 DMF:DCM with 15 % (w/w) CD:IC incorporated using a 20 gauge stainless steel needle at a distance of 8 cm from the needle tip to collector. A PCL control was electrospun at a concentration of 12 % (w/v) in 1:1 DMF:DCM using a 22 gauge stainless steel needle at a distance of 10 cm from the needle tip to collector.

The viscous polymer solution was transferred to a 0. 5 mL glass syringe which was then fixed horizontally on a syringe pump (KD101, KD Scientific, USA). The flow rate was maintained at 0.2 mL/h and connected to a high voltage supply (ES30P, Gamma High Voltage, USA) which applied a voltage of 15 kV. The polymer solution was refilled every 2.5 hours to electrospin a total volume of 3 mL. The fibers were collected on a grounded rotating mandrel collector which was covered with aluminum foil and a dryer sheet and

rotated at roughly 2000 RPM. Following this, the scaffolds were removed from the electrospinning assembly and the solvent was allowed to evaporate in the fume hood.

5.3.3 Dissolved Oxygen Study on Cyclodextrin Inclusion Complexes with Perfluoroperhydrophenanthrene

The dissolved oxygen was measured using a fiber optic oxygen sensor, NeoFox model FOXY-AL300 (Ocean Optics, Dunedin, FL), equipped with NeoFox software. The sensor uses ruthenium (II) complexes suspended in a support matrix and attached at the tip of a fiber optic cable. When excited by a light emitting diode at 475 nm, the ruthenium complex fluoresces and emission occurs at 620 nm. When the excited ruthenium complex encounters an oxygen molecule, the emission is quenched, allowing the intensity of the fluorescence to be related to the oxygen concentration. Accordingly, the more oxygen that is present, the lower the emission intensity and vice versa. In the absence of oxygen, the maximum fluorescent intensity of emitted light is observed. A multipoint calibration was carried out using the factory calibration file provided by Ocean Optics, followed by a single point reset at standard temperature and pressure, and 20.9 % oxygen. The oxygen sensor was placed in the solution and measured dissolved oxygen every 0.5 seconds.

Various concentrations (1, 2, 4 %) of PFP, α-CD, and CD:IC, with respect to the PFP concentration within complex, were suspended in phosphate buffered saline (PBS; pH 7.4) with and without 0.1 % Span80 as a surfactant. The samples were rocked for 90 minutes (Gel Surfer, DiaMed Supplies Inc., Mississauga, ON). PBS with and without 0.1 % Span80 was used as a control. The 300 nm diameter probe was placed in the solution while the assembly was left open to atmospheric air. Measurements were taken at both RT and 37 °C, maintained by immersing the assembly in a water bath (VWR International, Mississauga, ON). The dissolved oxygen, measured as the oxygen partial pressure (atm), was recorded until stable readings were achieved. Henry's law (**Equation 2-6**) was used to determine the oxygen concentration in the solution, and the Henry's law constant was determined at each temperature according to Blanch and Clark.[11] The samples were stored in a refrigerator at 4 °C for two weeks, at which point all dissolved oxygen measurements were taken again at both RT and 37 °C. All measurements were carried out in triplicates.

5.3.4 Dissolved Oxygen Study on 3D Scaffolds Incorporating Cyclodextrin/Perfluoroperhydrophenanthrene Inclusion Complexes

Squares of the electrospun fibrous mats (roughly 1 cm^2) were weighed, placed in a 24-well plate and covered with 1 mL of PBS (pH 7.4). The 24-well plates were placed in an incubating microplate shaker (VWR International, Mississauga, ON) at 37 °C with continuous shaking at 100 shakes/min. After 1, 3, 5, 7, 10, and 14 days, the dissolved oxygen was measured using the NeoFox fiber optic oxygen sensor. Following measurement of dissolved oxygen, the corresponding squares were removed from their well, dried in a desiccator with potassium hydroxide as a desiccant for 72 hours, and weighed. The PBS was replenished every 3 days. All measurements were carried out in triplicates.

5.3.5 Statistical Analysis

The results of the dissolved oxygen studies were analyzed using analysis of variance (ANOVA) with the Tukey post-test. The Pearson product-moment correlation coefficient was calculated in SigmaPlot (Systat Software Inc., USA). For all analyses, significance was assigned for $p<0.05$.

5.4 Results and Discussion

5.4.1 Dissolved Oxygen Study on Cyclodextrin Inclusion Complexes with Perfluoroperhydrophenanthrene

The ability of PFP to enhance oxygen delivery to cells seeded on 3D tissue engineering scaffolds was investigated. Because *in vitro* data using PFP is not reported, it was investigated if this molecule could be a candidate to enhance oxygen delivery in tissue engineering. Furthermore, the feasibility of utilizing the prepared cyclodextrin inclusion complexes from PFP and α-CD was explored.

Measurements of dissolved oxygen (DO) in the presence of different weight percentages of PFP, α-CD, and CD:IC were conducted in PBS with a fiber optic probe under a number

of conditions: with or without surfactant (0.1 % Span80), at RT or 37 °C, and immediately following sample preparation (Day 1) or after two weeks storage in a refrigerator (Day 14). It should be noted that the amount of CD:IC incorporated corresponded to the weight percent of PFP in the inclusion complex, that is, 2 % CD:IC contains 2 % PFP. **Table 5-1** shows the results of the DO measurements, reported as dissolved oxygen (mg/L) ± standard deviation (SD) and the statistical significance of the data, as determined by ANOVA, is reported in **Appendix 7-2**.

The DO measured in the PBS controls (**Table 5-1**) was comparable to the DO calculated using Henry's law (8.39 mg/L at 23 °C, 6.87 mg/L at 37 °C). When the dissolved oxygen was measured immediately following preparation (RT, no surfactant, Day 1), the data shows that by incorporating 2 % PFP in PBS, there was a significant increase in dissolved oxygen ($p=0.01$), whereas 1 % PFP was not sufficient to statistically increase the dissolved oxygen ($p=0.71$). This concurs with a previous study in our lab where a minimum threshold of 2 % perfluorodecalin was required to statistically increase the dissolved oxygen.[10] A similar relationship was observed with the incorporation of CD:IC, where a minimum threshold of 2 % was required in order to significantly increase the dissolved oxygen at RT ($p<0.001$). When the amount of PFP incorporated was increased from 2 to 4 %, a further statistically significant increase was observed ($p<0.001$). On the other hand, when the amount of CD:IC was likewise increased to 4 %, the dissolved oxygen did not increase significantly ($p=1.00$).

This experiment was also carried out at 37 °C, corresponding with body temperature. At 37 °C, for samples both with and without surfactant, incorporation of even 1 % PFP served to significantly increase the dissolved oxygen in PBS ($p<0.001$ for both). In both cases, increasing the concentration from 2 to 4 % resulted in a corresponding increase in dissolved oxygen ($p<0.001$ for both). Because they are the most relevant conditions to represent usage of these oxygen carriers in the human body, **Figure 5-1** shows the data for the dissolved oxygen measurements at 37 °C immediately following sample preparation (Day1) without the use of surfactant.

Table 5-1: Dissolved oxygen in PBS at various conditions in the presence of α-CD, PFP, and CD:IC. Dissolved oxygen was measured with a fiber optic probe. Data are means (mg/L) ± SD for experiments performed in triplicate.

RT, No Surfactant, Day 1		RT, Surfactant, Day 1		37 °C, No Surfactant, Day 1		37 °C, Surfactant, Day 1	
PBS Control	$8.64_{(\pm0.07)}$	PBS Control	$8.50_{(\pm0.09)}$	PBS Control	$6.81_{(\pm0.03)}$	PBS Control	$6.92_{(\pm0.04)}$
1% CD	$8.65_{(\pm0.03)}$	1% CD	$8.60_{(\pm0.03)}$	1% CD	$6.88_{(\pm0.02)}$	1% CD	$6.95_{(\pm0.05)}$
2% CD	$8.64_{(\pm0.04)}$	2% CD	$8.48_{(\pm0.10)}$	2% CD	$6.90_{(\pm0.02)}$	2% CD	$6.94_{(\pm0.07)}$
4% CD	$8.66_{(\pm0.01)}$	4% CD	$8.67_{(\pm0.021)}$	4% CD	$7.12_{(\pm0.04)}$	4% CD	$7.07_{(\pm0.027)}$
1% PFP	$8.73_{(\pm0.11)}$	1% PFP	$8.73_{(\pm0.03)}$	1% PFP	$7.10_{(\pm0.07)}$	1% PFP	$7.14_{(\pm0.02)}$
1% CD:IC	$8.70_{(\pm0.05)}$	1% CD:IC	$8.73_{(\pm0.03)}$	1% CD:IC	$7.29_{(\pm0.04)}$	1% CD:IC	$7.28_{(\pm0.03)}$
2% PFP	$8.85_{(\pm0.02)}$	2% PFP	$8.89_{(\pm0.05)}$	2% PFP	$7.34_{(\pm0.08)}$	2% PFP	$7.60_{(\pm0.002)}$
2% CD:IC	$8.96_{(\pm0.06)}$	2% CD:IC	$9.32_{(\pm0.04)}$	2% CD:IC	$7.41_{(\pm0.02)}$	2% CD:IC	$7.69_{(\pm0.02)}$
4% PFP	$9.13_{(\pm0.08)}$	4% PFP	$9.41_{(\pm0.14)}$	4% PFP	$7.63_{(\pm0.01)}$	4% PFP	$7.91_{(\pm0.02)}$
4% CD:IC	$8.98_{(\pm0.08)}$	4% CD:IC	$9.63_{(\pm0.03)}$	4% CD:IC	$7.87_{(\pm0.02)}$	4% CD:IC	$7.95_{(\pm0.005)}$
RT, No Surfactant, Day 14		**RT, Surfactant, Day 14**		**37 °C, No Surfactant, Day 14**		**37 °C, Surfactant, Day 14**	
PBS Control	$7.80_{(\pm0.04)}$	PBS Control	$7.84_{(\pm0.08)}$	PBS Control	$6.66_{(\pm0.02)}$	PBS Control	$6.82_{(\pm0.01)}$
1% CD	$7.62_{(\pm0.04)}$	1% CD	$7.80_{(\pm0.05)}$	1% CD	$6.78_{(\pm0.02)}$	1% CD	$6.92_{(\pm0.04)}$
2% CD	$7.74_{(\pm0.07)}$	2% CD	$7.98_{(\pm0.02)}$	2% CD	$6.78_{(\pm0.02)}$	2% CD	$6.88_{(\pm0.02)}$
4% CD	$8.29_{(\pm0.03)}$	4% CD	$8.16_{(\pm0.01)}$	4% CD	$6.93_{(\pm0.09)}$	4% CD	$6.84_{(\pm0.02)}$
1% PFP	$8.05_{(\pm0.03)}$	1% PFP	$8.26_{(\pm0.04)}$	1% PFP	$6.91_{(\pm0.02)}$	1% PFP	$7.04_{(\pm0.04)}$
1% CD:IC	$7.94_{(\pm0.07)}$	1% CD:IC	$8.36_{(\pm0.01)}$	1% CD:IC	$7.13_{(\pm0.02)}$	1% CD:IC	$7.27_{(\pm0.01)}$
2% PFP	$8.02_{(\pm0.004)}$	2% PFP	$8.47_{(\pm0.01)}$	2% PFP	$7.22_{(\pm0.01)}$	2% PFP	$7.51_{(\pm0.02)}$
2% CD:IC	$8.14_{(\pm0.04)}$	2% CD:IC	$8.91_{(\pm0.04)}$	2% CD:IC	$7.32_{(\pm0.01)}$	2% CD:IC	$7.61_{(\pm0.01)}$
4% PFP	$8.53_{(\pm0.01)}$	4% PFP	$9.29_{(\pm0.05)}$	4% PFP	$7.40_{(\pm0.01)}$	4% PFP	$7.75_{(\pm0.01)}$
4% CD:IC	$8.66_{(\pm0.04)}$	4% CD:IC	$9.54_{(\pm0.04)}$	4% CD:IC	$7.71_{(\pm0.001)}$	4% CD:IC	$7.92_{(\pm0.02)}$

The dissolved oxygen was also measured in samples containing 0.1 % Span80 as a surfactant, with the same weight percentages of α-CD, PFP, and CD:IC. Relevant statistical data comparing results obtained with and without the use of surfactant are presented in **Appendix 7-3**. Adding a surfactant had a considerable impact on the results at both RT and 37 °C, as well as on Day 1 and Day 14. Statistically significant increases in dissolved oxygen were observed in all cases at as low as 1 % for both PFP and CD:IC. This is specifically notable in comparison to RT, Day 1 conditions where a minimum threshold of 2 % PFP was required to produce a statistically significant increase without surfactant. These changes can likely be attributed to the emulsifying properties of the surfactant,

producing a more stable system between the PFP and PBS. Furthermore, increasing the concentration from 2 to 4 % served to further enhance the dissolved oxygen, in both the case of PFP and CD:IC under all conditions.
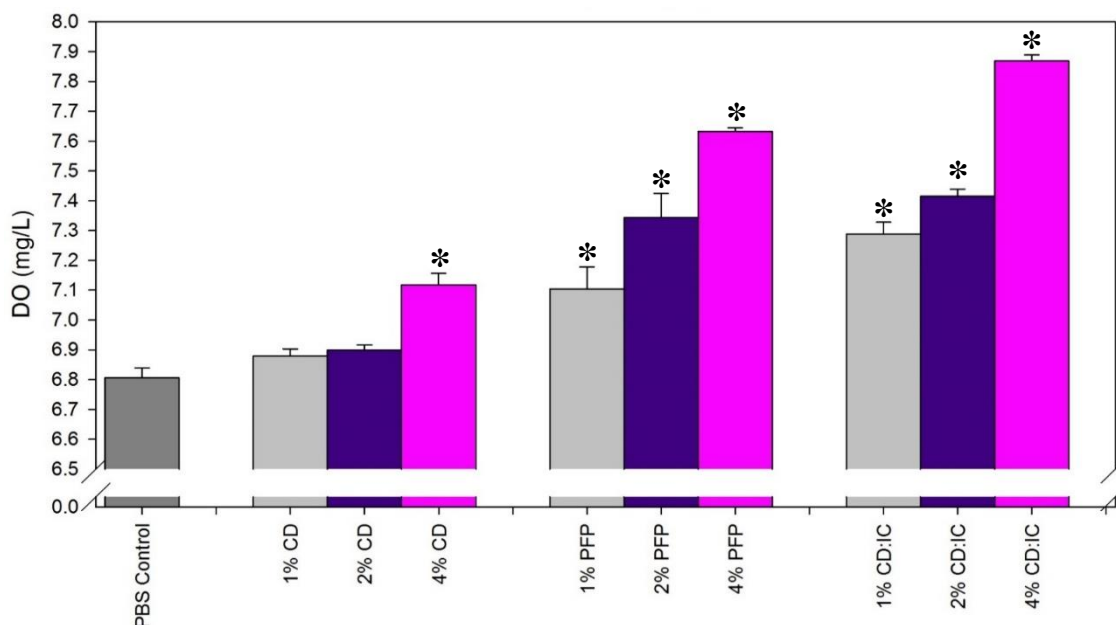
Figure 5-1: Dissolved oxygen in PBS (37 °C, no surfactant, Day 1), in the presence of different weight percentages of α-CD, PFP, and CD:IC. Dissolved oxygen was measured using a fiber optic probe. Data are means ± SD for experiments conducted in triplicate, * indicates statistical significance at *p*<0.05.

Following DO measurements on Day 1, the samples were stored in a refrigerator at 4 °C for two weeks in order to test the ability of the perfluorinated compounds, specifically in the form of the inclusion complex, to enhance oxygen delivery after storage. Relevant statistical data for these long term studies is presented in **Appendix 7-4**. Most interestingly, all of the measurements at 37 °C (without surfactant) were statistically comparable to those taken under the same conditions on Day 1. This indicates that including the PFC in the cyclodextrin cavity serves to enhance the stability of the PFC. These results are extremely relevant as one of the main disadvantages of using PFC emulsions is their lack of stability, resultant stringent storage requirements, and overall lack of user-friendliness.[1, 6] Furthermore, with the exception of two conditions, utilizing the CD:IC as opposed to unmodified PFP actually served to further enhance the dissolved oxygen. For example, at 37 °C (without surfactant, Day 1), the dissolved oxygen was (7.63±0.01) mg/L for 4 %

PFP and (7.87±0.03) mg/L for 4 % CD:IC, demonstrating a significant difference ($p<0.001$).

An interesting trend was observed with the incorporation of 1, 2, and 4 % α-CD when compared to PBS. At 37 °C (Day 1), both with and without surfactant, incorporation of 4 % α-CD resulted in a statistically significant increase in dissolved oxygen ($p<0.001$ for both). After 14 days of storage in a refrigerator at 4 °C, this effect was further enhanced with increases in dissolved oxygen occurring at both RT and 37 °C as well as with and without surfactant. Furthermore, the dissolved oxygen was statistically increased with as low as 1 % α-CD in a number of cases. It has been shown that cyclodextrins can store gases in their cavity, particularly α-CD because the small size of its cavity suits the low molecular weight of the gases.[12] Cramer and Henglein[13] showed that by bubbling various gases, such as chlorine, xenon, and oxygen in an α-CD/water solution at 7-120 atm, crystalline gas complexes could be isolated and remained stable for months at room temperature. The amount of gas complexed varied between 0.3 and 1.2 moles of gas per mole of α-CD and could be easily evolved by simply dissolving the crystalline complex in water.[12, 14] It is therefore possible that certain conditions, such as increasing the temperature to 37 °C, allowed the α-CD to form an inclusion complex with oxygen, effectively increasing the dissolved oxygen in solution.

Further statistical analysis was carried out on the dissolved oxygen measurements by computing the Pearson product-moment correlation coefficient in order to determine the linear dependence of the dissolved oxygen on the concentration of PFP and CD:IC. The results are presented in **Table 5-2** and indicate a clear significant linear relationship between the concentration of both PFP and CD:IC and dissolved oxygen in all cases. This relationship demonstrates that as the concentration of PFP or CD:IC is increased, the dissolved oxygen also increases.

Table 5-2: Pearson product-moment correlation coefficients and corresponding *p* values demonstrating linear dependence of DO on concentration of PFP and CD:IC

	PFP	CD:IC	PFP	CD:IC	PFP	CD:IC	PFP	CD:IC
	RT, No Surfactant, Day 1		*RT Surfactant Day 1*		*37 °C No Surfactant Day 1*		*37 °C Surfactant Day 1*	
Correlation Coefficient	0.94	0.84	0.98	0.96	0.97	0.97	0.97	0.96
p value	4.52 E-06	6.34E-04	7.32E-08	8.27E-07	1.26E-07	1.21E-07	9.39E-08	4.36E-07
	RT, No Surfactant Day 14		*RT Surfactant Day 14*		*37 °C No Surfactant Day 14*		*37 °C Surfactant Day 14*	
Correlation Coefficient	0.96	0.99	0.99	0.99	0.96	0.97	0.96	0.97
p value	1.16 E-06	5.50E-09	2.65E-10	2.20E-09	7.47E-07	1.06E-07	6.17E-07	2.98E-07

In summary, the feasibility of utilizing PFP as an oxygen carrier molecule was shown. At 37 °C, as low as 1 % PFP resulted in a significant increase in the dissolved oxygen in PBS as measured with a NeoFox fiber optic probe. Dissolved gases are transported by perfluorinated compounds due to increased solubility in accordance with Henry's Law. The increased solubility in attributed to the existence of loose, non-directional van der Waals interactions leading to low cohesive energy densities, which facilitate mutual solubilization of oxygen in the fluorine compound. The feasibility of using an inclusion complex prepared from α-CD and PFP was also established. In fact, the CD:IC served to further increase the dissolved oxygen when compared to the same concentration of PFP at a number of conditions. Furthermore, including the PFP within the CD cavity was shown to improve the stability over a period of two weeks when stored in a refrigerator at 4 °C. Overall, this study indicates that CD:ICs prepared with PFCs can be used as oxygen carriers to enhance oxygen delivery in tissue engineering applications.

5.4.2 Dissolved Oxygen Study on 3D Scaffolds Incorporating Cyclodextrin/Perfluoroperhydrophenanthrene Inclusion Complexes

The feasibility of utilizing a cyclodextrin inclusion complex prepared with a PFC as an oxygen carrier was explored with promising results. Theoretically, the complexes could be added directly to the culture media and the effect on dissolved oxygen would be similar to that reported in the previous section (5.4.1). However, this is not an improvement over other studies where the PFC was added directly to the culture medium and their high density caused them to settle, limiting their potential.[7, 15] For this reason, in this study the CD:ICs were incorporated into a tissue engineering construct, fabricated using the electrospinning technique. This serves to immobilize the PFC within the scaffold and delay or prevent settling of the PFC into the culture medium, while providing enhanced oxygen delivery throughout the construct, specifically in the center where it is difficult for oxygen to permeate by diffusion alone.

Two different materials were explored as polymer matrices for fabricating the tissue engineering constructs incorporating the CD:IC. PCU and PCL were selected as stable and biodegradable polymers, respectively. The constructs were fabricated via electrospinning from concentrations optimized previously (Section 4). The optimized concentration for PCU was 8 % (v/v) PCU with respect to solvent and 50 % (w/w) CD:IC with respect to PCU, referred to as 8PCU-50CD:IC. The optimized concentration for PCL was 8 % (v/v) PCL with respect to solvent, 15 % (w/w) CD:IC with respect to PCL, referred to as 8PCL-15CD:IC. The CD:IC-functionalized scaffolds were compared to scaffolds fabricated from unmodified PCU and PCL. Squares of the fibrous mats (roughly 1 cm^2) were placed in PBS at 37 °C and the DO was measured after 1, 3, 5, 7, 10, and 14 days with a fiber optic probe. **Table 5-3** shows the results of these measurements, reported as dissolved oxygen (mg/L) ± standard deviation. **Figure 5-2** and **Figure 5-3** graphically depict these measurements for the PCU- and PCL-based scaffolds, respectively.

Table 5-3: Dissolved oxygen in PBS in the presence of electrospun 3D fibrous mats fabricated from PCU or PCL incorporating an inclusion complex prepared from α-CD and PFP. Dissolved oxygen was measured with a fiber optic probe. Data are means (mg/L) ± SD for experiments performed in triplicate.

Day	PCU Control	PCU-CD:IC	PCL Control	PCL-CD:IC
1	$6.43_{(\pm 0.22)}$	$8.47_{(\pm 0.48)}$	$6.57_{(\pm 0.20)}$	$8.52_{(\pm 0.80)}$
3	$7.82_{(\pm 0.08)}$	$8.07_{(\pm 0.32)}$	$8.38_{(\pm 0.18)}$	$9.02_{(\pm 0.42)}$
5	$8.13_{(\pm 0.26)}$	$9.71_{(\pm 0.32)}$	$8.35_{(\pm 0.33)}$	$9.94_{(\pm 0.29)}$
7	$8.26_{(\pm 0.35)}$	$10.9_{(\pm 0.53)}$	$8.24_{(\pm 0.87)}$	$9.62_{(\pm 0.45)}$
10	$7.04_{(\pm 0.96)}$	$9.38_{(\pm 0.26)}$	$7.94_{(\pm 0.42)}$	$9.51_{(\pm 0.21)}$
14	$7.93_{(\pm 0.19)}$	$9.63_{(\pm 0.62)}$	$8.40_{(\pm 0.12)}$	$10.0_{(\pm 0.46)}$
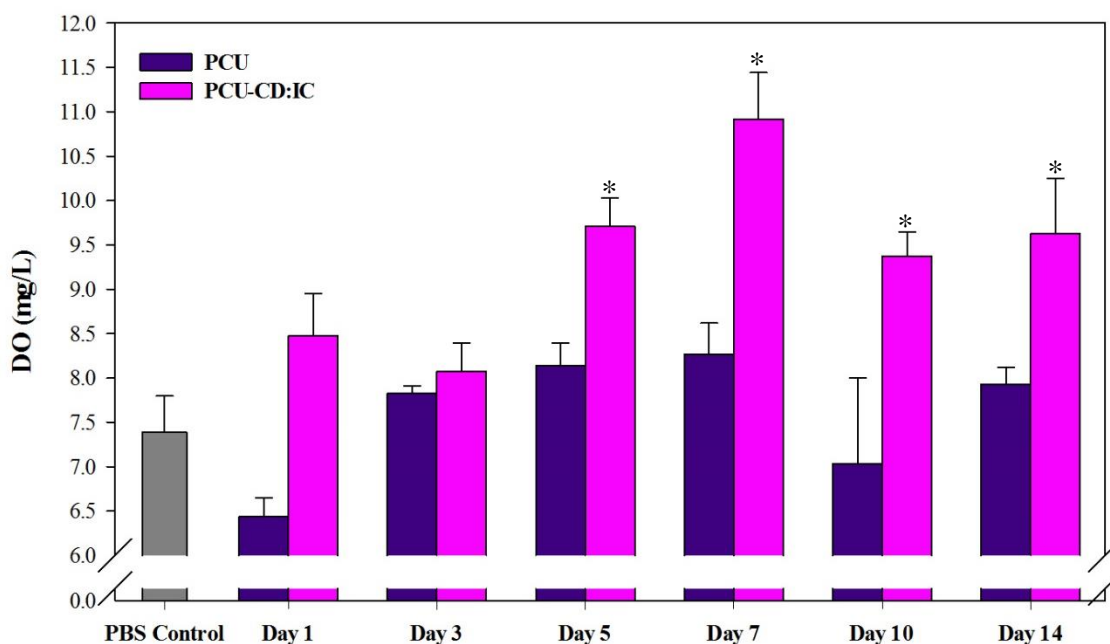
Figure 5-2: Dissolved oxygen measurements for PCU and PCU-CD:IC scaffolds in PBS at 37 °C. Dissolved oxygen was measured using a fiber optic probe. Data are means ± SD for experiments conducted in triplicate, * indicates statistical significance at $p<0.05$
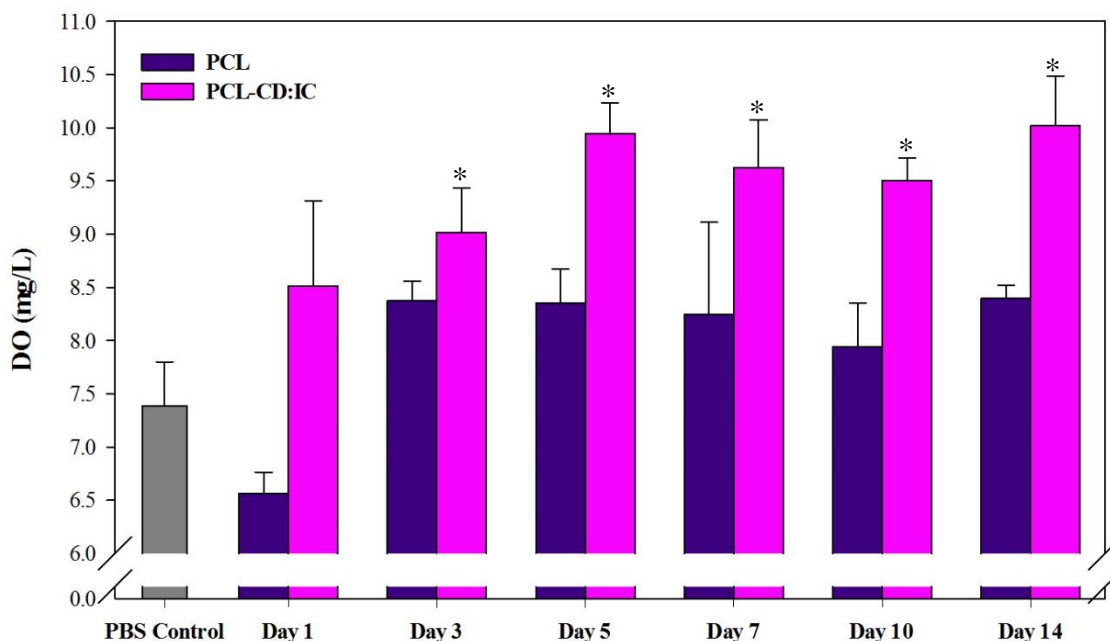
Figure 5-3: Dissolved oxygen measurements for PCL and PCL-CD:IC scaffolds in PBS at 37 °C. Dissolved oxygen was measured using a fiber optic probe. Data are means ± SD for experiments conducted in triplicate, * indicates statistical significance at $p<0.05$

When compared to the PBS control, neither the PCU nor the PCL scaffolds showed any significant increase in dissolved oxygen at any time point, as expected (statistical data is presented in **Appendix 7-5**). As indicated in **Figure 5-2**, the PCU-CD:IC scaffold showed a significant increase in DO on Day 5 ($p<0.001$). Likewise, the PCL-CD:IC scaffold showed a significant increase in DO on Day 3 ($p=0.01$), as indicated in **Figure 5-3**. The DO was observed to remain significantly increased over the remainder of the 14 day period in the presence of both PCU-CD:IC and PCL-CD:IC fibrous mats.

Further statistical analysis was carried out on the dissolved oxygen measurements by computing the Pearson product-moment correlation coefficient in order to determine the linear dependence of the dissolved oxygen measurement on time. The results are presented in **Table 5-4** and demonstrate a lack of significant linear relationship between time and the dissolved oxygen measured for all materials except the PCL-CD:IC nanofibers. The PCL-CD:IC nanofibers show a significant but weak relationship between the variables, with the

DO tending to increase with time. Because PCL is a degradable polymer whereas PCU is not, it is likely that this trend would be further enhanced with a stronger relationship evident over long-term studies, corresponding to the degradation of PCL.

Table 5-4: Pearson product-moment correlation coefficients for the dissolved oxygen concentration and time for CD:IC-functionalized scaffolds

	PCU Control	PCU-CD:IC	PCL Control	PCL-CD:IC
Correlation Coefficient	0.29	0.46	0.46	0.61
_p_ value	0.24	0.06	0.05	0.007

Figure 5-4 shows a graphical comparison of the two polymer materials, PCU and PCL with the CD:IC incorporated, and **Appendix 7-6** shows the corresponding statistical analysis of the DO measurements. There was no statistical difference between the DO measured in the presence of either material at any time point. This is interesting because it was possible to incorporate considerably more CD:IC in the PCU fibers than in the PCL fibers. This may be explained by the fact that PCL is degradable whereas PCU is not, thus only the complexes on the surface of the PCU-CD:IC fibers were available whereas when the PCL matrix began to degrade, increasingly more complex was released. Further studies are necessary to ascertain how the two materials would compare over the long term. It is predicted that the oxygen delivery provided by the PCL-CD:IC scaffold would exceed that of the PCU-CD:IC material because it is biodegradable. Over the lifespan of the PCL, (> 2 years)[16] CD:IC would become uncovered from the polymer matrix and/or completely released. This would serve to prolong the improvement of oxygen delivery to the cells seeded on the construct whereas the CD:IC contained within the PCU fibers would remain buried throughout the culture time.
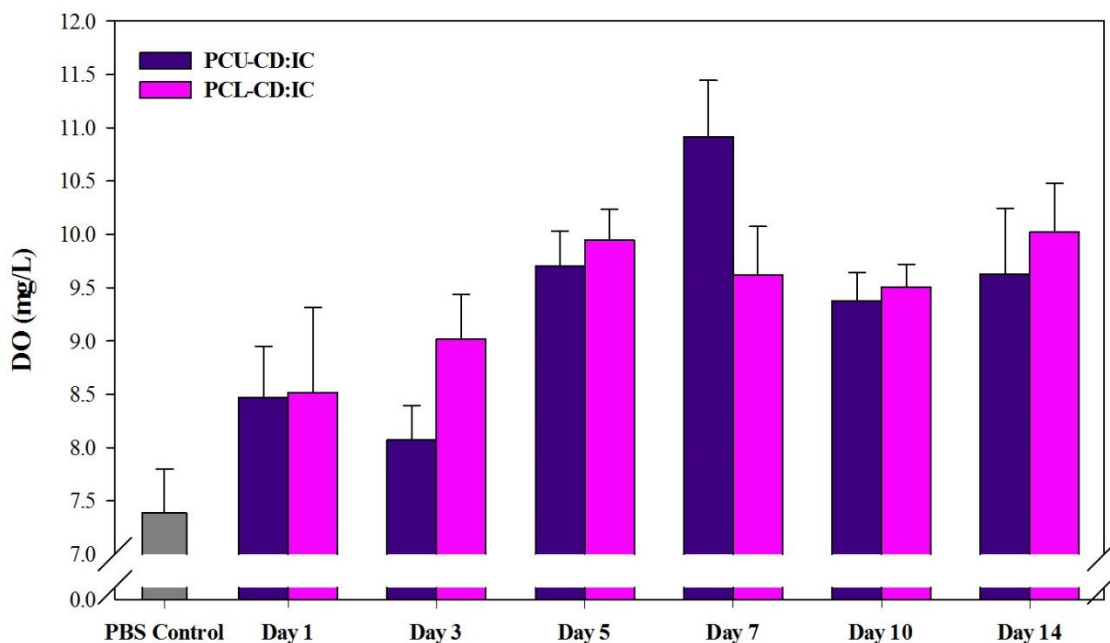
Figure 5-4: Dissolved oxygen measurements for PCU-CD:IC and PCL-CD:IC scaffolds in PBS at 37 °C. Dissolved oxygen was measured using a fiber optic probe. Data are means ± SD for experiments conducted in triplicate, * indicates statistical significance at $p<0.05$

A preliminary study was carried out in order to ascertain if there was a burst of CD:IC released from the polymer matrix upon submersion in PBS; the change in mass of the fibrous mats were studied alongside the DO measurements. The results of this study are presented in **Table 5-5**. Any increases in mass can be attributed to precipitation of PBS salts on the scaffold after they were dried for 72 hours. A desiccator was used instead of heat to dry to the scaffolds in order to prevent destruction of the inclusion complex and loss of the PFP guest. Consequently, it is possible that only the surface moisture was removed such that residual PBS on the fibers would cause a superficial increase in the final mass of the fibers. Due to the inconsistency in the change in mass of the fibers, the release of CD:IC from the fibers cannot be commented on conclusively. Nevertheless, it was observed that overall there was a greater release from the PCU-CD:IC fibers when compared to the PCU control fibers. Because PCU is not a degradable polymer, this loss can likely be attributed to the leaching of the CD:IC from the surface of the fibers. A similar trend was not distinguishable for the PCL-based scaffolds and the results were

inconclusive. Further studies should be carried out to better ascertain the changes in the electrospun fibers after submersion in PBS with respect to the release of CD:IC and its effect on dissolved oxygen. For instance, analysis of SEM images would allow for the observation of morphological changes occurring in the fibers with mass loss.

Table 5-5: Change in mass (%) recorded for 3D PCU and PCL scaffolds incorporating CD:IC and their corresponding controls

Day	PCU Control				PCU-CD:IC			
	A	B	C	Average	A	B	C	Average
1	-14.3	-1.85	-19.5	-119	-12.5	-23.8	-32.0	-22.8
3	5.26	5.56	10.3	7.04	-30.0	-36.0	-43.8	-36.6
5	-4.35	6.25	-2.63	-0.24	-25.0	-35.6	-47.1	-35.9
7	3.85	9.52	0.00	4.46	-43.4	-41.9	-51.4	-45.6
10	-2.04	4.55	0.00	0.83	-37.2	-38.3	-37.0	-37.5
14	-5.71	0.00	0.00	-1.90	-37.5	175	62.8	66.8

Day	PCL Control				PCL-CD:IC			
	A	B	C	Average	A	B	C	Average
1	-8.33	-25.0	-11.1	-14.8	-33.3	-21.2	-27.6	-27.4
3	-14.3	-3.23	-4.55	-7.36	-19.5	-4.17	-5.26	-9.64
5	-14.3	-9.09	-14.3	-12.6	-14.3	-17.0	-14.0	-15.1
7	-0.36	-0.31	-0.29	-0.32	-20.5	-20.4	-26.1	-22.3
10	-20.4	-23.3	-29.0	-24.2	-20.0	-15.4	-16.7	-17.4
14	-42.1	-16.0	-8.33	-22.1	128.0	16.7	36.7	60.5

Overall, incorporating the CD:IC within 3D electrospun scaffolds resulted in an increase in the DO measured in the surrounding PBS. The results of this study are promising and suggest that incorporating CD/PFC inclusion complexes in scaffolds would be an effective strategy for enhancing the oxygen delivery to cells seeded on the constructs. An increase in dissolved oxygen was observed with both biostable, PCU, and biodegradable, PCL, materials. This promotes the idea that this approach is incredibly versatile, such that the CD:IC could theoretically be incorporated in a plethora of different polymer materials via electrospinning. Furthermore, these results indicate that at least some of the CD:IC embedded within the constructs was on the surface of the fibers and available for oxygen delivery. This correlates with the data obtained from XPS (Section 4.4.2) which

demonstrated that there was increased oxygen content on the surface of the fibers. Although this study served as a proof of concept, further studies are required in order to ascertain the ability of these scaffolds to enhance oxygen delivery in the long term.

5.5 Conclusion

One unsolved problem in tissue engineering is overcoming the diffusional limitations of oxygen which lead to hypoxia in the center of tissue engineering constructs. In this study, the feasibility of using PFP as an oxygen carrier, specifically in the form of a cyclodextrin inclusion complex, was explored. Dissolved oxygen concentration significantly increased in the presence of PFP at all conditions tested, with as low as 1% PFP required for a statistically significant increase in most cases. At a number of conditions, it was observed that incorporating the PFP in the form of a cyclodextrin inclusion complex actually served to further enhance the dissolved oxygen in solution. Moreover, including the PFP within the α-CD cavity served to enhance the stability of the PFP and the complexes provided a statistically significant increase in DO after storage in the refrigerator for 2 weeks.

The CD:IC was then embedded in 3D PCU and PCL scaffolds fabricated via electrospinning. Dissolved oxygen concentration increased in PBS in the presence of these scaffolds on Day 3 for PCL-CD:IC and Day 5 for PCU-CD:IC, and remained statistically higher than the PBS control for both materials over the remainder of the 14 day period. This indicates that at least some of the CD:IC remained available for oxygen delivery when contained within the polymer matrix.

Taken together, these data suggest the potential for scaffolds functionalized with CD:IC to enhance oxygen delivery to seeded cells for application in tissue engineering. Incorporating the oxygen carrier directly in the scaffold enables the delivery of oxygen throughout the construct, especially in the center where it is difficult to reach by diffusion alone. Furthermore, it is an improvement upon using PFCs and their emulsions directly in the culture media because the oxygen carriers are embedded within the scaffold and therefore will not settle in the media.

5.6 References

1.   Langer, R.; Vacanti, J. P., Tissue engineering. *Science* **1993,** 260, (5110), 920-6.

2.   Malda, J.; Rouwkema, J.; Martens, D. E.; Le Comte, E. P.; Kooy, F. K.; Tramper, J.; van Blitterswijk, C. A.; Riesle, J., Oxygen gradients in tissue-engineered PEGT/PBT cartilaginous constructs: measurement and modeling. *Biotechnol Bioeng* **2004,** 86, (1), 9-18.

3.   Radisic, M.; Deen, W.; Langer, R.; Vunjak-Novakovic, G., Mathematical model of oxygen distribution in engineered cardiac tissue with parallel channel array perfused with culture medium containing oxygen carriers. *Am J Physiol Heart Circ Physiol* **2005,** 288, (3), H1278-89.

4.   Radisic, M.; Malda, J.; Epping, E.; Geng, W.; Langer, R.; Vunjak-Novakovic, G., Oxygen gradients correlate with cell density and cell viability in engineered cardiac tissue. *Biotechnol Bioeng* **2006,** 93, (2), 332-43.

5.   Yu, X.; Botchwey, E. A.; Levine, E. M.; Pollack, S. R.; Laurencin, C. T., Bioreactor-based bone tissue engineering: the influence of dynamic flow on osteoblast phenotypic expression and matrix mineralization. *Proc Natl Acad Sci U S A* **2004,** 101, (31), 11203-8.

6.   Riess, J. G., Highly fluorinated systems for oxygen transport, diagnosis and drug delivery. *Colloids Surf., A* **1994,** 84, 33-48.

7.   Radisic, M.; Park, H.; Chen, F.; Salazar-Lazzaro, J. E.; Wang, Y.; Dennis, R.; Langer, R.; Freed, L. E.; Vunjak-Novakovic, G., Biomimetic approach to cardiac tissue engineering: oxygen carriers and channeled scaffolds. *Tissue Eng* **2006,** 12, (8), 2077-91.

8.   Oh, S. H.; Ward, C. L.; Atala, A.; Yoo, J. J.; Harrison, B. S., Oxygen generating scaffolds for enhancing engineered tissue survival. *Biomaterials* **2009,** 30, (5), 757-62.

9.   Harrison, B. S.; Eberli, D.; Lee, S. J.; Atala, A.; Yoo, J. J., Oxygen producing biomaterials for tissue regeneration. *Biomaterials* **2007,** 28, (31), 4628-34.

10.   Seifu, D. G.; Isimjan, T. T.; Mequanint, K., Tissue engineering scaffolds containing embedded fluorinated-zeolite oxygen vectors. *Acta Biomater* **2011,** 7, (10), 3670-8.

11.   Blanch, H. W.; Clark, D. S., Biochemical Engineering. In *Biochemical Engineering*, CRC Press: New York, 1997.

12.   Trotta, F.; Cavalli, R.; Martina, K.; Biasizzo, M.; Vitillo, J.; Bordiga, S.; Vavia, P.; Ansari, K., Cyclodextrin nanosponges as effective gas carriers. *J Incl Phenom Macrocycl Chem* **2011,** 71, 189-194.

13.   Cramer, F.; Henglein, M., Einschlußverbindungen der Cyclodextrine mit Gasen. *Angewandte Chemie* **1956,** 68, (20), 649.

14.   Rudkevich, D. M.; Leontiev, A., Molecular encapsulation of gases. *Australian Journal of Chemistry* **2004,** 57, 713-722.

15.   Spiess, B. D., Perfluorocarbon emulsions as a promising technology: a review of tissue and vascular gas dynamics. *J Appl Physiol (1985)* **2009,** 106, (4), 1444-52.

16.   Cipitria, A.; Skelton, A.; Dargaville, T. R.; Dalton, P. D.; Hutmacher, D. W., Design, fabrication and characterization of PCL electrospun scaffolds - a review. *Journal of Materials Chemistry* **2011,** 21, 9419-9453.

6 GENERAL DISCUSSION AND CONCLUSIONS

Overview: This chapter provides a general summery of the overall work of this thesis as per the specific objectives mentioned in Section 2.5. The strengths and limitations of this work are summarized with directions for future work. Finally, the overall significance of this work for tissue engineering is included.

6.1 Conclusions

The main goal of this study was to enhance the delivery of oxygen to cells seeded on scaffolds for application in tissue engineering. The fundamental basis for the strategy explored was the ability of PFCs to transport large quantities of oxygen due to increased solubility according to Henry's Law. The initial step involved preparing an inclusion complex between cyclodextrin and a perfluorocarbon. Specifically, α-CD and PFP were selected as the host and guest, respectively, following preliminary experiments and according to the close match between the dimensions of the α-CD cavity and PFP diameter. Of the numerous complexation techniques available, co-precipitation, paste mixing, and dry mixing were conducted. The products were characterized with FTIR, TGA, and XRD in order to establish the most effective complexation technique for the specific host and guest molecules utilized. Taken together, the characterization techniques showed that paste mixing and dry mixing, at a molar ratio of 2:1 α-CD to PFP, were the most effective complexation techniques. Further tests were conducted with the CD:IC prepared by paste mixing.

The next step involved incorporating the CD:IC into a 3D tissue engineering construct. Electrospinning was selected as the fabrication technique, with PCU and PCL as the stable and biodegradable polymer matrices, respectively. SEM micrographs were used to characterize the resulting fibrous mats in terms of fiber diameter and uniformity. The optimized concentrations were determined to be 8 % (v/v) PCU with respect to solvent, 50 % (w/w) CD:IC with respect to polymer and 8 % (v/v) PCL with respect to solvent, 15 % (w/w) CD:IC with respect to polymer. The fibers in these mats had average diameters of (232 ± 31) nm and (342±56) nm for PCU-CD:IC and PCL-CD:IC, respectively, which is

within the acceptable margin for most tissue engineering applications. XPS survey scans of the fibers indicated that at least some of the CD:IC was present on the surface of both the PCU and PCL fibers.

Finally, the ability of the CD:IC and the CD:IC-containing scaffolds to enhance oxygen delivery *in vitro* was studied. Dissolved oxygen, measured with a fiber optic probe in PBS, was significantly increased in the presence of as low as 1 % PFP. Furthermore, in some cases incorporating the PFC as a CD:IC actually served to further enhance the dissolved oxygen. After being embedded within a polymer matrix and electrospun into a 3D fibrous mat, the CD:ICs maintained their ability to enhance the oxygen delivery. Statistically significant increases in dissolved oxygen measured in the PBS surrounding the fibrous mats were observed for both the PCU- and PCL-based materials on Day 5 and 3, respectively. This increase was maintained over the remainder of the 14 day period of the experiment for both materials.

Taken together, the experiments conducted over the course of this study demonstrate that CD:ICs prepared with a PFC are viable oxygen carriers. Embedding the CD/PFC inclusion complexes within a 3D scaffold is a feasible approach to enhance oxygen delivery to cells seeded on tissue engineering constructs with the ultimate goal of developing clinically thick tissues.

6.2 Strengths and Limitations

In this study, a strategy for enhancing oxygen delivery in scaffold-guided tissue engineering was developed. The strategy involved incorporating cyclodextrin inclusion complexes with perfluorocarbons as oxygen carriers in tissue engineering scaffolds. One of the strengths of this approach is that by incorporating the PFC within the CD cavity, the limitations with stability and user-friendliness of PFC emulsions are overcome. Moreover, incorporating the oxygen carriers directly within the scaffold prevents, or at least hinders, the settling of the PFC droplets in either the culture well or medium reservoir. Having the CD:ICs embedded directly in the scaffold also serves to provide enhanced oxygen delivery throughout the scaffold, particularly in the center which is difficult to reach by diffusion

alone. Furthermore, the advantage of using CD/PFC complexes over oxygen generating compounds, such as calcium peroxide[1] or sodium percarbonate,[2] is that they are not depleted and theoretically have an unlimited lifespan.

One of the major strengths with the use of a cyclodextrin/perfluorocarbon inclusion complex as an oxygen carrier is that there is potential to incorporate the CD:IC within virtually any polymer via electrospinning. In this study alone, it was possible to embed the CD:ICs within both stable and degradable polymer matrices. Additionally, the application of the CD:ICs as oxygen carriers could be extended to other biomaterials; for example, hydrogels containing cyclodextrin have been reported.[3-5] Another advantage of utilizing cyclodextrin as the oxygen carrier is that cyclodextrins are natural and relatively non-toxic, making them suitable for biological applications, they have a low price, and are commercially available.[6] In the body, CDs are mainly excreted in their intact form by renal filtration as they are minimally susceptible to hydrolytic cleavage or degradation by human enzymes.[7]

A limitation of this work is the absence of *in vitro* cell studies. Preliminary cell culture experiments were carried out on the CD:IC-functionalized fibrous mats (**Appendix 7-7**), however, they were not comprehensive enough to conclusively draw conclusions on the cytotoxicity of the α-CD/PFP inclusion complex. Although CD is well-known to be relatively non-toxic,[6] PFC emulsions are generally considered to be cytotoxic to cultured human fibroblast cells in a concentration-dependent manner.[8, 9] Previous experiments carried out in our lab on HCASMCs, on the other hand, demonstrated cell viability in the presence of perfluorodecalin.[10] In future work, it is therefore necessary to clarify the cytotoxicity of the PFC used in this study in the form of a cyclodextrin inclusion complex embedded within 3D tissue engineering constructs.

Another limitation of this work is the lack of characterization for the complexes prepared from all techniques attempted. As the ultimate objective of this work was to test the ability of the inclusion complex to enhance oxygen delivery when embedded within a tissue engineering scaffold, once sufficient characterization was carried out to confirm complex

formation the focus was shifted to fabricating the scaffolds and carrying out analysis *in vitro*. Theoretically, an entire thesis work could be dedicated to varying the parameters associated with each complexation technique and thoroughly characterizing the resulting products.

6.3 Future Directions

In light of the work presented here, future work on this project should include:

- Short-term *in vitro* cell studies on the electrospun fibers incorporating CD:IC to evaluate cytotoxicity and cell spreading

- Long-term *in vitro* cell studies on the 3D PCU-CD:IC and PCL-CD:IC scaffolds to further explore their capacity to enhance oxygen delivery, specifically in terms of increased proliferation overall and decreased necrosis in the center of the construct

- Long-term studies to investigate the release of the CD:IC from the degradable PCL and stable PCU scaffolds

- Further characterization of the PCU-CD:IC and PCL-CD:IC scaffolds to clarify the positioning of the CD:IC in the fibers

- Mechanical testing on the 3D PCU-CD:IC and PCL-CD:IC scaffolds to ensure appropriateness for tissue engineering applications

- Electrospinning with different polymers and further research different types of biomaterials in order to confirm the versatility of this approach

6.4 Significance

The focus of this research was the development of a novel inclusion complex, prepared between α-cyclodextrin and perfluoroperhydrophenanthrene, and the incorporation of the inclusion complex in three-dimensional scaffolds. This study serves as the foundation for the use of cyclodextrin/perfluorocarbon inclusion complexes as oxygen carriers in

scaffold-guided tissue engineering. Alternative oxygen delivery strategies utilizing different cyclodextrins, perfluorocarbons, scaffold polymers, or fabrication techniques may yet be developed.

6.5 References

1.   Oh, S. H.; Ward, C. L.; Atala, A.; Yoo, J. J.; Harrison, B. S., Oxygen generating scaffolds for enhancing engineered tissue survival. *Biomaterials* **2009,** 30, (5), 757-62.

2.   Harrison, B. S.; Eberli, D.; Lee, S. J.; Atala, A.; Yoo, J. J., Oxygen producing biomaterials for tissue regeneration. *Biomaterials* **2007,** 28, (31), 4628-34.

3.   Garcia-Fernandez, M. J.; Brackman, G.; Coenye, T.; Concheiro, A.; Alvarez-Lorenzo, C., Antiseptic cyclodextrin-functionalized hydrogels and gauzes for loading and delivery of benzalkonium chloride. *Biofouling* **2013,** 29, (3), 261-71.

4.   Chee, P. L.; Prasad, A.; Fang, X.; Owh, C.; Yeo, V. J.; Loh, X. J., Supramolecular cyclodextrin pseudorotaxane hydrogels: a candidate for sustained release? *Mater Sci Eng C Mater Biol Appl* **2014,** 39, 6-12.

5.   Liu, S.; Chen, X.; Zhang, Q.; Wu, W.; Xin, J.; Li, J., Multifunctional hydrogels based on β-cyclodextrin with both biomineralization and anti-inflammatory properties. *Carbohydr Polym* **2014,** 102, 869-76.

6.   Lo Nostro, P.; Santoni, I.; Bonini, M.; Baglioni, P., Inclusion compound from a semifluorinated alkane and beta-cyclodextrin. *Langmuir* **2003,** 19, 2313-2317.

7.   van de Manakker, F.; Vermonden, T.; van Nostrum, C. F.; Hennink, W. E., Cyclodextrin-based polymeric materials: synthesis, properties, and pharmaceutical/biomedical applications. *Biomacromolecules* **2009,** 10, (12), 3157-75.

8.   Wake, E. J.; Studzinski, G. P.; Bhandal, A., Changes in human cultured cells exposed to a perfluorocarbon emulsion. *Transfusion* **1985,** 25, (1), 73-7.

9.   Centis, V.; Doillon, C. J.; Vermette, P., Perfluorocarbon emulsions cytotoxic effects on human fibroblasts and effect of aging on particle size distribution. *Artif Organs* **2007,** 31, (8), 649-53.

10.   Seifu, D. G.; Mequanint, K., Experimental and modeling studies of oxygen tension in vascular tissue engineering with and without an oxygen carrier. *Journal of Biomaterials and Tissue Engineering* **2011,** 1, 49-59.

7 APPENDICES
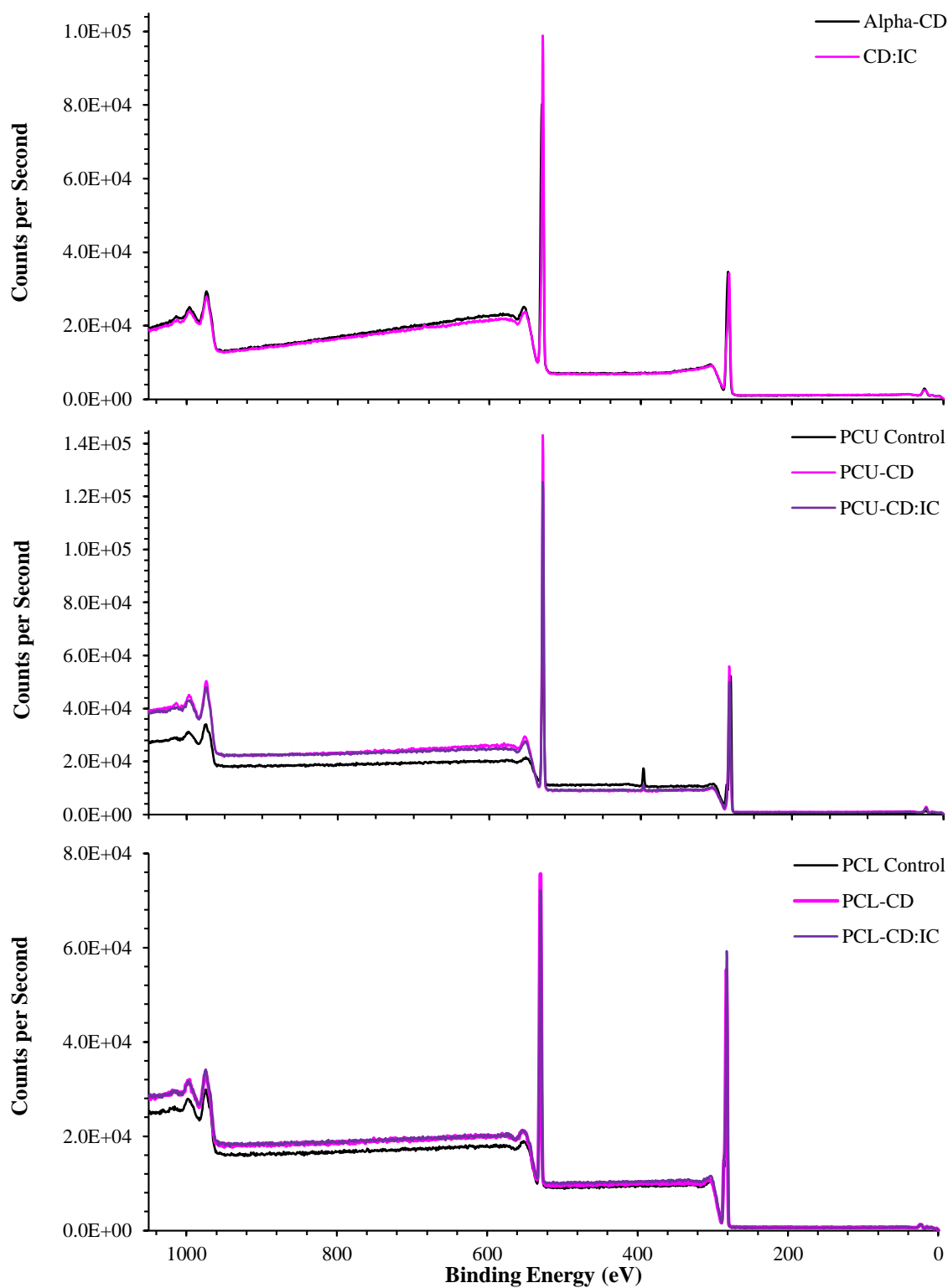
Appendix 6-1: XPS spectra of the unmodified α-CD and prepared CD:IC, and the 3D PCU and PCL scaffolds incorporating the α-CD and CD:IC

Appendix 7-2: Statistical data for dissolved oxygen measurements in PBS at various conditions in the presence of α-CD, PFP, and α-CD/PFP CD:ICs. Dissolved oxygen was measured with a fiber optic probe. Data are means ± SD for experiments performed in triplicate. Statistical significance: x indicates $p{>}0.05$, * indicates $p{\leq}0.05$. *** indicates $p{\leq}0.001$.

		RT, No Surfactant, Day 1			
PBS Control vs.	$8.64_{(\pm0.07)}$	1% PFP	$8.73_{(\pm0.11)}$	0.71	x
		1% CD:IC	$8.70_{(\pm0.05)}$	0.96	x
		2% PFP	$8.85_{(\pm0.02)}$	0.01	*
		2% CD:IC	$8.96_{(\pm0.06)}$	<0.001	***
		4% PFP	$9.13_{(\pm0.08)}$	<0.001	***
		4% CD:IC	$8.98_{(\pm0.08)}$	<0.001	***
PBS Control vs.	$8.64_{(\pm0.07)}$	1% CD	$8.65_{(\pm0.03)}$	1	x
		2% CD	$8.64_{(\pm0.04)}$	1	x
		4% CD	$8.66_{(\pm0.006)}$	1	x
1% CD vs.	$8.65_{(\pm0.03)}$	1% CD:IC	$8.70_{(\pm0.05)}$	0.99	x
2% CD vs.	$8.64_{(\pm0.04)}$	2% CD:IC	$8.97_{(\pm0.06)}$	<0.001	***
4% CD vs.	$8.66_{(\pm0.01)}$	4% CD:IC	$8.98_{(\pm0.08)}$	<0.001	***
1% CD:IC vs.	$8.70_{(\pm0.05)}$	2% CD:IC	$8.96_{(\pm0.06)}$	0.001	***
2% PFP vs.	$8.85_{(\pm0.02)}$	2% CD:IC	$8.96_{(\pm0.06)}$	0.42	x
2% PFP vs.	$8.85_{(\pm0.02)}$	4% PFP	$9.13_{(\pm0.08)}$	<0.001	***
2% CDIC vs.	$8.96_{(\pm0.06)}$	4% CD:IC	$8.98_{(\pm0.08)}$	1	x
4% PFP vs.	$9.13_{(\pm0.08)}$	4% CD:IC	$8.98_{(\pm0.08)}$	0.18	x
		RT, Surfactant, Day 1			
PBS Control vs.	$8.50_{(\pm0.09)}$	1% PFP	$8.73_{(\pm0.03)}$	0.01	*
		1% CD:IC	$8.73_{(\pm0.03)}$	0.01	*
		2% PFP	$8.89_{(\pm0.05)}$	<0.001	***
		2% CD:IC	$9.32_{(\pm0.04)}$	<0.001	***
		4% PFP	$9.41_{(\pm0.14)}$	<0.001	***
		4% CD:IC	$9.63_{(\pm0.03)}$	<0.001	***
PBS Control vs.	$8.50_{(\pm0.09)}$	1% CD	$8.60_{(\pm0.03)}$	0.64	x
		2% CD	$8.48_{(\pm0.10)}$	1	x
		4% CD	$8.67_{(\pm0.02)}$	0.11	x
1% CD vs.	$8.60_{(\pm0.03)}$	1% CD:IC	$8.73_{(\pm0.03)}$	0.48	x
2% CD vs.	$8.48_{(\pm0.10)}$	2% CD:IC	$9.32_{(\pm0.04)}$	<0.001	***
4% CD vs.	$8.67_{(\pm0.02)}$	4% CD:IC	$9.63_{(\pm0.03)}$	<0.001	***
1% CD:IC vs.	$8.73_{(\pm0.03)}$	2% CD:IC	$9.32_{(\pm0.04)}$	<0.001	***
2% PFP vs.	$8.89_{(\pm0.05)}$	2% CD:IC	$9.32_{(\pm0.04)}$	<0.001	***
2% PFP vs.	$8.89_{(\pm0.05)}$	4% PFP	$9.41_{(\pm0.14)}$	<0.001	***

2% CDIC vs.	$9.32_{(\pm0.03)}$	4% CD:IC	$9.63_{(\pm0.03)}$	<0.001	***
4% PFP vs.	$9.41_{(\pm0.137)}$	4% CD:IC	$9.63_{(\pm0.0299)}$	0.02	*

37°C, No Surfactant, Day 1

PBS Control vs.	$6.81_{(\pm0.03)}$	1% PFP	$7.10_{(\pm0.07)}$	<0.001	***
		1% CD:IC	$7.29_{(\pm0.04)}$	<0.001	***
		2% PFP	$7.34_{(\pm0.08)}$	<0.001	***
		2% CD:IC	$7.41_{(\pm0.02)}$	<0.001	***
		4% PFP	$7.63_{(\pm0.01)}$	<0.001	***
		4% CD:IC	$7.87_{(\pm0.02)}$	<0.001	***
PBS Control vs.	$6.806_{(\pm0.0333)}$	1% CD	$6.88_{(\pm0.02)}$	0.06	x
		2% CD	$6.90_{(\pm0.02)}$	0.25	x
		4% CD	$7.12_{(\pm0.04)}$	<0.001	***
1% CD vs.	$6.879_{(\pm0.0238)}$	1% CD:IC	$7.29_{(\pm0.04)}$	<0.001	***
2% CD vs.	$6.899_{(\pm0.0167)}$	2% CD:IC	$7.41_{(\pm0.02)}$	<0.001	***
4% CD vs.	$7.118_{(\pm0.038)}$	4% CD:IC	$7.87_{(\pm0.02)}$	<0.001	***
1% CD:IC vs.	$7.288_{(\pm0.0397)}$	2% CD:IC	$7.41_{(\pm0.02)}$	0.04	*
2% PFP vs.	$7.343_{(\pm0.0809)}$	2% CD:IC	$7.41_{(\pm0.02)}$	0.60	x
2% PFP vs.	$7.343_{(\pm0.0809)}$	4% PFP	$7.63_{(\pm0.01)}$	<0.001	***
2% CDIC vs.	$7.414_{(\pm0.0244)}$	4% CD:IC	$7.87_{(\pm0.02)}$	<0.001	***
4% PFP vs.	$7.632_{(\pm0.0119)}$	4% CD:IC	$7.87_{(\pm0.02)}$	<0.001	***

37°C, Surfactant, Day 1

PBS Control vs.	$6.925_{(\pm0.0423)}$	1% PFP	$7.14_{(\pm0.02)}$	<0.001	***
		1% CD:IC	$7.28_{(\pm0.03)}$	<0.001	***
		2% PFP	$7.60_{(\pm0.002)}$	<0.001	***
		2% CD:IC	$7.69_{(\pm0.02)}$	<0.001	***
		4% PFP	$7.91_{(\pm0.02)}$	<0.001	***
		4% CD:IC	$7.95_{(\pm0.005)}$	<0.001	***
PBS Control vs.	$6.925_{(\pm0.0423)}$	1% CD	$6.95_{(\pm0.05)}$	0.99	x
		2% CD	$6.94_{(\pm0.07)}$	1	x
		4% CD	$7.07_{(\pm0.03)}$	0.001	***
1% CD vs.	$6.953_{(\pm0.0467)}$	1% CD:IC	$7.28_{(\pm0.03)}$	<0.001	***
2% CD vs.	$6.942_{(\pm0.0668)}$	2% CD:IC	$7.69_{(\pm0.02)}$	<0.001	***
4% CD vs.	$7.071_{(\pm0.0270)}$	4% CD:IC	$7.95_{(\pm0.005)}$	<0.001	***
1% CD:IC vs.	$7.281_{(\pm0.03)}$	2% CD:IC	$7.69_{(\pm0.02)}$	<0.001	***
2% PFP vs.	$7.602_{(\pm0.00210)}$	2% CD:IC	$7.69_{(\pm0.02)}$	0.12	x
2% PFP vs.	$7.602_{(\pm0.00210)}$	4% PFP	$7.91_{(\pm0.02)}$	<0.001	***
2% CDIC vs.	$7.687_{(\pm0.0165)}$	4% CD:IC	$7.95_{(\pm0.005)}$	<0.001	***
4% PFP vs.	$7.906_{(\pm0.0240)}$	4% CD:IC	$7.95_{(\pm0.005)}$	0.8	x

RT, No Surfactant, Day 14

PBS Control vs.	$7.81_{(\pm0.04)}$	1% PFP	$8.05_{(\pm0.03)}$	<0.001	***

		1% CD:IC	$7.94_{(\pm0.07)}$	0.02	*
		2% PFP	$8.02_{(\pm0.004)}$	<0.001	***
		2% CD:IC	$8.14_{(\pm0.04)}$	<0.001	***
		4% PFP	$8.53_{(\pm0.006)}$	<0.001	***
		4% CD:IC	$8.66_{(\pm0.04)}$	<0.001	***
PBS Control vs.	$7.80_{(\pm0.04)}$	1% CD	$7.62_{(\pm0.04)}$	0.001	***
		2% CD	$7.74_{(\pm0.07)}$	0.76	x
		4% CD	$8.29_{(\pm0.03)}$	<0.001	***
1% CD vs.	$7.62_{(\pm0.04)}$	1% CD:IC	$7.94_{(\pm0.07)}$	<0.001	***
2% CD vs.	$7.74_{(\pm0.07)}$	2% CD:IC	$8.14_{(\pm0.04)}$	<0.001	***
4% CD vs.	$8.29_{(\pm0.03)}$	4% CD:IC	$8.66_{(\pm0.04)}$	<0.001	***
1% CD:IC vs.	$7.94_{(\pm0.07)}$	2% CD:IC	$8.14_{(\pm0.04)}$	<0.001	***
2% PFP vs.	$8.02_{(\pm0.004)}$	2% CD:IC	$8.14_{(\pm0.04)}$	0.05	*
2% PFP vs.	$8.02_{(\pm0.004)}$	4% PFP	$8.53_{(\pm0.006)}$	<0.001	***
2% CDIC vs.	$8.14_{(\pm0.04)}$	4% CD:IC	$8.66_{(\pm0.04)}$	<0.001	***
4% PFP vs.	$8.53_{(\pm0.006)}$	4% CD:IC	$8.66_{(\pm0.04)}$	0.04	*

RT, Surfactant, Day 14

PBS Control vs.	$7.84_{(\pm0.08)}$	1% PFP	$8.26_{(\pm0.04)}$	<0.001	***
		1% CD:IC	$8.36_{(\pm0.01)}$	<0.001	***
		2% PFP	$8.47_{(\pm0.01)}$	<0.001	***
		2% CD:IC	$8.91_{(\pm0.04)}$	<0.001	***
		4% PFP	$9.29_{(\pm0.05)}$	<0.001	***
		4% CD:IC	$9.54_{(\pm0.04)}$	<0.001	***
PBS Control vs.	$7.84_{(\pm0.08)}$	1% CD	$7.80_{(\pm0.05)}$	0.97	x
		2% CD	$7.98_{(\pm0.02)}$	0.01	*
		4% CD	$8.16_{(\pm0.01)}$	<0.001	***
1% CD vs.	$7.80_{(\pm0.05)}$	1% CD:IC	$8.36_{(\pm0.01)}$	<0.001	***
2% CD vs.	$7.98_{(\pm0.02)}$	2% CD:IC	$8.91_{(\pm0.04)}$	<0.001	***
4% CD vs.	$8.16_{(\pm0.01)}$	4% CD:IC	$9.54_{(\pm0.04)}$	<0.001	***
1% CD:IC vs.	$8.36_{(\pm0.01)}$	2% CD:IC	$8.91_{(\pm0.04)}$	<0.001	***
2% PFP vs.	$8.47_{(\pm0.01)}$	2% CD:IC	$8.91_{(\pm0.04)}$	<0.001	***
2% PFP vs.	$8.47_{(\pm0.01)}$	4% PFP	$9.29_{(\pm0.05)}$	<0.001	***
2% CDIC vs.	$8.91_{(\pm0.04)}$	4% CD:IC	$9.54_{(\pm0.04)}$	<0.001	***
4% PFP vs.	$9.29_{(\pm0.05)}$	4% CD:IC	$9.54_{(\pm0.04)}$	<0.001	***

37°C, No Surfactant, Day 14

PBS Control vs.	$6.66_{(\pm0.02)}$	1% PFP	$6.91_{(\pm0.02)}$	<0.001	***
		1% CD:IC	$7.13_{(\pm0.02)}$	<0.001	***
		2% PFP	$7.22_{(\pm0.01)}$	<0.001	***
		2% CD:IC	$7.32_{(\pm0.01)}$	<0.001	***
		4% PFP	$7.40_{(\pm0.01)}$	<0.001	***

		4% CD:IC	$7.71_{(\pm 0.01)}$	<0.001	***
PBS Control vs.	$6.66_{(\pm 0.02)}$	1% CD	$6.78_{(\pm 0.02)}$	0.004	*
		2% CD	$6.78_{(\pm 0.02)}$	0.01	*
		4% CD	$6.93_{(\pm 0.09)}$	<0.001	***
1% CD vs.	$6.78_{(\pm 0.02)}$	1% CD:IC	$7.13_{(\pm 0.02)}$	<0.001	***
2% CD vs.	$6.78_{(\pm 0.02)}$	2% CD:IC	$7.32_{(\pm 0.01)}$	<0.001	***
4% CD vs.	$6.93_{(\pm 0.09)}$	4% CD:IC		<0.001	***
1% CD:IC vs.	$7.13_{(\pm 0.02)}$	2% CD:IC	$7.32_{(\pm 0.01)}$	<0.001	***
2% PFP vs.	$7.22_{(\pm 0.01)}$	2% CD:IC	$7.32_{(\pm 0.01)}$	0.04	*
2% PFP vs.	$7.22_{(\pm 0.01)}$	4% PFP	$7.40_{(\pm 0.01)}$	<0.001	***
2% CDIC vs.	$7.32_{(\pm 0.01)}$	4% CD:IC	$7.71_{(\pm 0.01)}$	<0.001	***
4% PFP vs.	$7.40_{(\pm 0.01)}$	4% CD:IC	$7.71_{(\pm 0.01)}$	<0.001	***

37°C, Surfactant, Day 14

PBS Control vs.	$6.82_{(\pm 0.01)}$	1% PFP	$7.04_{(\pm 0.04}$	<0.001	***
		1% CD:IC	$7.27_{(\pm 0.01)}$	<0.001	***
		2% PFP	$7.51_{(\pm 0.02)}$	<0.001	***
		2% CD:IC	$7.61_{(\pm 0.01)}$	<0.001	***
		4% PFP	$7.75_{(\pm 0.01)}$	<0.001	***
		4% CD:IC	$7.92_{(\pm 0.02)}$	<0.001	***
PBS Control vs.	$6.82_{(\pm 0.01)}$	1% CD	$6.92_{(\pm 0.04)}$	0.01	*
		2% CD	$6.88_{(\pm 0.02)}$	0.16	x
		4% CD	$6.84_{(\pm 0.02)}$	0.50	x
1% CD vs.	$6.92_{(\pm 0.043)}$	1% CD:IC	$7.27_{(\pm 0.01)}$	<0.001	***
2% CD vs.	$6.88_{(\pm 0.02)}$	2% CD:IC	$7.61_{(\pm 0.01)}$	<0.001	***
4% CD vs.	$6.84_{(\pm 0.02)}$	4% CD:IC	$7.92_{(\pm 0.02)}$	<0.001	***
1% CD:IC vs.	$7.27_{(\pm 0.01)}$	2% CD:IC	$7.61_{(\pm 0.01)}$	<0.001	***
2% PFP vs.	$7.51_{(\pm 0.02)}$	2% CD:IC	$7.61_{(\pm 0.01)}$	0.004	*
2% PFP vs.	$7.51_{(\pm 0.02)}$	4% PFP	$7.75_{(\pm 0.01)}$	<0.001	***
2% CDIC vs.	$7.61_{(\pm 0.01)}$	4% CD:IC	$7.92_{(\pm 0.02)}$	<0.001	***
4% PFP vs.	$7.75_{(\pm 0.01)}$	4% CD:IC	$7.92_{(\pm 0.02)}$	<0.001	***

Appendix 7-3: Statistical data showing the effect of surfactant on dissolved oxygen measurements in PBS at various conditions in the presence of α-CD, PFP, and α-CD/PFP CD:ICs. Dissolved oxygen was measured with a fiber optic probe. Data are means ± SD for experiments performed in triplicate. Statistical significance: x indicates $p>0.05$, * indicates $p≤0.05$. * indicates $p≤0.001$.**

	No Surfactant	Surfactant	p value	Significance
		RT, Day 1		
PBS Control	8.64$_{(±0.07)}$	8.50$_{(±0.09)}$	0.52	x
1% CD	8.65$_{(±0.03)}$	8.60$_{(±0.03)}$	1.00	x
2% CD	8.64$_{(±0.04)}$	8.48$_{(±0.10)}$	0.38	*
4% CD	8.66$_{(±0.01)}$	8.67$_{(±0.02)}$	1.00	x
1% PFP	8.73$_{(±0.11)}$	8.73$_{(±0.03)}$	1.00	x
1% CD:IC	8.70$_{(±0.04)}$	8.73$_{(±0.03)}$	1.00	x
2% PFP	8.85$_{(±0.02)}$	8.89$_{(±0.05)}$	1.00	x
2% CD:IC	8.97$_{(±0.06)}$	9.32$_{(±0.04)}$	<0.001	***
4% PFP	9.13$_{(±0.08)}$	9.41$_{(±0.14)}$	<0.001	***
4% CD:IC	8.98$_{(±0.08)}$	9.63$_{(±0.03)}$	<0.001	***
		37°C, Day 1		
PBS Control	6.81$_{(±0.03)}$	6.92$_{(±0.04)}$	0.05	x
1% CD	6.88$_{(±0.02)}$	6.95$_{(±0.05)}$	0.67	x
2% CD	6.90$_{(±0.02)}$	6.94$_{(±0.07)}$	1	x
4% CD	7.12$_{(±0.04)}$	7.07$_{(±0.03)}$	0.99	x
1% PFP	7.10$_{(±0.07)}$	7.14$_{(±0.02)}$	1.00	x
1% CD:IC	7.29$_{(±0.04)}$	7.28$_{(±0.03)}$	1.00	x
2% PFP	7.34$_{(±0.08)}$	7.60$_{(±0.002)}$	<0.001	***
2% CD:IC	7.41$_{(±0.02)}$	7.69$_{(±0.02)}$	<0.001	***
4% PFP	7.63$_{(±0.01)}$	7.91$_{(±0.02)}$	<0.001	***
4% CD:IC	7.868$_{(±0.0207)}$	7.952$_{(±0.00461)}$	0.461	x

RT, Day 14				
PBS Control	$7.80_{(\pm0.04)}$	$7.84_{(\pm0.08)}$	1	x
1% CD	$7.62_{(\pm0.04)}$	$7.80_{(\pm0.052)}$	<0.001	***
2% CD	$7.74_{(\pm0.07)}$	$7.98_{(\pm0.02)}$	<0.001	***
4% CD	$8.29_{(\pm0.03)}$	$8.16_{(\pm0.01)}$	0.02	*
1% PFP	$8.05_{(\pm0.03)}$	$8.26_{(\pm0.04)}$	<0.001	***
1% CD:IC	$7.94_{(\pm0.07)}$	$8.36_{(\pm0.01)}$	<0.001	***
2% PFP	$8.02_{(\pm0.004)}$	$8.47_{(\pm0.01)}$	<0.001	***
2% CD:IC	$8.14_{(\pm0.04)}$	$8.91_{(\pm0.04)}$	<0.001	***
4% PFP	$8.53_{(\pm0.01)}$	$9.29_{(\pm0.047)}$	<0.001	***
4% CD:IC	$8.66_{(\pm0.04)}$	$9.54_{(\pm0.04)}$	<0.001	***
37°C, Day 14				
PBS Control	$6.66_{(\pm0.02)}$	$6.82_{(\pm0.01)}$	<0.001	***
1% CD	$6.78_{(\pm0.02)}$	$6.92_{(\pm0.04)}$	<0.001	***
2% CD	$6.78_{(\pm0.02)}$	$6.88_{(\pm0.02)}$	0.01	*
4% CD	$6.93_{(\pm0.09)}$	$6.84_{(\pm0.02)}$	0.02	*
1% PFP	$6.91_{(\pm0.02)}$	$7.04_{(\pm0.04)}$	<0.001	***
1% CD:IC	$7.13_{(\pm0.02)}$	$7.27_{(\pm0.01)}$	<0.001	***
2% PFP	$7.22_{(\pm0.01)}$	$7.51_{(\pm0.02)}$	<0.001	***
2% CD:IC	$7.32_{(\pm0.01)}$	$7.61_{(\pm0.01)}$	<0.001	***
4% PFP	$7.40_{(\pm0.01)}$	$7.75_{(\pm0.01)}$	<0.001	***
4% CD:IC	$7.71_{(\pm0.01)}$	$7.92_{(\pm0.02)}$	<0.001	***

Appendix 7-4: Statistical data showing the effect of storage for 14 days in a refrigerator on dissolved oxygen measured in PBS in the presence of α-CD, PFP, and α-CD/PFP CD:ICs. Dissolved oxygen was measured with a fiber optic probe. Data are means ± SD for experiments performed in triplicate. Statistical significance: x indicates $p>0.05$, * indicates $p\leq0.05$. * indicates $p\leq0.001$.**

	Day 1	Day 14	p value	Significance
RT, No Surfactant				
PBS Control	$8.64_{(\pm0.07)}$	$7.80_{(\pm0.044)}$	<0.001	***
1% CD	$8.65_{(\pm0.03)}$	$7.62_{(\pm0.04)}$	<0.001	***
2% CD	$8.64_{(\pm0.04)}$	$7.74_{(\pm0.07)}$	<0.001	***
4% CD	$8.66_{(\pm0.01)}$	$8.29_{(\pm0.03)}$	<0.001	***
1% PFP	$8.73_{(\pm0.11)}$	$8.05_{(\pm0.03)}$	<0.001	***
1% CD:IC	$8.70_{(\pm0.05)}$	$7.94_{(\pm0.07)}$	<0.001	***
2% PFP	$8.85_{(\pm0.02)}$	$8.02_{(\pm0.004)}$	<0.001	***
2% CD:IC	$8.96_{(\pm0.06)}$	$8.14_{(\pm0.04)}$	<0.001	***
4% PFP	$9.13_{(\pm0.08)}$	$8.53_{(\pm0.01)}$	<0.001	***
4% CD:IC	$8.98_{(\pm0.08)}$	$8.66_{(\pm0.04)}$	<0.001	***
RT, Surfactant				
PBS Control	$8.50_{(\pm0.09)}$	$7.84_{(\pm0.08)}$	<0.001	***
1% CD	$8.60_{(\pm0.03)}$	$7.80_{(\pm0.05)}$	<0.001	***
2% CD	$8.48_{(\pm0.10)}$	$7.98_{(\pm0.02)}$	<0.001	***
4% CD	$8.67_{(\pm0.02)}$	$8.16_{(\pm0.01)}$	<0.001	***
1% PFP	$8.73_{(\pm0.03)}$	$8.26_{(\pm0.04)}$	<0.001	***
1% CD:IC	$8.73_{(\pm0.03)}$	$8.36_{(\pm0.01)}$	<0.001	***
2% PFP	$8.89_{(\pm0.05)}$	$8.47_{(\pm0.01)}$	<0.001	***
2% CD:IC	$9.32_{(\pm0.04)}$	$8.91_{(\pm0.04)}$	<0.001	***
4% PFP	$9.41_{(\pm0.14)}$	$9.29_{(\pm0.05)}$	0.49	x

4% CD:IC	9.63$_{(\pm0.03)}$	9.54$_{(\pm0.04)}$	0.87	x

	37°C, No Surfactant			
PBS Control	6.806$_{(\pm0.0333)}$	6.66$_{(\pm0.01)}$	0.76	x
1% CD	6.88$_{(\pm0.02)}$	6.78$_{(\pm0.02)}$	0.83	x
2% CD	6.90$_{(\pm0.02)}$	6.78$_{(\pm0.02)}$	1.09	x
4% CD	7.12$_{(\pm0.04)}$	6.93$_{(\pm0.09)}$	0.93	x
1% PFP	7.10$_{(\pm0.07)}$	6.91$_{(\pm0.02)}$	0.83	x
1% CD:IC	7.29$_{(\pm0.04)}$	7.13$_{(\pm0.02)}$	0.99	x
2% PFP	7.34$_{(\pm0.08)}$	7.22$_{(\pm0.01)}$	0.79	x
2% CD:IC	7.41$_{(\pm0.02)}$	7.32$_{(\pm0.01)}$	0.66	x
4% PFP	7.63$_{(\pm0.01)}$	7.40$_{(\pm0.01)}$	0.63	x
4% CD:IC	7.87$_{(\pm0.02)}$	7.71$_{(\pm0.01)}$	0.30	x

	37°C, Surfactant			
PBS Control	6.92$_{(\pm0.04)}$	6.82$_{(\pm0.01)}$	0.02	*
1% CD	6.95$_{(\pm0.05)}$	6.92$_{(\pm0.04)}$	0.99	x
2% CD	6.94$_{(\pm0.07)}$	6.88$_{(\pm0.02)}$	0.58	x
4% CD	7.07$_{(\pm0.0270)}$	6.84$_{(\pm0.02)}$	<0.001	***
1% PFP	7.14$_{(\pm0.02)}$	7.04$_{(\pm0.04)}$	0.02	*
1% CD:IC	7.28$_{(\pm0.03)}$	7.27$_{(\pm0.01)}$	1	x
2% PFP	7.60$_{(\pm0.002)}$	7.51$_{(\pm0.02)}$	0.07	x
2% CD:IC	7.69$_{(\pm0.02)}$	7.61$_{(\pm0.01)}$	0.17	x
4% PFP	7.91$_{(\pm0.02)}$	7.75$_{(\pm0.01)}$	<0.001	***
4% CD:IC	7.95$_{(\pm0.005)}$	7.92$_{(\pm0.02)}$	1	x

Appendix 7-5: Statistical analysis for dissolved oxygen measured in PBS at 37 °C in the presence of 3D electrospun fibrous mats compared to a PBS control. Dissolved oxygen was measured with a fiber optic probe. Data are means ± SD for experiments performed in triplicate. Statistical significance: x indicates $p > 0.05$, * indicates $p \leq 0.05$. * indicates $p \leq 0.001$.**

	DO (mg/L)	p value	Significance	DO (mg/L)	p value	Significance
Day	**PCU**			**PCU-CD:IC**		
1	$6.43_{(\pm0.22)}$	0.34	x	$8.47_{(\pm0.48)}$	0.18	x
3	$7.82_{(\pm0.08)}$	0.99	x	$8.07_{(\pm0.32)}$	0.78	x
5	$8.14_{(\pm0.26)}$	0.68	x	$9.71_{(\pm0.32)}$	<0.001	***
7	$8.26_{(\pm0.35)}$	0.45	x	$10.9_{(\pm0.53)}$	<0.001	***
10	$7.04_{(\pm0.96)}$	1.00	x	$9.38_{(\pm0.26)}$	<0.001	***
14	$7.93_{(\pm0.19)}$	0.94	x	$9.63_{(\pm0.62)}$	<0.001	***
Day	**PCU**			**PCU-CD:IC**		
1	$6.57_{(\pm0.20)}$	0.59	x	$8.52_{(\pm0.80)}$	0.16	x
3	$8.38_{(\pm0.18)}$	0.32	x	$9.02_{(\pm0.42)}$	0.01	*
5	$8.35_{(\pm0.33)}$	0.35	x	$9.94_{(\pm0.29)}$	<0.001	***
7	$8.24_{(\pm0.87)}$	0.52	x	$9.62_{(\pm0.45)}$	<0.001	***
10	$7.94_{(\pm0.42)}$	0.94	x	$9.51_{(\pm0.21)}$	<0.001	***
14	$8.40_{(\pm0.12)}$	0.29	x	$10.0_{(0.46)}$	<0.001	***

Appendix 7-6: Statistical analysis comparing dissolved oxygen measured in the presence of 3D electrospun fibrous mats fabricated from PCU and PCL containing α-CD/PFP CD:ICs in PBS at 37 °C. Dissolved oxygen was measured with a fiber optic probe. Data are means ± SD for experiments performed in triplicate. Statistical significance: x indicates $p > 0.05$, * indicates $p \leq 0.05$. * indicates $p \leq 0.001$.**

Day	PCU-CD:IC	PCL-CD:IC	p value	Significance
1	$8.47_{(\pm0.48)}$	$8.52_{(\pm0.80)}$	1	x
3	$8.07_{(\pm0.32)}$	$9.02_{(\pm0.42)}$	0.37	x
5	$9.71_{(\pm0.32)}$	$9.94_{(\pm0.29)}$	1	x
7	$10.9_{(\pm0.53)}$	$9.62_{(\pm0.45)}$	0.07	x
10	$9.38_{(\pm0.26)}$	$9.51_{(\pm0.21)}$	1	x
14	$9.63_{(\pm0.62)}$	$10.0_{(0.46)}$	0.99	x

Appendix 7-7: Preliminary Cell Studies

Materials and Methods

Cell Culture on 3D Scaffolds

Three-dimensional polymer scaffolds with an area of approximately 3.2 cm^2 were cut from PCU, PCU-CD:IC, PCL, and PCL-CD:IC electrospun fibrous mats. The scaffolds were exposed to UV irradiation for 1 hour per side for disinfection. The mats were transferred to culture plates, rinsed once with Hank's Balanced Salt Solution (HBSS), and soaked in fresh HBSS overnight for conditioning (Invitrogen Canada Inc., Burlington, ON) at RT. Mouse embryonic fibroblasts (NIH-3T3 cell-line) were seeded directly on the surface of the scaffolds, at a density of 100,000 cells/scaffold, affixed to the bottom of the well using an O-ring. The cells were maintained in a humidified incubator at 37 °C and 5 % CO$_2$ after adding with 0.5 mL/well of advanced DMEM (GIBCO® Invitrogen, Burlington, ON, Canada) containing 5 % FBS, 1 % antibiotics, and 0.2 mM L-glutamine.

Cytotoxicity Assay

Cell toxicity and proliferation were quantified by colorimetric assays of the metabolic activity of viable cells using 3-(4,5-dimethylthiazol-2-yl)-2,5-diphenyltetrazolium bromide (MTT) (Vybrant® MTT Cell Proliferation Assay Kit, Invitrogen Canada Inc.). The MTT tetrazolium dye is reduced to insoluble formazan salts in correspondence to the activity level of NADPH-dependent oxidoreductase enzymes of metabolically active cells producing a purple colour. The concentration of the formazan salts, and therefore metabolic activity level of the cells present, is determined using optical density at $\lambda = 570$ nm.

At time points of 1, 3, 5, and 7 days, the spent culture media was aspirated and replaced with 300 µL of fresh phenol-red free DMEM (GIBCO® Invitrogen, Burlington, ON, Canada) followed by MTT (30 µL, Component A) and allowed to incubate for 4 hours. Sodium dodecyl sulphate in dilute acid (300 µL, Component B) was added to the wells to solubilize the water insoluble formazan salts upon thorough mixing and incubation overnight. The resultant coloured solution was quantified using a BioTek EL307C multiplate reader (BioTek Instruments, Inc., Winooski, VT) at the maximum absorbance

wavelength of the formazan solution (570 nm). The results of the MTT assays are presented as the mean ± standard deviation for experiments conducted with 3 replicates.

Cytotoxicity Assay and Cell Spreading

The ultimate application of the 3D fibrous scaffolds incorporating CD:ICs prepared with a PFP is to enhance oxygen delivery to cells seeded on the construct during *in vitro* maturation. It was therefore necessary to evaluate the interaction of the materials with cells to ensure their cytocompatibility. For this, the 3D mats were fixed to the bottom of a tissue culture plate well, and cytotoxicity and cell proliferation were analyzed using MTT assays. A mouse fibroblast cell line (NIH-3T3) was used to evaluate the effect of the CD:IC-functionalized fibers on cell viability and metabolic activity over a time period of 7 days. The CD:IC-functionalized scaffolds were compared to PCU or PCL scaffolds without any modification as a control. As shown in Figure 7-1, there is no significant difference in the metabolic activity observed on the CD:IC-functionalized scaffolds as compared to the unmodified controls. Both PCU and PCL are well-known biocompatible materials,[1] so the similarity in metabolic activity suggests that, at the concentrations tested, the CD:IC-functionalized materials were not cytotoxic. The differences observed between the PCU- and PCL-based materials is potentially due to the different amount of CD:IC incorporated within the polymer material. It was possible to incorporate 50 % (w/w) CD:IC in the PCU scaffold while maintaining adequate fiber morphology, but only 15 % (w/w) CD:IC was incorporated in the PCL scaffold. This data could indicate that there is a threshold above which the CD:IC becomes toxic to fibroblasts. Moreover, if there is any uncomplexed CD in the electrospinning solution, solvent could be retained in the cavity leading to cytotoxicity. Further studies are necessary to elicit the effect of the α-CD/PFP complex on cytotoxicity and proliferation, especially over the long-term.
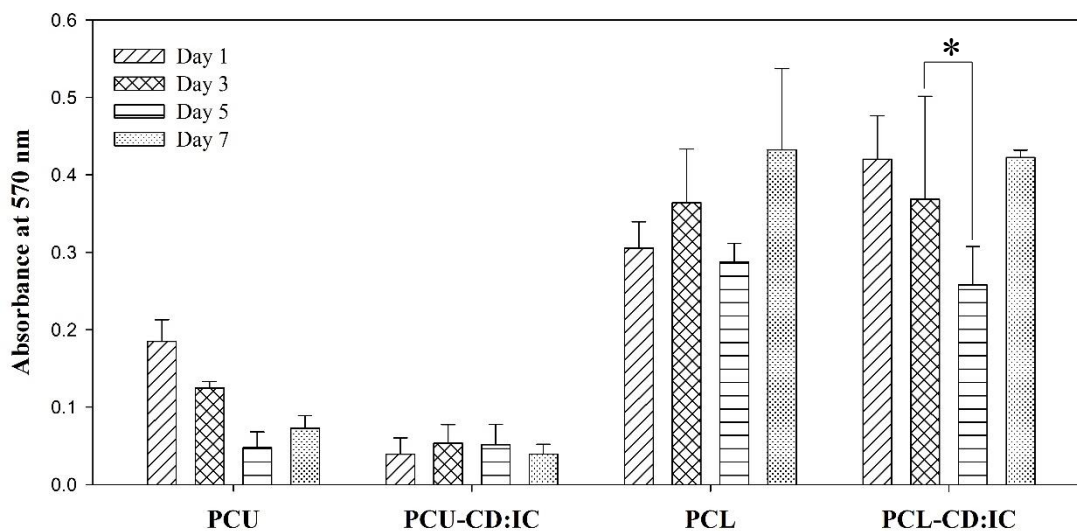
Figure 7-1: Fibroblast metabolic activity as determined by MTT assay over a 7 day period. Metabolic activity on CD:IC-functionalized materials are compared to that on the unmodified base polymer. The data are presented as mean ± standard deviation. Experiments were carried out in triplicate.

References

1.   Cipitria, A.; Skelton, A.; Dargaville, T. R.; Dalton, P. D.; Hutmacher, D. W., Design, fabrication and characterization of PCL electrospun scaffolds - a review. *Journal of Materials Chemistry* **2011,** 21, 9419-9453.

Appendix 7-8: Copyright Permissions

Subject: **RE: Copyright Permission**   Date: 07/21/14 10:11 AM
To: From: "Ballen, Karen"

Dear Tierney:

Copyright permission is granted for use of this figure in your dissertation.

Kind regards,

Karen Ballen

From:
Sent: Saturday, July 19, 2014 2:21 AM
To: Ballen, Karen
Subject: Copyright Permission

Hello,

I would like to use a figure from the following publication for use in my thesis and was hoping to get copyright permission.

The Roles of Hypoxia in the In Vitro Engineering of Tissues

Jos Malda, Travis J. Klein, and Zee Upton. Tissue Engineering. Volume 13, Number 9, 2007

Figure 3

8 CURRICULUM VITAE

Tierney Grace Blakeborough Deluzio

EDUCATION

May 2012-present	Candidate for Master of Engineering Science (M.E.Sc) June 2014 Specialization in Biomaterials and Biochemical Engineering University of Western Ontario, London, Canada *Supervisor:* Dr. Kibret Mequanint
September 2008- June 2012	Bachelor of Engineering Science, with distinction (B.E.Sc.) Specialization in Chemical Engineering Biochemical & Environmental Option University of Western Ontario, London, Canada
September 2004- June 2008	Korah Collegiate and Vocational School, Sault Ste. Marie, Ontario International Baccalaureate Diploma Ontario Secondary School Diploma Third highest academic average

HONOURS, AWARDS, and DISTINCTIONS

May 2012-present   Western Graduate Research Scholarship
- awarded to full-time graduate students with an entrance and continued average above 80%
- Institutional
- **Tuition and $12,000/year**

November 2013   Speaker of the Month, Graduate Seminar Series
- Awarded to graduate student achieving the highest mark on their seminar presentation
- Institutional

May 2012, May 2011, May 2010 Dean's Honor List
- Awarded to a full-time student who has maintained an academic average above 80%
- Institutional

March 2012   2nd Place Western Engineering Capstone Design & Competition
- Oral Presentation of Capstone Design Project
- Institutional
- **$500**

September 2008   Continuing Admission Scholarship
- Awarded to full-time student with an entrance average above 95%
- Institutional
- **$2,500/year**

DESIGN PROJECTS

September 2011-April 2012   Capstone Fourth Year Design Project
Supervisor: Dr. Argyrios Margaritis
Thesis: Production of Iso-butanol from Anaerobic Fermentation of Sugar Beets

- design of a chemical plant for the production of iso-butanol from sugar beets
- completed both team and individual tasks
- lead writer for all technical reports
- received second place award in category

RELATED WORK EXPERIENCE

Summer 2011   Engineering Co-op – Lake Superior Power (Cogeneration Plant)
- researched alternative water treatment technologies for proposed process upgrade
- participated in all safety and environmental meetings, focusing on future initiatives
- assisted with administrative, clerical, and operations related engineering tasks

Summer 2010   Student – Brookfield Renewable Power Wind Operations (Wind Farm)
- assisted with administrative, clerical, and operational tasks related engineering tasks
- performed school and public presentations on company operations and environmental initiatives
- completed review and update of documents related to operations and maintenance

September 2006-August 2009   Pool Lifeguard and Swim Instructor – City of Sault Ste. Marie
- Head Instructor (summer 2009) supervising co-workers during morning lessons and swims
- teaching swimming skills and water safety while providing a safe and enjoyable environment
- maintaining the safety of varied numbers of patrons during swims

December 2011-April 2014   Graduate Teaching Assistant
- ES2211F/G Engineering Communications
- Faculty of Engineering
- University of Western Ontario

August 2012   Teaching Assistant Training Program
- An interdisciplinary course for Graduate Teaching Assistants on the strategies and practice of university teaching
- Teaching Support Centre, University of Western Ontario

PUBLICATIONS and PRESENTATIONS

Refereed Journal Manuscripts (1)

- **Tierney G.B. Deluzio**, Dawit G. Seifu, and Kibret Mequanint. 3D scaffolds in tissue engineering and regenerative medicine: beyond structural templates? *Pharmaceutical Bioprocessing* 2013; 1(3), 267-281

Conference Presentations (1)

- **Deluzio, Tierney GB***; Mequanint, Kibret, Perfluorinated Molecules as Novel Oxygen Vectors for Tissue Engineering. 30th Annual Meeting of the Canadian Biomaterials Society (CBS), University of Ottawa, Ottawa, Ontario, Canada (May 29, 2013-June 1, 2013)